# A novel strategy for estimating groundwater recharge in arid mountain regions and its application to parts of the Jebel Akhdar Mountains (Sultanate of Oman)

D I S S E R T A T I O N

in partial fulfilment of the requirements for the degree of

Doctor rerum naturalium (Dr. rer. nat.)

submitted to the Faculty of Environmental Sciences

Dresden University of Technology

by

Dipl.-Hydrol. Alexander Gerner

born March 26th, 1971 in Schwäbisch Gmünd

**Referees:**

Prof. em. Dr.-Ing. Gerd H. Schmitz, TU Dresden

Prof. Dr. Martin Sauter, University of Göttingen

Prof. Dr. Rudolf Liedl, TU Dresden

Examination location and date: Dresden, November 21th, 2013

# Abstract

In arid regions, mountain catchments are the major contributor to the total natural water yield. Due to generally low groundwater tables, subsurface underflow - referred to as mountain-front recharge - is important in distinction to the surface runoff at the mountain front. The extent of the groundwater basin is hereby often vague. Approaches to assess mountain-front recharge are mostly based on groundwater data and integrate over time and space. This, however, cannot provide prognostic and time-dependent estimates of subsurface inflow to the adjacent alluvial basin aquifer. Consequently, the proposed strategy builds on rainfall based approaches. Temporal and spatial resolution is in this case mostly limited by data scarcity regarding hydrological characteristics of the catchment area and high-resolution rainfall data.

The proposed novel strategy combines three approaches to tackle these challenges. A newly developed conceptual hydrologic model provides time-dependent estimates based on fully distributed monthly rainfall. For distinct response units and seasons, non-linear relationships between rainfall and recharge describe the hydrogeologic response. The derivation of the response functions is based on a mass balance and considers the principal recharge mechanisms. Parameterisation makes use of available expert knowledge on geomorphology and seasonal rainfall characteristics. As an efficient tool to assess uncertainties, fuzzy arithmetic is used for complementary long-term average water balance estimates. This technique allows considering fuzziness in rainfall input, crop water use in mountain oases, and best available assumptions on recharge as portion of rainfall. Uncertainty regarding the potential, albeit unknown extent of groundwater basins is portrayed based on continuous surfaces which represent the degree of membership to a distinct geographical entity (termed as fuzzy regions). Distinct subsets of these fuzzy regions represent potential groundwater basins for water balance assessment.

The proposed strategy was applied on the large scale in an arid karst mountain range in northern Oman. The two complementary assessment approaches result in similar ranges of values. They are in good agreement with inversely computed inflow to a steady state groundwater model for the adjacent basin aquifer. The results of the conceptual hydrologic model are confirmed by the plausibility of average recharge rates for distinct response units and seasons. This shows that less intense winter rainfall contributes mainly to groundwater recharge. Uncertainties due to the vague extent of the groundwater basin are about 30 % of the total mean annual value. An option to mitigate this uncertainty is the complementary consideration of adjacent aquifer systems in future studies. Hydrogeologic survey and observation of groundwater levels in the alluvial basin aquifer in near distance to the mountains is a way to underpin these findings in future studies. This recommenddation applies not only to the discussed study area, but also to mountain block systems in general.

## Kurzfassung

In ariden Gebieten haben Gebirgseinzugsgebiete einen wesentlichen Anteil am gesamten natürlichen Wasserdargebot. Aufgrund i. Allg. tief liegender Grundwasserspiegel ist – in Abgrenzung zum Oberflächenabfluss am Gebirgsrand – auch der unterirdische Abstrom (*mountain-front recharge*) von besonderer Bedeutung. Die Ausdehnung des unterirdischen Einzugsgebiets ist dabei oft vage. Ansätze zur Abschätzung des *mountain-front recharge* basieren meist auf Grundwasserdaten und integrieren in Zeit und Raum. Damit können allerdings keine prognostischen oder zeitabhängigen Schätzungen für den Zustrom zur benachbarten alluvialen Aquifer gemacht werden. Daher wird im folgenden ein niederschlagsbasierter Ansatz vorgeschlagen.

Das vorgeschlagene neue Konzept kombiniert drei Ansätze, um den genannten Herausforderungen zu begegnen. Mit einem neu entwickelten konzeptionellen hydrologischen Modell auf Basis verteilter Niederschläge werden monatliche Werte für die Grundwasserneubildung bereitgestellt. Es basiert auf nicht-linearen Beziehungen zwischen Niederschlag und Grundwasserneubildung für definierte hydrologisch homogene Einheiten und Jahreszeiten. Deren Ableitung basiert auf einer Massenbilanz und berücksichtigt die wesentlichen Neubildungsmechanismen. Die Parametrisierung basiert auf Expertenwissen zu Geomorphologie und Niederschlagscharakteristika. Fuzzy Arithmetik wird zur Berücksichtigung von Unsicherheiten in einer ergänzenden mittleren jährlichen Wasserbilanz verwendet. Damit können Unschärfen im Niederschlagsinput, beim Pflanzenwasserbedarf in Gebirgsoasen und best verfügbaren Schätzungen der Neubildung als Bruchteil des Niederschlags effizient berücksichtigt werden. Mittels kontinuierlicher Oberflächen, die den Grad der Zugehörigkeit zu einer bestimmten geographischen Entität anzeigen (*fuzzy regions*) werden Unsicherheiten in der räumlichen Ausdehnung der unterirdischen Einzugsgebiete beschrieben. Definierte Teilmengen dieser *fuzzy regions* werden dann bei den Wasserhaushaltsbetrachtungen als potentielle Grundwassereinzugsgebiete verwendet.

Der vorgeschlagene Ansatz wurde in einer ariden, teils verkarsteten Gebirgsregion im Norden des Sultanats Oman angewendet. Die beiden sich ergänzenden Ansätze zur Abschätzung der Grundwasserneubildung ergaben im langjährigen Mittel vergleichbare Werte. Diese stimmten auch gut mit den Ergebnissen einer inversen Grundwassermodellierung überein. Die Plausibilität der Neubildungsraten für bestimmte hydrologisch homogene Einheiten und Jahreszeiten spricht für die Verlässlichkeit der Ergebnisse des konzeptionellen hydrologischen Modells. Offensichtlich tragen insbesondere die weniger intensiven Winterniederschläge wesentlich zur Grundwasserneubildung bei. Die Unsicherheiten bezüglich der Ausdehnung des Grundwassereinzugsgebiets belaufen sich auf ca. 30 % des mittleren jährlichen Dargebots. Die komplementäre Betrachtung benachbarter Grundwassereinzugsgebiete ist ein denkbarer Weg, diese Unsicherheit in Zukunft zu reduzieren. Ein wesentlicher Beitrag um die Ergebnisse dieser Studie zukünftig weiter zu untermauern wären hydrogeologische Erkundung und Beobachtung von Grundwasserständen im alluvialen Aquifer, insbesondere nahe dem Gebirgsrand. Diese Empfehlung gilt über dieses Fallbeispiel hinaus für vergleichbare Systeme, in denen ein Gebirgseinzugsgebiet den Aquifer in der angrenzende Ebene speist.

*„You will never miss the water,*
*until your falaj runs dry."*

*(Dr. Slim Zekri)*

*"The real voyage of discovery*
*consists not in seeking new landscapes,*
*but in having new eyes."*

*(Marcel Proust)*


# Acknowledgments

*I want to express my sincere thanks to all those, who supported me in coming closer to the nature of things.*

*First and foremost, I am grateful to my supervisor Prof. Gerd H. Schmitz, who gave me the opportunity to gather a wealth of experiences, for his motive force and careful guidance. I also thank Prof. Martin Sauter and Prof. Rudolf Liedl for their valuable comments.*

*The manuscript was prepared within the research project IWAS Middle East, funded by the German Federal Ministry of Education and Research (BMBF) under grant N°02WM1166.*

*This thesis wouldn't have been possible without the fruitful cooperation and exchange with the Ministry of Rural Municipalities and Water Resources at Muscat (Sultanate of Oman). My special thank goes to the colleagues from Monitoring Section and Aflaj Section for their efforts in providing the data. I also highly appreciated the great hospitality that I have experienced during my stays in the Sultanate.*

*During my time at the Chair of Hydrology, I had fruitful discussions and exchange with Dr. Klemens Barfus, Marco Brettschneider, Dr. Werner Dröge, Hamed Al-Dhuhli, Markus Giese, Ayisha Al Khatri, Sebastian Kloß, Dr. Thomas Krauße, Dr. Franz Lennartz, Ruben Müller, Tinh Pham Van, Dr. Andy Phillip, Dr. Robert Schwarze, Yohannes Subagadis and Dr. Michael Wagner. Jutta Hoffmann and Anke Deuchert are the good spirits of the Chair. In addition to the appreciation for his efforts all around the project, I thank Jens Grundmann for his support for my personal work. Dr. Niels Schütze gave valuable support to organize myself and to finalize my work in an appropriate time and form.*

*Beyond that, I appreciated the exchange of experiences with Marc Walther from the Institute of Groundwater Management. I also thank Jule Gottschlich for proofreading. Niels Rackwitz gave me the link to the 'Fermi's Approach', which led me to interesting discussions in current hydrology. While preparing fort the defense, my colleagues from Dr. Dittrich & Partner Hydro-Consult Ltd. provided care and valuable scientific feedback.*

*I want to express my warm thanks to all the friends and relatives, who provided social backing, encouragement and also valuable comments on my work. Last but not least, my heartfelt thanks and appreciation to my family, Anja, Julian and Johanna. You were brave enough to tackle that project together. Hats off!*

# Table of Contents

# 1 Mountains – 'water towers' for water resources systems in arid regions

"Mountains of the world, water towers for humanity" is the heading of a paper, which focuses on the global importance of mountain catchments as freshwater resources (Viviroli et al., 2007). Higher precipitation due to orographic effects, lower potential evapotranspiration (ETP) and relatively high recharge rates in relation to precipitation due to shallow or even absent soils and fractured bedrock are the main reasons, why mountain catchments generally yield more water than the adjacent basin plain. In arid regions, a limited natural water yield due to generally scarce rainfall meet with a continuously increasing water demand for agriculture, industries, and urban water supply. Thus, the yield of mountain catchments is often crucial for water resources management.

The total yield can be subdivided into surface and subsurface shares. Their relative proportions depend on the characteristics of the study area. Besides, these water balance variables differ regarding relevant time scale (single events or (long-term) water balance considerations) and process dynamics. Depending on the study area, surface drainage basins and underground catchment areas can differ as well. Thus, with respect to their assessment, a clear distinction is reasonable.

The subsurface runoff components at the mountain front are often referred to as mountain-front recharge (MFR). According to Wilson and Guan (2004), it is an important, if not predominant source of recharge to the adjacent basins in arid and semiarid climates. Simultaneously, it is the least well quantified. The quantification of its current rate is a prerequisite for an efficient and sustainable groundwater management. Hence, reliable assessment approaches are urgently needed.

Varying groundwater use implies the need for transient groundwater management. Consequently, time dependent inflow boundary conditions are required. Moreover, prognostic rainfall-recharge relationships are desirable to assess the impacts of climate change. These two aspects indicate the use of rainfall based assessment approaches. However, the availability of respective studies is very limited. Research in this field is challenged by the size, complexity and accessibility of mountain systems. Additionally, the availability of data in an appropriate temporal or spatial resolution is a limiting factor.

The determination of the relevant catchment area is the starting point of any hydrological analysis. Especially in arid regions with recharge controlled water tables, regional groundwater flow across surface drainage divides is common (Gleeson and Manning, 2008). Hence, groundwater basins are often subject to considerable uncertainties. As a consequence, this issue has to be addressed in assessing MFR.

Against this background, the focus of this thesis is the rainfall based assessment of mountain-front recharge in the context of integrated water resources management (IWRM). Though, the calibration or validation of respective approaches has to consider the water resources system as a whole, including the groundwater surface in the adjacent alluvial basin aquifer.

# 2 Mountain hydrology and water resources assessment

## 2.1 Mountain hydrology and mountain-front recharge

Figure 2.1 illustrates a so called mountain block system consisting of the mountain block and an adjacent alluvial plain. Herein, the mountain block is defined as all the mass composing the mountains, including vegetation, soil, bedrock (exposed and unexposed), and water. The mountain front zone is the not exactly defined transition zone between the mountain block and the basin plain (Wilson and Guan, 2004).

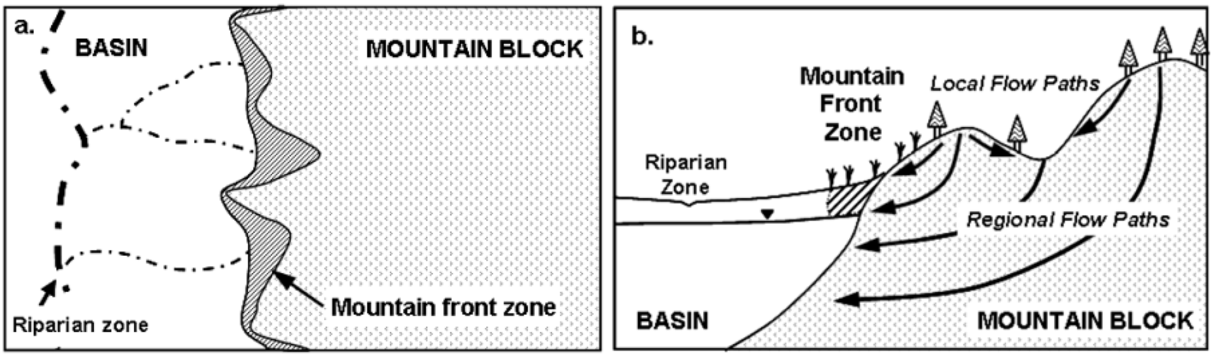


Figure 2.1: Schematic diagram showing hydrologically distinctive units of the landscape in map view (a) and in cross-section (b). The cross section also shows various groundwater flow paths in the mountain block (Wilson and Guan, 2004).

The total of the subsurface and near-surface water fluxes entering the basin aquifer in the mountain block or in the mountain front zone is often termed mountain-front recharge (MFR). The main components are illustrated in Figure 2.2. The near-surface component is the water flowing in alluvial channels or fans while subsurface flow comprises the groundwater in the mountain aquifer after (deep) percolation. In the context of groundwater modelling, MFR can also be seen as inter aquifer flow from the mountain aquifer to the alluvial basin aquifer.

Precipitation is the most important control on MFR. It is related to elevation, relief and orientation of the mountain. Winter precipitation is primarily responsible for MFR. Permeability of soils and bedrock in the mountains affects the way in which MFR occurs, as well as the rate and volume of recharge. The proportions of near-surface or subsurface inflow depend on the topography of the mountain. Finally, the stratigraphy of the mountain front deposit controls the distribution of recharge in space (Lerner et al., 1990).

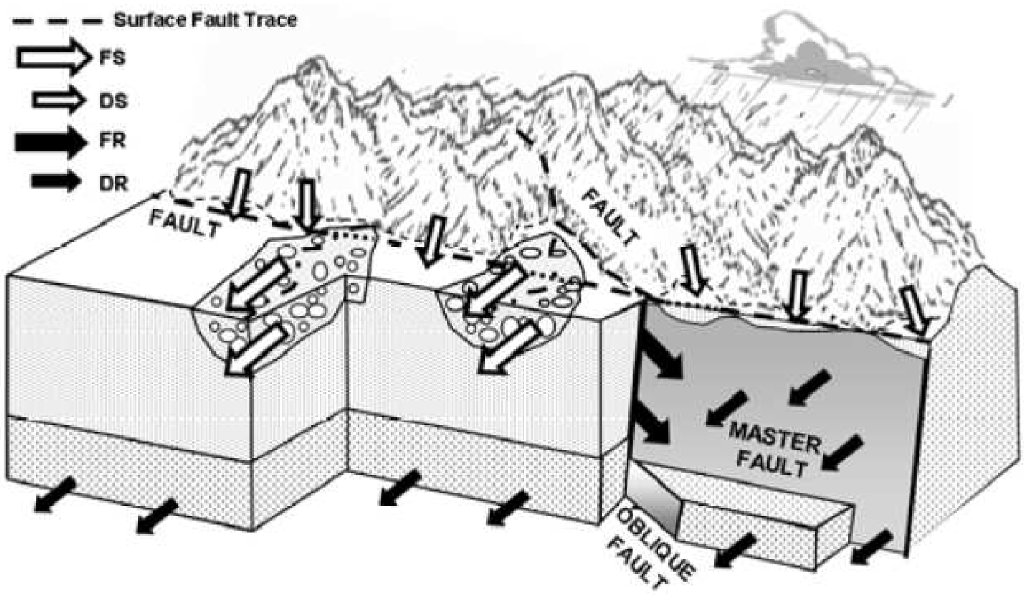


Figure 2.2: Schematic diagram illustrating MFR components. FS = focused near-surface recharge, DS = diffuse near-surface recharge, FR = focused subsurface recharge, DR = diffuse subsurface recharge (Wilson and Guan, 2004)

Evapotranspiration (ET), i.e. the moisture transfer from bare soil surface (evaporation) and from vegetated surface (transpiration) is an important aspect. In water resources assessment, the actually removed amount of water is of main interest. However, data about this is usually not available. Its measurement at site, for example based on the eddy covariance method carried out by Canton et al. (2010), is complex, uncertain and costly. Consequently, assessment of actual evapotranspiration ($ET_{actual}$) is a main issue in water balance assessment at any scale. An important basis therefore is the potential evapotranspiration (ETP). This represents the atmosphere’s ability to remove water from a saturated surface.

To date, the quantification of MFR is mostly limited to long-term average considerations avoiding the complexity of the interacting hydrologic processes within the catchment area. With regard to an improved understanding of the interacting processes, but also to quantify the link between precipitation and recharge to basins bounding the mountain front, Wilson and Guan (2004) propose a comprehensive integrated approach which is summarized under the term mountain block hydrology. An important challenge in this regard is the link between plot or hill slope scale and the entire mountain block in time (see section 2.2.1) and space (representatively of site-specific experimental data on the catchment or regional scale). Amongst other things, this complex approach aims at predicting the impact of water use, land use change, or climate variability on MFR rates.

The definition of MFR excludes surface runoff at the mountain front, which is likewise generated in the mountain catchment. Its proportional infiltration during runoff on the basin plain is another important mechanism regarding recharge to the alluvial basin aquifer. In the context of hydrological modelling, the infiltration of surface runoff during runoff routing is termed as transmission loss (Wheater and Al-Weshah, 2002). From the viewpoint of groundwater management, it can be seen as potential indirect recharge (de Vries and Simmers, 2002; Lerner, 1997). As illustrated in Figure 2.3, it occurs both in the mountain block and on the basin plain. The ratio of MFR and surface runoff at the mountain front can differ considerably, depending on the hydrological setting of the respective study area.

The links between those two water balance variables are runoff generation (division of rainfall into initial losses, infiltration and effective precipitation $P_{eff}$) and transmission losses (division of $P_{eff}$ into potential indirect recharge and surface runoff). In Figure 2.3, the first aspect is illustrated by the first branching of *'precipitation reaching the surface'*. Transmission losses are represented by infiltration after a lateral movement, which is labelled as *'Runoff and Interflow'*.

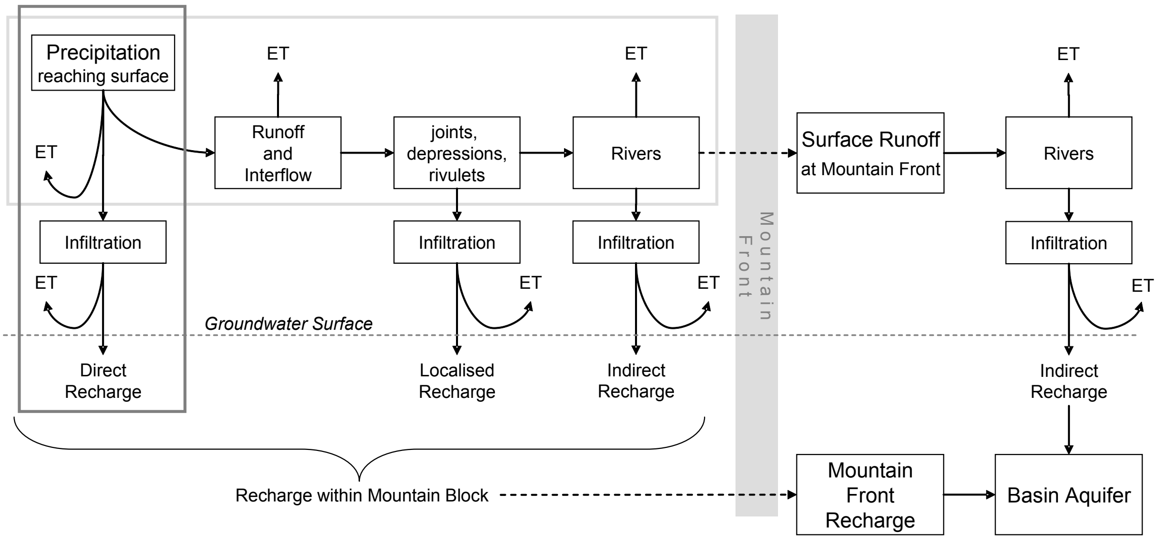


Figure 2.3: Subdivision of precipitation based recharge (modified after Lerner, 1997)

A main difference in the subsequent routing is the temporal dynamic. MFR and indirect recharge subsequent to surface runoff at the mountain front show different response times from rainfall to entry into the saturated zone of the adjacent alluvial aquifer. While the time scale of flash flood runoff is minutes or hours, percolation, retention in the mountain aquifer and subsurface flow rather extends over days, months, or even years. Moreover, MFR is a lateral inflow from the mountain front zone to the basin aquifer, while surface runoff induces a lateral movement. Subsequent transmission losses (or potential indirect recharge) often occur only far downstream to the mountain front zone. Thus, the groundwater surface in the basin aquifer is the integral result of different processes and mechanisms over different temporal and spatial scales.

Table 2.1: Characteristics of the two main water balance variables related to the mountain front

| variable | reference area | empirical reference | relevant time scales | promoted by | adequate tempo-spatial resolution |
|---|---|---|---|---|---|
| $Q_{Wadi}$ | (surface) drainage basin | stream gauging | event | low infiltration rates, high rainfall intensity | necessarily very high (minutes, hours) |
| MFR | groundwater basin | GW surface in alluvial basin aquifer | event, season, years | high infiltration rates, low to med. rainfall intensity | days, months, years |

Table 2.1 summarizes the characteristics of surface runoff discussed above at the mountain front and MFR. On this basis, it is reasonable to assess these variables separately. In section 2.3, various approaches to assess groundwater recharge are discussed. It includes more or less process oriented integrated approaches which allow assessing both variables separately and also approaches which integrate in time or in space.

## 2.2 Essential aspects to advance mountain hydrology

### *2.2.1 Rainfall characteristics and options for data acquisition*

Rainfall distribution in time and space is the most important driver of hydrological processes. In arid regions, it is generally characterised by a rare, erratic occurrence. If rainfall occurs, it results in a very high variability in space (Lange et al., 1999; Warner, 2004; Wheater and Al-Weshah, 2002). Therefore, the analysis of rainfall-runoff processes depends on the availability of monitoring data in an appropriate spatio-temporal resolution. Observed rainfall without observed runoff in the major wadis can be explained by transmission losses after local rainstorms in minor wadis (Lerner et al., 1990). Observed runoff without observed rainfall is often the case due to the limited spatial resolution of the rainfall monitoring network (see section 5.7).

The effects of spotty rainfall, which cover only a fraction of the drainage area in the context of hydrologic modelling, were investigated in various studies. They outline the increase of errors with decreasing density of the monitoring network (Michaud and Sorooshian, 1994; Osborn and Lane, 1972; Wheater and Al-Weshah, 2002). According to the last-named authors, the typical density of flash flood warning systems is 1 station per 20 km². On average, this results in errors of simulated peak runoff of more than 50 %.

So far, an area wide ground-based recording or of short duration rain storms in a spatio-temporal resolution corresponding to the process dynamic is limited to experimental catchments like, for example, Walnut Gulch in Arizona/USA. Rainfall radar is a useful supplement to ground based rainfall monitoring. In various studies, it has been applied in mountain catchments in both humid and arid regions (Germann et al., 2006; Morin and

Gabella, 2007; Peleg and Morin, 2012). Morin and Gabella (2007) investigated radar measurements under dry climatic conditions in Israel. Within certain limitations, for example distance to the radar station, they found that the applied methods provided useful rain depth estimates. More recently, cellular networks were investigated as an advancing alternative (Chwala et al., 2012; Kraemer et al., 2012; Messer et al., 2012; Rayitsfeld et al., 2011).

An option for remote or poorly gauged regions are the satellite-based PERSIANN rainfall estimates (Sorooshian et al., 2008). Since 2000, time series in a temporal resolution of 6 hours are globally available. However, the spatial resolution is only 0.25°. Additionally, a higher spatio-temporal resolution ($\Delta x = 0.04°$ and $\Delta t = 3$ h) is available for selected areas since 2006.

With regard to water resources assessment, the inter-linkage of temporal and spatial scales is an important issue. Single, local events appear rather randomly within a time window of a few years. On the long-term, they often result in typical cyclic patterns which are of vital importance in water resources management (Brook and Sheen, 2000). Consequently, conclusions based on a narrow time window can be misleading with regard to mid- or long-term conditions.

The geochemistry and isotopy of groundwater resources provides information on moisture sources or rainfall mechanisms, which are predominantly responsible for groundwater recharge (Stanger, 1986; Weyhenmeyer et al., 2002). Thus, monitoring and analysis rainfall chemistry and isotopy is an important issue besides its quantity in time and space.

### *2.2.2 Groundwater-surface water interactions and availability of reference values*

The effects of topographic and hydrogeologic controls on groundwater flow in mountainous terrain was investigated by Gleeson and Manning (2008) based on three-dimensional simulations of idealized multi-basin systems. The main conclusions are shortly summarized in Table 2.2. According to this, shallow or so called topography controlled groundwater tables are promoted by high rates of groundwater recharge, low hydraulic conductivity and a low relief. In contrast, low recharge, highly permeable aquifers and a rough topography lead to deep water tables. Local flow implies that the yield of a drainage basin discharges at the outlet of this watershed in contrast to regional flow, where groundwater flows from one surface watershed to another.

Table 2.2: Hydrologic controls and groundwater flow in mountainous terrain following Gleeson and Manning (2008)

| hydrologic controls | | | | promoted groundwater flow regime | | | | streamflow characteristics |
|---|---|---|---|---|---|---|---|---|
| climate | groundwater recharge | hydraulic conductivity | relief | water table | | flow range | hydraulic conditions | |
| | | | | type | depth | | | |
| humid | high | low | low | topography controlled | shallow | local flow | effluence ('gaining stream') | perennial |
| arid | low | high | rough | recharge controlled | deep | regional flow | influence ('losing stream) | ephemeral |

The terms influence and effluence describe the relation between the water level of surface water courses and groundwater surface next to it. If the groundwater table lies above surface water level, effluent conditions prevail. The opposite direction is termed as influence or influent conditions. Figure 2.4 (left graphs) illustrates these distinct conditions. They decide on the drainage direction from the groundwater to the surface water course (gaining stream) or vice versa (losing stream).

In humid zones with predominantly effluent conditions, the gauged hydrograph of a (gaining) stream represents the integral hydrologic response of its catchment area. Many hydrologic approaches are based on the assumption of a gaining stream. They are reaching from hydrograph separation approaches, e.g. DIFGA (Schwarze et al., 1999), to conceptual hydrologic models, e.g. the HBV model (Bergström, 1995). In this perception, groundwater recharge in the sense of water entering the saturated zone, can be derived from the slower flow components of the hydrograph. Water that does not contribute to actual evapotranspiration does, in either case, contribute to the hydrograph at the catchments outlet. For this reason, the measuring cross section in the Wernersbach experimental catchment, 25 km southwest to the city of Dresden/Germany, was equipped with an underflow barrier to really ensure effluent conditions.

In arid zones, generally deep lying groundwater tables prevail. Consequently, influent conditions are predominant (see Figure 2.4). Thus, the response of a mountain catchment is divided into (subsurface or near-surface) mountain-front recharge and surface runoff in a (losing) wadi channel. Further downstream, these components either contribute to indirect recharge or they discharge to its recipient. As a result, in contrast to effluent conditions, not only the surface runoff hydrograph reflects the interacting hydrological processes in the respective catchment, but especially the groundwater table in the alluvial basin aquifer does so. Stated more generally, under influent conditions, a surface runoff hydrograph alone is an appropriate reference for rainfall-runoff-modelling in a narrow sense, aiming at surface runoff at the catchment’s outlet. Calibration or validation of water balance approaches concluding on effective infiltration and actual evapotranspiration, however, requires basically information on the actual groundwater response.

Mostly, these references are limited to long-term averages (see section 2.3). An empirical database to evaluate the time dependent recharge estimates is, eventually, only the observed groundwater surface within or in an adequate distance to the mountain front zone. As Figure 2.5 shows, the empirical data base is a set of observed groundwater levels. In contrast, the output of a rainfall-recharge-relationship is a flux of water. Consequently, the observed changes in groundwater levels have to be transferred to fluxes by the use of appropriate models. The latter in turn require hydrogeologic survey.

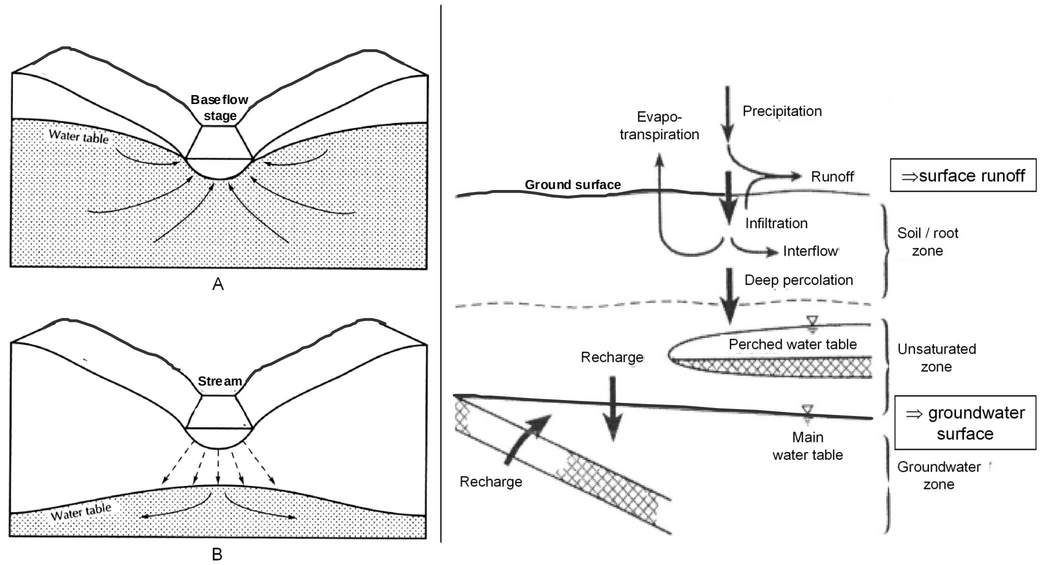


Figure 2.4: Left: Groundwater - surface water interactions (Fetter, 2001); A: Cross section of a gaining stream, which is typical of humid regions, where ground water recharges streams. B: Cross section of a losing stream, which is typical of arid regions, where streams can recharge ground water. Right: Infiltration, deep percolation and recharge - modified after Lerner (1997)

Thus, the calibration or validation of time-dependent approaches to assess MFR requires adequate hydrogeologic investigations, including observations of groundwater levels in an appropriate distance to the mountain front zone. Its availability is a crucial point for the interconnection between mountain catchment and basin aquifer.

The usual lack of appropriate groundwater observations is a general issue in arid zone hydrology. With regard to the Walnut Gulch experimental catchment, Wheater et al. (1997) outline this as follows: "*It is interesting to note that despite the very high quality of surface hydrology data at Walnut Gulch, subsurface information is limited, and there is a major international need for arid zone research basins to include integrated monitoring of both surface and subsurface processes.*"

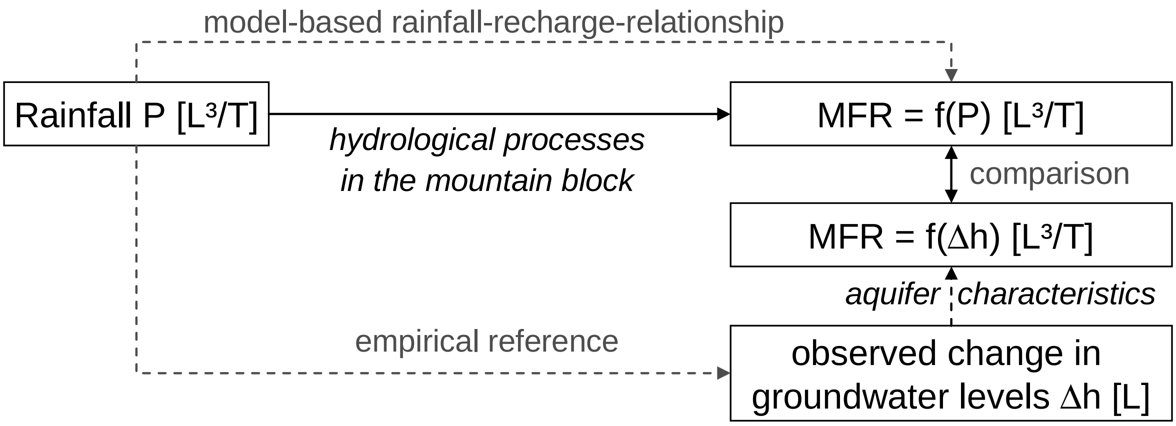


Figure 2.5: Interlink between mountain-front recharge and observed groundwater surface

## 2.3 Approaches to the assessment of mountain-front recharge

### *2.3.1 Options to assess groundwater recharge*

A “*Global synthesis of groundwater recharge in semiarid and arid regions*” (Scanlon et al., 2006) compiles the findings of about 140 studies in arid and semiarid regions. It covers different settings in terms of physical geography and spatial extent of the study area, the purpose of the study, and applied approaches. However, it contains hardly any study which focuses especially on mountain-front recharge. The study reported on a study of Anderholm (2001) using the Chloride Mass Balance approach (CMB) for the Middle Rio Grande Basin in New Mexico (7900 km²). Manning and Solomon (2003) were using noble gases in the salt lake valley in Utah. In a study about the Yucca Mountains (Flint et al., 2002) however, several methods were applied (see below). Additionally, Scanlon (pers. comm., January 25, 2012) stated: *“I think mountain front/block recharge is extremely important. I don't think there is a lot of information about this topic [...]”*.

Wilson and Guan (2004) compiled 12 studies featuring different hydrological settings regarding geology, mean annual precipitation, estimated mean recharge rate, and assessment approaches. Half of these studies comprised methods based on groundwater data (CMB, numerical modelling, Darcy’s law, i.e. estimating flow through a cross section). Furthermore, empirical relationships and water balance approaches based on estimations of evapotranspiration were applied.

Two conclusions can be drawn from this short overview:

- The data base for inter-site comparisons as a preliminary approach to a study area is extremely limited. Likewise, reference data for derivation or validation of assessment approaches is hardly available.
- The approaches applied are generally in accordance with established literature on groundwater recharge as provided by (de Vries and Simmers, 2002; Healy and Scanlon, 2010; Lerner, 1997; Scanlon and Cook, 2002; Scanlon et al., 2002).

There is a wide range of methods for quantifying recharge in the wider sense of water forming an addition to the groundwater reservoir from any direction (Scanlon et al., 2002). In summary, these are physical techniques, tracer techniques and modelling techniques. It is distinguished between surface water, unsaturated zone and saturated zone studies.

The water balance approach is a superior principle which is, implicitly or explicitly, connected to a number of these approaches. Its accuracy generally depends on the accuracy of the various components or parameters. Often, the sought groundwater recharge and the uncertainty range of other water balance variables are in a similar order of magnitude. Especially the assessment of actual evapotranspiration is subject to a considerable uncertainty.

The choice and success of each approach depends on the aim of the study and the spatial and temporal scale. While vulnerability assessment is focused on site-specific information, water resources assessment (WRA) rather has to deal with the integral response of a distinct catchment area. In addition to the larger spatial scales, a time scale of decades is considered in the context of WRA.

Studies based on groundwater data are a common way for large scale assessment of water resources. The most widely used approach for estimating recharge is the chloride mass balance technique (CMB) (Scanlon et al., 2006). However, (Weyhenmeyer et al., 2002) point out, that this method is limited by the availability of detailed long-term records of precipitation and chloride deposition. Another option is the inverse estimate of recharge based on numerical groundwater modelling. These 'basin centred' methods provide results for the whole catchment of the aquifer. However, they are integrating over space and (mostly) over time (Wilson and Guan, 2004).

In contrast, spatially distributed water balance modelling is an option for both, time dependent, and prognostic assessment. However, the data requirements are demanding and subject to the above mentioned limitations of the water balance approach regarding the accuracy. In more detail, this is discussed in section 2.3.2.

(Semi-) empirical approaches are mainly restricted to long term mean annual considerations. However, it can be highly misleading to describe mean annual recharge or recharge as a proportion of mean annual precipitation, if recharge results from only infrequent large events, which is often the case in arid regions (de Vries and Simmers, 2002). Nonetheless, it is common, not least due to a lack of alternatives. Additionally, it is an option to estimate recharge with manageable data requirements as a complementary approach to any other available method. An example for catchment wide estimates is the simple linear rainfall-recharge relationship for catchments in South Africa provided by Bredenkamp (1990).

Flint et al. (2002) cited a spatially distributed method by Maxey and Eakin (1950) which is based on distinct recharge rates as percentage of annual precipitation for different zones. This approach was adopted by other authors and adjusted or recalibrated for the respective study area.

Andreo et al. (2008) used data of several well investigated semi-arid catchments in southern Spain to derive a spatially distributed regionalisation approach named APLIS to estimate the annual recharge in carbonate aquifers based on geomorphologic variables.

A time dependent approach was provided by Kessler (1967) for the yield of a karstic spring in Hungary. Although not for a semi-arid region, it is interesting because it is based on the finding, that the hydrologic response depends, besides the rainfall input in the respective month, on antecedent rainfall or, more generally, on the seasonality. This is in accordance with one of the main controls mentioned in section 2.1 regarding MFR in arid regions.

Various authors point out, that recharge assessment is an iterative process. It starts with the review of previous studies and analysis of available data. On this basis, a conceptual model can be outlined. The choice of appropriate methods and the necessary data collection provides the basis for numerical models. Within a number of loops, data base, conceptualisation and models can be refined. Different independent complementary approaches, as allowed by available data, are highly desirable, because every approach is subject to certain limitations and considerable uncertainties (de Vries and Simmers, 2002; Healy and Scanlon, 2010; Scanlon et al., 2002). The discussion in section 2.2.2 where validation of rainfall based approaches relies on groundwater data, but the fact that numerical groundwater modelling relies on reliable inflow boundary conditions, supports that.

A unique example for such an iterative process using complementary approaches is the investigation of recharge mechanisms in the Yucca Mountains with regard to nuclear waste disposal. Flint et al. (2002) provided a comprehensive overview on applied approaches, their scales, parameters, strengths and limitations. They state: *"All of these methods produce estimates that are highly approximate, but complementary rather then redundant because they are based on vastly different assumptions."*

### *2.3.2 Arid zone water balance modelling – options and limitations*

Wilson and Guan (2004) promoted a comprehensive mountain block hydrology. The main motivation for that is the need for a time dependent and prognostic assessment. Nonetheless, the state of the art relies rather on inverse or (semi-)empirical approaches (see above). In the following, different water balance modelling approaches are reviewed and discussed with regard to their advantages and limitations. On this basis, the question about these processes and mechanisms, which are essential to assess mountain-front recharge is raised. The cited studies do not necessarily focus on MFR. However, the challenges and limitations are comparable because they eventually deal with the same basic processes and mechanisms.

Various authors (e.g. Al-Qurashi et al., 2008; Wheater et al., 1997) focus explicitly on rainfall-runoff-processes, i.e. the assessment of stream runoff at the catchments outlet. This approach provides an upper boundary for the assessment of indirect recharge due to transmission losses downstream to the considered reference cross section. With regard to an overall water balance assessment including direct recharge over the catchment area, it is only one part of the problem.

A further developed version of the lumped conceptual HBV light (Seibert, 2002) was used by Love et al. (2011) for meso-scale catchments in semi-arid environments. They concluded, that the model is unreliable for more ephemeral and drier catchments. It is stated that *"without more reliable and longer rainfall and runoff data, regionalisation in semi-arid ephemeral catchments will remain highly challenging."*

Likewise, a conceptual hydrologic modelling approach was presented by Sheffer et al. (2010). However, regarding 6 non-physical parameters, the applicability highly depends on available reference data. In this case, they could meet this challenge using a 3 stage calibration approach based on a 16 year calibration period, and another 5 observed years for validation based on the link of the water balance model to a groundwater model.

A distributed water balance approach for a mountain catchment in Iran, featuring a flow equation for the subsurface flow processes in valley alluvium and recharge from the beds of ephemeral rivers, was provided by Khazaei et al. (2003). Direct recharge in the highland area is explicitly out of consideration. This simplification can be acceptable in this special case. However, in the case of very permeable surfaces, direct recharge is supposed to be a main portion of groundwater recharge. Infiltration in the alluvium is described as a function of actual and maximal storage, and in addition, 2 non-physical parameters. The authors used a daily time step because of insufficient data to justify a smaller time step.

The work of Gunkel and Lange (2011) combined the fully distributed event based rainfall-runoff model ZIN (Lange et al., 1999) in a 5-7 minutes resolution with the continuous daily water balance model TRAIN (Menzel, 1997), applied in the lower Jordan River basin. This approach is a possible solution for a largely process based assessment of groundwater recharge. It gives insights to the spatial and temporal dynamics of the considered system. However, its application is demanding in terms of required input data (e.g. rainfall data in adequately high spatio-temporal resolution) and field data on catchment morphology (e.g. infiltration characteristics, geometry and hydraulic properties of alluvial channels etc.). For example, Gunkel and Lange (2011) point out that radar data was only available for about 2 years. Consequently, they discussed the distinct conditions for a single rather wet and a single drier year, but they did not conclude on mid- or long-term conditions.

Hughes et al. (2008) argue, that distributed watershed modelling is preferable to assess groundwater recharge in a structurally complex upland karst limestone aquifer in the West Bank. As one reason, they point out that the empirical approaches, applied in earlier recharge studies in this study area, defy the complexity of the partly karst, fractured aquifer and ignore the nature of a semi-arid climate with regard to variability in time. Additionally, it is mentioned that spring discharge can be subject to anthropogenic influences which has an impact on empirical relationships for the respective study area. Thus, they present a distributed water balance model on a daily time step. The assessment of groundwater recharge is carried out either by a soil moisture deficit (SMD) approach (Penman, 1948) or wetting thresholds (WT) according to Lange et al. (2003). The latter reference is, actually, the documentation of a 2 day sprinkling experiment on a large plot (18 x 10 m²) of a steep hill slope with a variety of different terrain elements. Hughes et al. (2008) documented the assumed wetting thresholds, but they do not reveal if it is just a threshold value above which recharge is equal to rainfall input, or if it is a more sophisticated modelling concept. The approach results in a spatially distributed picture. The authors point out that the complexity of the methods can be enlarged as understanding of the processes increases.

The following crucial points are summarised:

Availability of reference data:

Only in the study of Sheffer et al. (2010), a reference was available in the form of an interlinked groundwater model. In all the other cited studies, no reference data was available which really reflects the integral groundwater response to rainfall over the catchment as a whole. This general problem is one reason for the request for complementary approaches (seeFlint et al., 2002; cited in section 2.3.1) and it is a considerable source of uncertainty with regard to the calibration of non-physical model parameters. Consequently, concepts which rely on more or less physical parameters or at least proxy values for key processes are generally preferable compared to largely conceptual approaches. Furthermore, the enhancement of monitoring in the frame of an iterative approach should pay at least the same attention to reference data as to input data and catchment characteristics.

In the case of Wadi Kafrein (Jordan) both, a largely process based water balance model (Alkhoury, 2011) and a groundwater model (Wu et al., 2011) were set up recently. Therefore, an optimal setup for an iterative approach as outlined in section 2.3.1 is available.

Modelling concepts versus availability of input data and model parameters:

The approach of Gunkel and Lange (2011) relies on high resolution input data which is generally not available for time periods which are necessary for reliable water balance considerations. This is beneficial regarding process understanding. However, it does hardly support water resources assessment in an actual application. For this reason, Hughes et al. (2008) and Khazaei et al. (2003) chose a daily time step. In this case, considerable simplifications in process conceptualisation are unavoidable. For example the infiltration process is highly instationary.

Stochastic simulation is an option to deal with this issue. For example, Wheater et al. (1991) provided a model for stochastic rainfall simulation on the Arabian peninsula. Analogously, Fleckenstein and Fogg (2008) used geostatistical models to upscale hydraulic characteristics. However, in the given context it has to be considered, to what extent these models provide input data or model parameters which really represent a real-world case.

Consequently, a differentiation in the purpose is necessary between process understanding, which can be supported by stochastically generated high resolution data, and an actual application in a data scarce region for a recent time period. The latter must necessarily go along with a reduced complexity according to data availability.

With this in mind, Blöschl (2006) favours the synthesis of available approaches. He argues that complex system models clearly have their role in hydrology, but alternative models and alternative model uses are equally valuable in hydrologic synthesis across processes, places, and scales. In '*Searching for Simplicity in Hydrology*', Dooge (1997) argued in the same direction. He distinguished between rather micro-scale phenomena which can be tackled with deterministic approaches and, on the other hand, macro-scale processes with a very high degree of randomness. The problems faced in hydrology fall in the intermediate region. As a result, in his strategy for synthesis *"a systematic search for simple models, involving as few assumptions as possible and a small number of parameters, together with a sound knowledge of the conditions under which the models fail to give and adequate representation of the data"* is an important aspect.

### *2.3.3 Key components for assessing mountain-front recharge*

The flowchart showing the subdivision of precipitation based recharge including vertical and lateral movement of water (Figure 2.3) is supposed to be a valuable outline to derive an appropriate approach in order to assess mountain-front recharge in regions with scarce data.

Runoff generation and soil moisture budget can be considered one-dimensional vertically. Surface runoff routing and transmission losses range over the whole flow distance, and are therefore subject to all the uncertainties in physical properties along that flow distance. Infiltration characteristics and antecedent moisture conditions decide on the portion of surface runoff or indirect recharge in proportion to infiltration or direct recharge. Infiltration is considered to be a key issue: Its sensitivity should be considered whenever possible.

Which portion of the infiltrated water amount will enter the saturated zone and which portion will get lost by evapotranspiration? A site specific answer is a challenge for above discussed modelling approaches and for experimental approaches. In the context of water resources assessment on the meso- or large scale, the primary aim is a good agreement with reference data representing the whole catchment area on the mid- or long-term. The actual soil moisture status at a certain site and for a certain date is subordinated at this point. Nonetheless, a best possible consideration of the soil storage characteristics is an important aspect.

Variability of rainfall input in space is an important issue. Subdivision of rainfall into recharge, evapotranspiration and surface runoff depends highly on site-specific rainfall characteristics. Spatially averaged characteristics can be misleading. Therefore, a distributed approach is highly desirable. There is a conflict between desirable process orientation and temporal resolution of available rainfall data, however (see above). Regionalisation of rainfall is a necessary step in the pre-processing of input data. Additionally, regionalisation of the temporal variability is a critical point, where uncertainty is supposed to increase with increasing temporal resolution. Thus, an alignment of tempo-spatial resolution of available data and modelling concept is necessary.

To summarise, the following issues should, implicitly or explicitly, be considered regarding rainfall based assessment of mountain-front recharge:

- spatial distribution of rainfall and (seasonal) rainfall characteristics like occurrence, intensity and duration
- infiltration characteristics
- soil water balance as a function of soil storage characteristics, climate conditions and vegetation cover.

Furthermore, spatial and temporal resolution should correspond to available data.

Flint et al. (2002) emphasized, that every approach is to a certain degree approximate. Thus, analysis and portrayal of vagueness or uncertainties is important. For this reason, uncertainty analysis based on likelihoods is common in the context of hydrologic modelling. A distinction is made between input, parameter and model structural uncertainty (Beven, 1993; Grundmann, 2010). The last-named author combined several statistical and numerical methods to analyze both, the uncertainty of single model components and the global uncertainty. A comprehensive hydrogeological decision analysis framework in which geological uncertainty and parameter uncertainty is included was provided by Freeze et al. (1990). Alternative approaches to handle uncertainties based on fuzzy set theory will be discussed in section 3.

## 2.4 Linear reservoir models to describe base flow recession

In addition to runoff generation, concentration and channel routing, subsurface routing is an important aspect in water balance modelling. Reservoir models based on a single linear reservoir (SLR) or combinations of two or more linear reservoirs are widely used for this task. Dewandel et al. (2005) compared different conceptual methods for baseflow recession in porous media and concluded that only the equation by Boussinesq (1903) is an exact approximation of the respective flow equations for flow in porous media. Schwarze et al. (1999) show, that the linear combination of two storages with defined proportions of reservoir constants and input result in a sufficient approximation for the analytical solution of the underlying geohydraulic model. They are using this setup to describe the 'low' base flow components in the frame of conceptual water balance modelling. Their SLOWCOMP-approach includes another parallel storage for fast base flow components. Recharge $Q_{Rh}$ to this high permeable storage is limited by a constant number.

For karst aquifers, the explicit consideration of the conduits and the so called duality of recharge are essential. Király (2002) presents a conceptual two-reservoir model for karst aquifers. In this model, the low permeability storage Sl is representing the fissured matrix block. The highly permeable storage Sh, however, represents the conduit system.

Table 2.3 presents a comparison of the essential points. As a summary, the serial approach of Király (2002) is a recommendable option especially for karst aquifers (Geyer et al., 2008). The work of Schwarze et al. (1999) provide a proficient approximation of the analytical solution and parameters for different lithological classes. With regard to the distribution between low and high conducting storage, the approach of Király (2002) is more adaptable.

Table 2.3: reservoir models for hard rock or karst aquifers with lowly permeable (‘slow’) component Sl and highly permeably (‘fast’) component Sh

| lithological class | hard rock (in general) | karst aquifers |
|---|---|---|
| approach | SlowComp (Schwarze et al., 1999) | two-reservoir model<br>(Király, 2002) |
| order of storages | parallel | serial; release Ql flows into highly permeable storage Sh |
| distribution of input QR | limited capacity Vl_max of highly permeable storage Sh | proportion Rl/Rh of inflow to lowly and highly permeable storages |
| miscellaneous | slow component Sl: split-up into two storages Sl1 and Sl2 with reservoir constant<br>Kl2 =°1/9*Kl1 and distribution of inflow Rl1/Rl2 = $^{8/9}/_{1/9}$ | |
| physical interpretation \| *interpretation in the context of conceptual modelling* | *slow and fast baseflow components* | slow component :<br>Porous or fissured matrix<br>Fast Component:<br>Karst conduit system |
| reference values of reservoir constants K (as reciprocal of re-cession coefficient α) for carbonate aquifers | reservoir constant of low permeability storage Kl | |
| | see (Schwarze et al., 1999); carbonates (incl. different degrees of karstification):<br>120 d – **180 d** – 210 d | (Geyer et al., 2008):<br>100 d |
| | reservoir constant of highly permeable storage Kh | |
| | see (Schwarze, 2004); range for limestone (incl. different degrees of karstification):<br>6 d – **10 d** - 13 d | (Geyer et al., 2008):<br>2 d – 4 d |
| availablitity of reference values for non-carbonatic hard rock | available; see Schwarze et al. (1999), Schwarze (2004): | none |
| reference values for distribution of inflow | Schwarze (2004):<br>empirical values as function of annual P and lithology for annual P > 500 mm; thus, transferability limited | Geyer et al. (2008):<br>Rl = 50 % - 95 % |
| benefits | • commendable approximation of analytical solution for the slow component<br>• reference values for different lithological classes beyond karst | commendable conceptual approach for karst aquifers |
| limitations | distribution between slow and fast component: the higher the input, the lower the relative portion of the fast component | applicability for other lithological classes? |

# 3 Approaches to deal with uncertainty with a special focus on fuzzy sets

## 3.1 Probability based uncertainty assessment versus fuzzy reasoning

Hydrological analyses or models are subject to vagueness or uncertainty. Reasons are, for example, inaccurate or even lacking data, limited validity of site-specific measurements on a larger scale, or necessary simplifications in process conceptualisation. Their consideration is an important aspect in hydrology or water resources management. A major motivation for this is the equifinality of hydrologic models. This means, that different combinations of parameter values or input variables can result in the same output or goodness of fit, respectively (Beven, 1993; Grundmann, 2010).

Uncertainty analyses based on probabilities are widely used in hydrologic modelling. Parameters and variables of a hydrologic model are herein treated as random variables with distinct probability distributions. The necessary mathematical methods have been well founded for a long time. Consequently, their practical application is well established.

Probabilities are based on classical (binary) logic (CL). This means that a proposition is either (absolutely) true or (absolutely) false. In fuzzy logic (FL), however, it is a matter of degree. As illustrated in Figure 3.1, rainfall intensity is rather high or rather low in the fuzzy representation (right graph) instead of either high or low (left graph). The term crisp is often used in the context of fuzzy reasoning as an opposite to the term fuzzy.

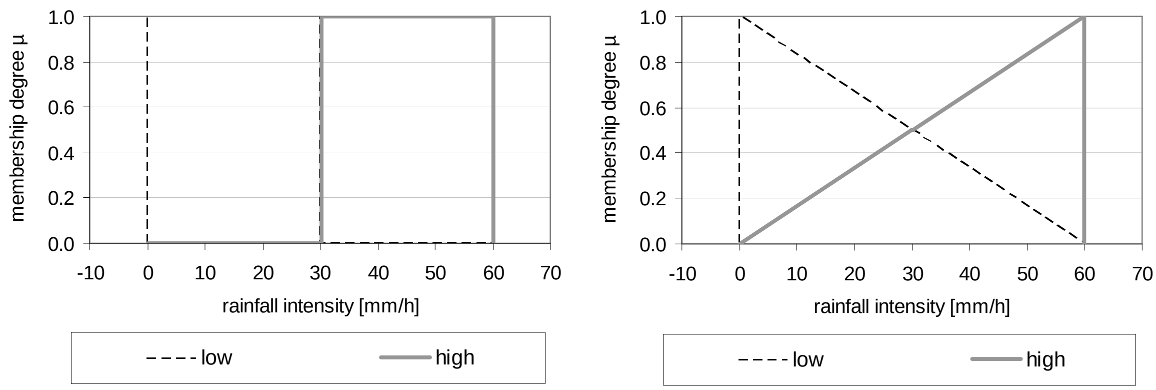


Figure 3.1: Crisp and fuzzy representation of rainfall intensities

In many respects, this approximate reasoning is much closer to reality. Hence, Şen (2010) states: *"It is better to start with FL principles and arrive at a set of fuzzy conclusions than to conclude with classical logic (CL) (two-valued logic) a mathematical approach with only one crisp result, which may never appear in real life."*

In the practical application, stochastic approaches rely on computationally demanding Monte-Carlo procedures. In this regard, fuzzy logic approaches can be an efficient alternative for consideration of uncertainty and are an integral part of model application. Additionally, fuzzy approaches are able to incorporate qualitative and heuristic information.

Fuzzy principles are able to use linguistic rather than quantitative variables to represent imprecise concepts. Linguistic variables (e.g. *rainfall intensity*) describe universal sets. They can be broken down into so called fuzzy words (e.g. *high*, *medium*, *low*) which imply numerical values. Therefore, fuzzy reasoning is very close to the nature of human language. Consequently, real world problems can be, in the first instance, described intuitively. This can be a common basis in problem solving for experts of different scientific or professional background (Sen, 2010).

However, fuzzy logic is not widely known or understood. Besides that, traditional stochastic methods are often preferred because of the inability to convert fuzzy predictions into probability distribution functions (Eder et al., 2005).

## 3.2 Fuzzy sets and related methods

In the following chapter, essential basics of fuzzy set theory are presented. Unless otherwise indicated, it is based on Dubois and Prade (1992) and Şen (2010). Ranges of application in water resources assessment are discussed in section 3.3. The flowchart in Figure 3.2 gives an overview on selected aspects which are relevant for this thesis. The upper part of the flow chart focuses on basic concepts, while the highlighted bottom line mentions potential applications in the fields of water resources management.

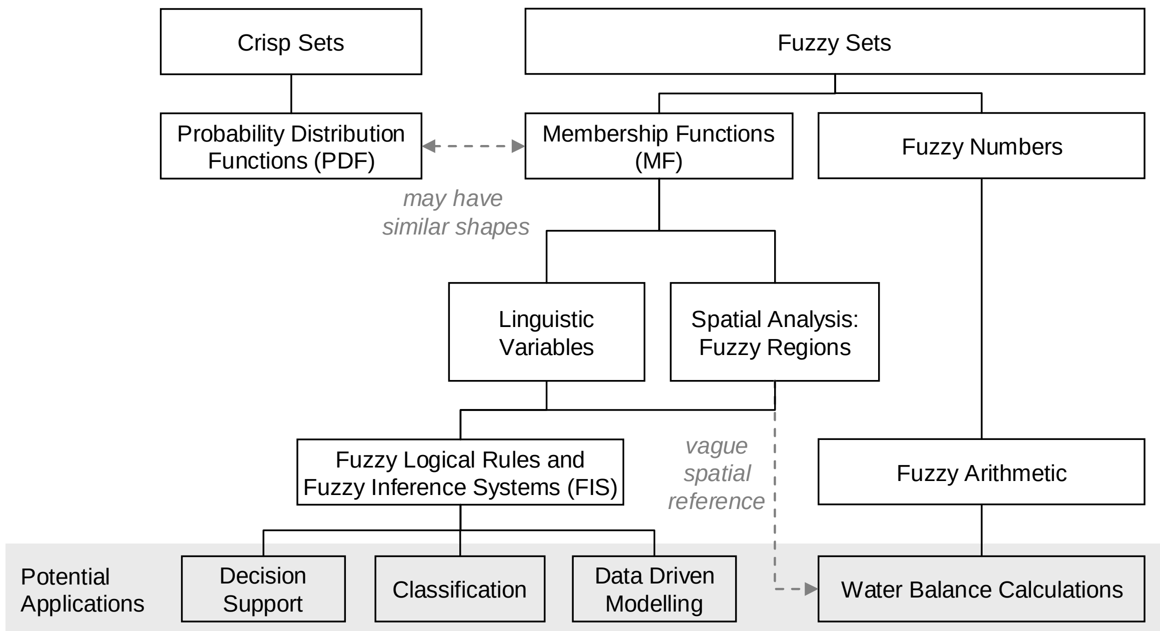


Figure 3.2: Fuzzy sets – related concepts and application range

Fuzzy sets

In classical (crisp) sets a membership degree (MD) of 1 is assigned, if an item belongs to a set. Otherwise, an MD of 0 is assigned. Symbolically, this can be shown as:

$$\mu_A(x) = \begin{cases} 1 & if\ x \in A \\ 0 & if\ x \notin A \end{cases} \tag{3.1}$$

In contrast, fuzzy sets can have MDs in the defined interval [0,1]. In other words, a point x of a fuzzy subset A can have a partial membership to a universe X (see Equ. 3.2). In the following, a fuzzy subset is referred to as fuzzy set.

$$A = \{(x, \mu_A(x)) : x \in X ; \mu_A(x) \in [0,1]\} \tag{3.2}$$

If $\mu_A(x) = 0$, then point x does not belong to the fuzzy set A. $\mu_A(x)$ is the so called membership function (MF) of the fuzzy subset A. It represents the MD of x in A. Therefore, the fuzzy set A is a set of n ordered pairs which can be expressed as follows:

$$A = \left\{ \frac{\mu_A(x_1)}{x_1}, \frac{\mu_A(x_2)}{x_2}, \ldots, \frac{\mu_A(x_n)}{x_n} \right\} \tag{3.3}$$

The support of a fuzzy set A includes all elements x with $\mu_A(x) > 0$.

$$\operatorname{supp}(A) = \{x \in X ; \mu_A(x) > 0\} \tag{3.4}$$

If the support of a fuzzy set A is only a single element, it is denoted as a fuzzy singleton. Its MD is $\mu_A \leq 1$. An ordinary number is likewise a subset with a single element. In contrast to the singletons, its MD is always unity ($\mu_A = 1$).

The most common shapes of membership functions are the triangular (Equ. 3.5) and the trapezoidal MF (Equ. 3.6). They are illustrated in Figure 2.1

Triangular MF:

$$\mu(x) = \begin{cases} \frac{x-a}{b-a} & if\ x \in [a,b] \\ \frac{c-x}{c-b} & if\ x \in [b,c] \\ 0 & else \end{cases} \tag{3.5}$$

Trapezoidal MF:

$$\mu(x)=\begin{cases}\dfrac{x-a}{b-a} & if\ x\in[a,b]\\ 1 & if\ x\in[b,c]\\ \dfrac{d-x}{d-c} & if\ x\in[c,d]\\ 0 & else\end{cases} \tag{3.6}$$

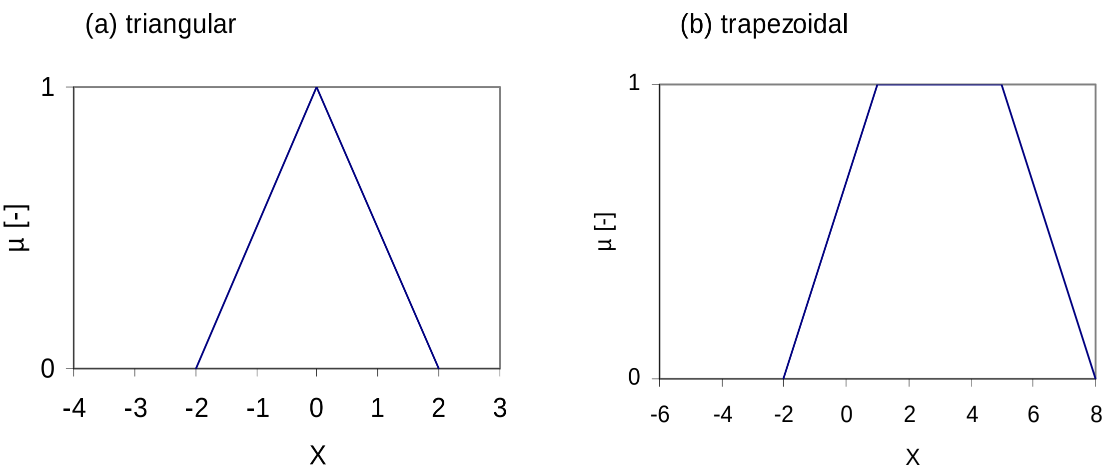


Figure 3.3: Triangular and trapezoidal membership functions

Normality and Convexity

A fuzzy set A is called normal, if at least one point of A has an MD $\mu_A(x)$ equal to 1. It is convex, if the MF consists of an increasing and a decreasing part. This means, that the MF does not include local minima. With $x_1, x_2 \in X$ and $\lambda \in [0,1]$, the respective criterion can be written as follows:

$$\mu_A(\lambda x_1 + (1-\lambda)x_2) \geq \min(\mu_A(x_1), \mu_A(x_2)) \tag{3.7}$$

An $\alpha$-cut is the crisp subset with MD $\mu_A(x) \geq \alpha$. If the MF is convex, then it is an interval which can be represented as

$$A(\alpha) = [x_1(\alpha), x_2(\alpha)] \tag{3.8}$$

with $A(\alpha)$ fuzzy set at $\alpha$-cut level $\alpha$

$x_1(\alpha)$ lower bound of the $\alpha$-cut

$x_2(\alpha)$ upper bound of the $\alpha$-cut

Operations on fuzzy sets

In the context of fuzzy-rule based systems (see below), logical operations are applied to fuzzy sets. On the basis of two fuzzy sets A and B of the universe X and the respective membership functions $\mu_A(x)$ and $\mu_B(x)$, there are three Boolean operations described in the following. The names in brackets are alternative terms used by Şen (2010).

Complement ('NOTing'):

The complement of a fuzzy set A is referred to as $\overline{A}$. Its MF is defined by

$$\mu_{\overline{A}}(x) = 1 - \mu_A(x) \tag{3.9}$$

Union ('ORing'):

The union of two fuzzy sets A and B is $C = A \cup B$. Its MF is defined by

$$\mu_C(x) = \max(\mu_A(x), \mu_B(x)) \tag{3.10}$$

Intersect ('ANDing'):

The intersection of two fuzzy sets A and B is $D = A \cap B$. Its MF is defined by

$$\mu_D(x) = \min(\mu_A(x), \mu_B(x)) \tag{3.11}$$

Fuzzy numbers and fuzzy arithmetic

Fuzzy numbers are a special case of a general fuzzy set. They are normal and convex fuzzy subsets of the set of real numbers $\Re$:

$$A = \{(x, \mu_A(x)) : x \in \Re; \mu_A(x) \in [0,1]\}: \tag{3.12}$$

Any real number can be considered as a fuzzy number with a single point support. It is referred to as crisp number. Consequently, fuzzy numbers can be seen as a generalization of the usual concept of numbers.

In contrast to the general fuzzy sets discussed above, arithmetic operations can be applied to fuzzy numbers beyond the above mentioned Boolean operations. Additionally, it has to be mentioned that union and intersection of fuzzy numbers do not result in fuzzy numbers because the normality assumption is not fulfilled any more.

Equations 3.13 to 3.16 show the four main fuzzy operators: addition, subtraction, multiplication and division. In this context, the lower and upper bounds of the $\alpha$-cuts of the fuzzy numbers A and B according to Equ. 3.8 are considered as operands. In the different operations, they are combined in such a way, that each operation results in the maximal possible interval width for the respective $\alpha$-cut level.

Fuzzy addition: $A(\alpha)(+)B(\alpha) = [x_{A,1}(\alpha) + x_{B,1}(\alpha), x_{A,2}(\alpha) + x_{B,2}(\alpha)]$ (3.13)

Fuzzy subtraction: $A(\alpha)(-)B(\alpha) = [x_{A,1}(\alpha) - x_{B,2}(\alpha), x_{A,2}(\alpha) - x_{B,1}(\alpha)]$ (3.14)

Fuzzy multiplication: $A(\alpha)(*)B(\alpha) = [x_{A,1}(\alpha) * x_{B,1}(\alpha), x_{A,2}(\alpha) * x_{B,2}(\alpha)]$ (3.15)

Fuzzy division: $A(\alpha)(/)B(\alpha) = [x_{A,1}(\alpha) / x_{B,2}(\alpha), x_{A,2}(\alpha) / x_{B,1}(\alpha)]$ (3.16)

Instead of two fuzzy operands, the operations can also be applied to a fuzzy operand A(α) and a crisp number.

The fuzzy arithmetic operators are based on the extension principle (Zadeh, 1965). This basically means that every value $x_A(\alpha)$ is transformed while its membership degree $\mu_A(x) = \alpha$ is kept. In the case of multiple operands different membership degrees are considered according to defined rules. Ultimately, it allows to generalize any crisp mathematical concept to the fuzzy set framework.

Fuzzy logic and Fuzzy Inference Systems (FIS)

Fuzzy Inference Systems (FIS) map different input fuzzy sets to an output using fuzzy logical rules. Among other things, it is an efficient way to describe non-linear relationships.

Figure 3.4 illustrates the general structure of a Mamdani type FIS. Linguistic variables represent single or multiple input variables (often referred to as antecedents) and single or multiple output variables (also referred to as consequents). Fuzzification means to define two or more overlapping membership functions (MFs) for each defined linguistic variable. For example, an antecedent ‘rainfall’ or a consequent ‘runoff’ can be represented by the MFs ‘low’, ‘medium’ and ‘high’ , each covering a certain support.

Fuzzy logic rules connect selected MFs of one or more antecedents with corresponding MFs of the consequents. During inference, the respective membership degrees (MDs) μ(x) of actual values x of the antecedents are evaluated and applied to the conclusion part of the rule. This results in a fuzzy subset for each output variable for each rule. Subsequently, the results of each rule are combined (‘Composition’), which results in a single fuzzy subset for each output variable. At last, the fuzzy output set is converted to a crisp number. This step is referred to as defuzzification. Different defuzzification methods can result in different crisp numbers for the same fuzzy output.

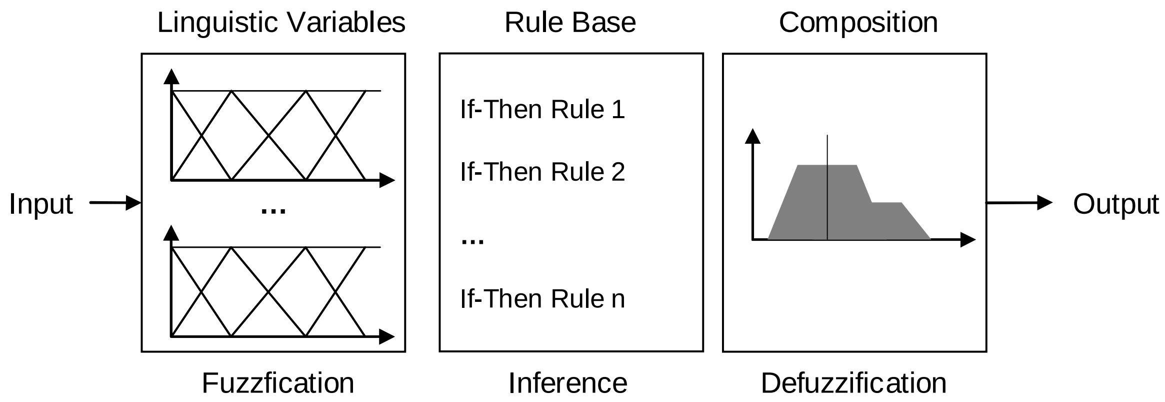


Figure 3.4: General structure of a Mamdani type Fuzzy Inference System (FIS) (own representation following Sen, 2010)

Due to the linguistic variables, the Mamdani type FIS described above supports a rather intuitive modelling approach. In contrast, the likewise widely applied Sugeno FIS or adaptive network based FIS (ANFIS) relate sets of crisp in- and output data instead of fuzzy sets.

<u>Fuzzy approaches in spatial analysis</u>

Transferring the basic concepts of fuzzy logic to spatial analysis, a thematic layer (e.g. landuse) can be seen as an analogue to a linguistic variable. However, the subsets (e.g. cropland or forest) are referred to as fuzzy geographical entities (Lodwick et al., 2008) or fuzzy regions (FR) (Morris and Kokhan, 2007). In the subsequent text, they are referred to as fuzzy regions. Figure 3.5 shows an example, where the grey tone indicates the degree of membership. Accordingly, fuzzy regions are continuous surfaces which represent membership degrees $\mu(x,y)$ in relation to certain locations. As shown in the lower sketch in Figure 3.5, a corresponding membership function can be derived as well. The abscissa hereby shows the value (in this context a measure of extension), while the ordinate indicates the degree of membership $\mu(x)$. The $\alpha$-cut is the crisp subset with membership degrees $\mu(x,y)$ of at least $\alpha$. Hence, the (2D-)$\alpha$-cut of a fuzzy region is an area with a crisp $\alpha$-cut boundary referring to a certain $\alpha$-cut level.

Fuzzy regions are usually applied in connection with fuzzy inference systems. In the frame of this thesis, they are used to portray the actually unknown extent of underground catchment areas as spatial reference for water resources assessment (see section 3.1).

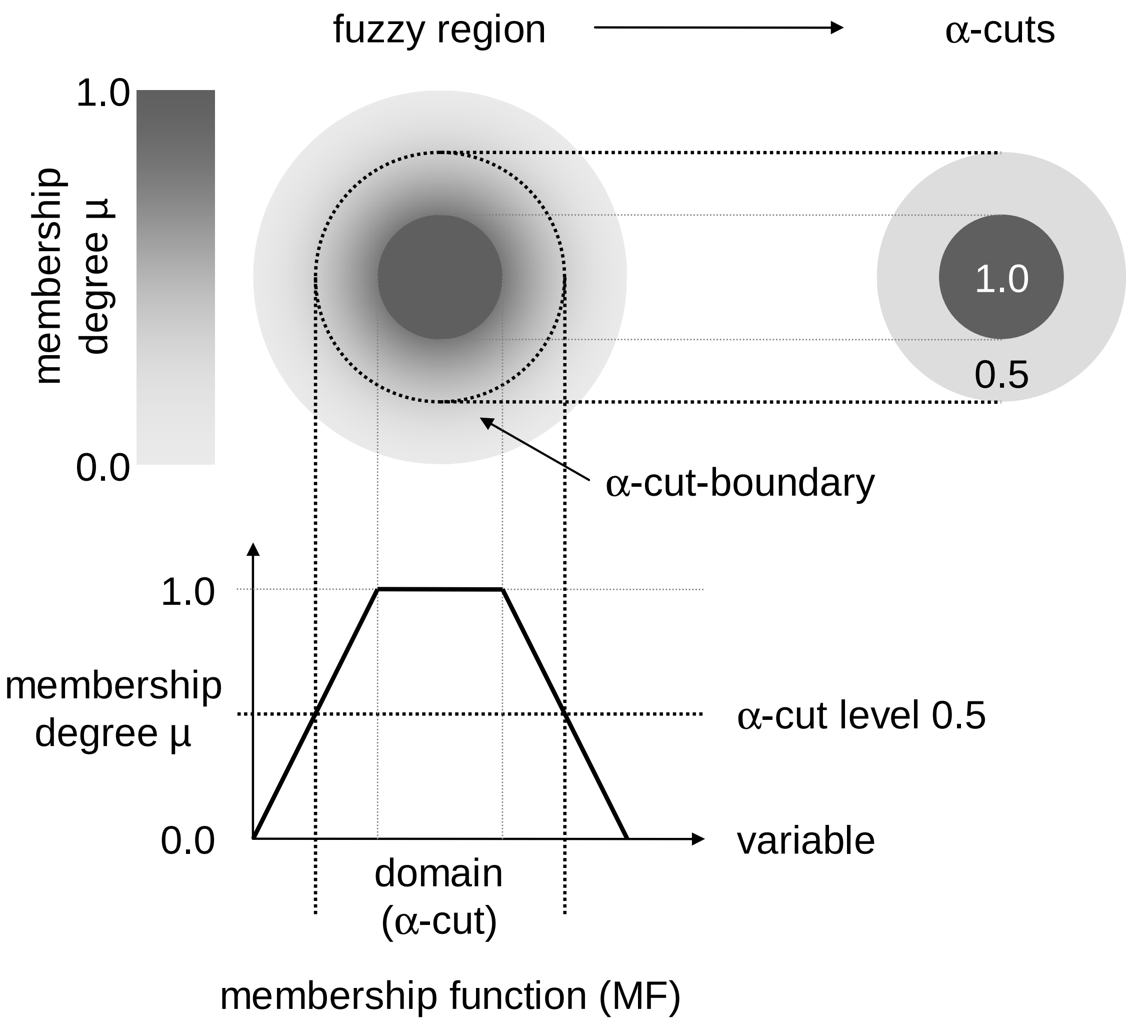


Figure 3.5: Representation of a fuzzy region and its fuzzy set membership function (modified after Zhan and Lin, 2003)

## 3.3 Ranges of application in hydrology and water resources management

FIS are supposed to be the most widely used application of fuzzy set theory. Often, they are used for decision support (Makropoulos et al., 2008). This means, the most appropriate out of several options is chosen according to selected values of the antecedents. Additionally, the classification of data is a typical application. For example, it was used to derive a soil map in the context of watershed modelling under data scarcity (Tavares Wahren et al., 2012). In the water balance approach in section 3.2, it is used to classify carbonates according to the expected degree of karstification according to selected input variables. In decision support as well as classification, the option to consider qualitative knowledge is of special benefit. Furthermore, FIS are an option for data driven modelling in the fields of hydrology. For example, FIS have been used as an alternative description of hydrological processes in conceptual hydrologic modelling (Hundecha et al., 2001). In addition to the clear and comprehensible structure, small computation times compared to common models are a motivation to use rule-based fuzzy systems. Pakosch (2011) used FIS to set up a flash flood forecasting system including uncertainty assessment instead of using a common model and respective ensembles of input data. Peters (2011) derived a FIS based on physically based 1D-SVAT modelling for selected sites to reduce computation time in raster based applications over large areas. Consequently, FIS can be an equal alternative to artificial neural networks (ANN).

Water balance assessment is a potential application of fuzzy arithmetic in hydrology. Fuzzy components of the water balance equation can be computed by using fuzzy arithmetic operators. In section 5, a respective approach is presented in combination with fuzzy regions to portray uncertainty regarding the extent of the underground catchment area.

A matter of research with regard to continuous water balance modelling is the increase of fuzziness in consecutive time steps (Eder et al., 2005).

# 4 A novel strategy for estimating groundwater recharge in arid mountain regions

Based on the prior discussions on the assessment of mountain-front recharge (MFR) in general and rainfall based approaches in particular, the following research questions arise:

How is it possible to assess MFR as a fraction of spatially distributed rainfall considering limited spatio-temporal resolution of rainfall input and data scarcity regarding catchment characteristics (infiltration, soil storage) and reference data for calibration?

How to deal with uncertainties regarding recharge rates or, more general, the response to rainfall input and the actual extent of the groundwater basins?

Is there a way to derive time dependent estimates of MFR capturing the essence of the prevailing processes and mechanisms but not all the details, complementarily to existing modelling concepts which are either oversimplified or over-parameterised and, thus, likewise subject to a considerable uncertainty?

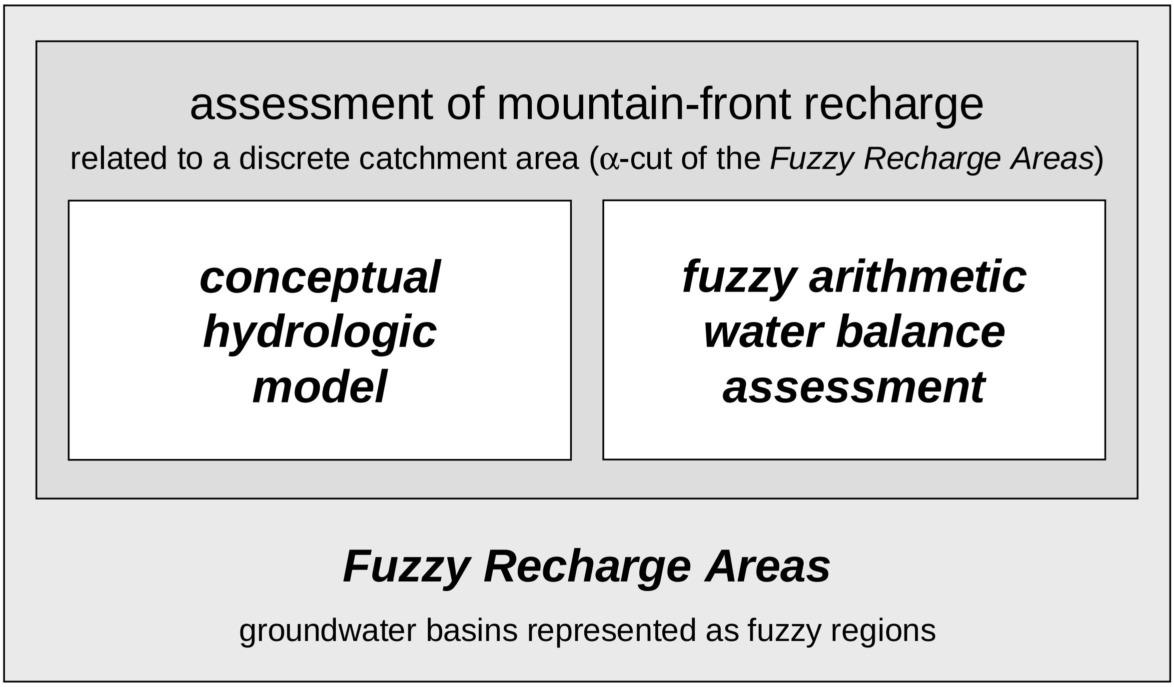


Figure 4.1: Assessment of mountain-front recharge considering limitations of data availability via combination of three complementary modules

A novel strategy is proposed as a possible answer, combining three complementary modules. According to Figure 4.1, the main components are a conceptual hydrologic model aiming at time dependent estimates, a fuzzy based tool for long-term average water balance assessment and a fuzzy approach to portray uncertainty in the actual extent of groundwater basins. Each approach covers certain aspects of the requirements mentioned above. In combination, all requirements are adequately considered.

The conceptual hydrologic modelling approach is based on fully distributed, monthly rainfall data. Recharge rates are herein non-linear functions of actual rainfall at site for distinct response units and seasons. The approach is based on the above discussed search for minimal necessary complexity – aiming at a model that captures the essence of the issue, but not all the details. For retention in the mountain aquifer, a serial two-reservoir model following Geyer et al. (2008) is used. The water use in mountain oases is considered. In addition to monthly output, long-term averages are computed to compare the outcome with complementary approaches. This approach is presented in detail in section 6.

Fuzzy arithmetic is used for long-term average annual water balance estimates. The single water balance variables are herein considered as fuzzy numbers (see section 3.2). Similar to the conceptual hydrologic model, it is based on fully distributed rainfall. The assessment of the single water balance variables can include available data or assessment approaches. It is an efficient tool to assess uncertainties in the water balance. The approach provides complementary estimates of mountain-front recharge independent from the hydrologic model mentioned above. A detailed description is presented in section 5.2.

As mentioned in section 1, the actual extent of groundwater basins can be a source of uncertainty. The concept of the Fuzzy Recharge Areas (Gerner et al., 2012) provides a means to consider this issue in the context of water balance modelling. Based on qualitative expert knowledge on the hydrogeology of the study area, potential extents of the groundwater basins are represented as fuzzy regions. Distinct subsets of these fuzzy regions provide the discrete catchment areas for water balance assessment. Ultimately, the parameter representing these distinct spatial extents can be considered as an additional variable in applying the two presented assessment approaches. Furthermore, the consideration of adjacent aquifer systems is supported. It is presented in section 5.1 in more detail.

Based on a detailed description of the hydrological setting (section 7.1), the case study in chapter 7 applies the approaches presented above to a pilot study area in the Batinah Region (Sultanate of Oman). In addition to mountain-front recharge, the role of further sources of recharge to the alluvial aquifer on the basin plain, for example (artificial) indirect recharge and direct precipitation recharge, is addressed. In this way, a comprehensive view upon this water resources system is provided. The focus, however, lies on assessing MFR based on the strategy presented above. The results are compared with inversely computed inflow to a steady state groundwater model (Walther et al., 2012). In section 7.6 the discussion addresses the distinct conditions in that study area (section 7.6.1) as well as methodical aspects based on the experiences in the case study application section (7.6.2).

Section 8 summarizes the work and evaluates the findings. Recommendations for future work are given in section 9.

# 5 Fuzzy-based tools to portray uncertainties in water balance assessment

## 5.1 Fuzzy Recharge Areas: From qualitative data to quantitative conclusions

### *5.1.1 The concept of the Fuzzy Recharge Areas*

Every approach for water resources assessment or hydrologic modelling refers to a distinct catchment area with a defined spatial extent. However, in some cases, its actual extent is not clear. While (surface) drainage divides can be reliably delineated, groundwater divides are often vague. Thus, the concept of the Fuzzy Recharge Areas introduces the application of fuzzy regions (see section 3.2) to water resources management as a means to describe potential, but actually unknown spatial extents of groundwater basins. Unless otherwise stated, the following text is based on Gerner et al. (2012).

Fuzzy Recharge Areas are an approach to transform qualitative expert knowledge referring to the hydrogeology of a study area into possible extents of the groundwater basin. These are represented as a fuzzy region. Subsequently, quantitative information, namely groundwater recharge $Q_R(\alpha)$ related to a certain $\alpha$-cut level, can be derived (see Figure 5.1). In this context, the expression *recharge area* is set equal with groundwater basin or underground catchment area, respectively.

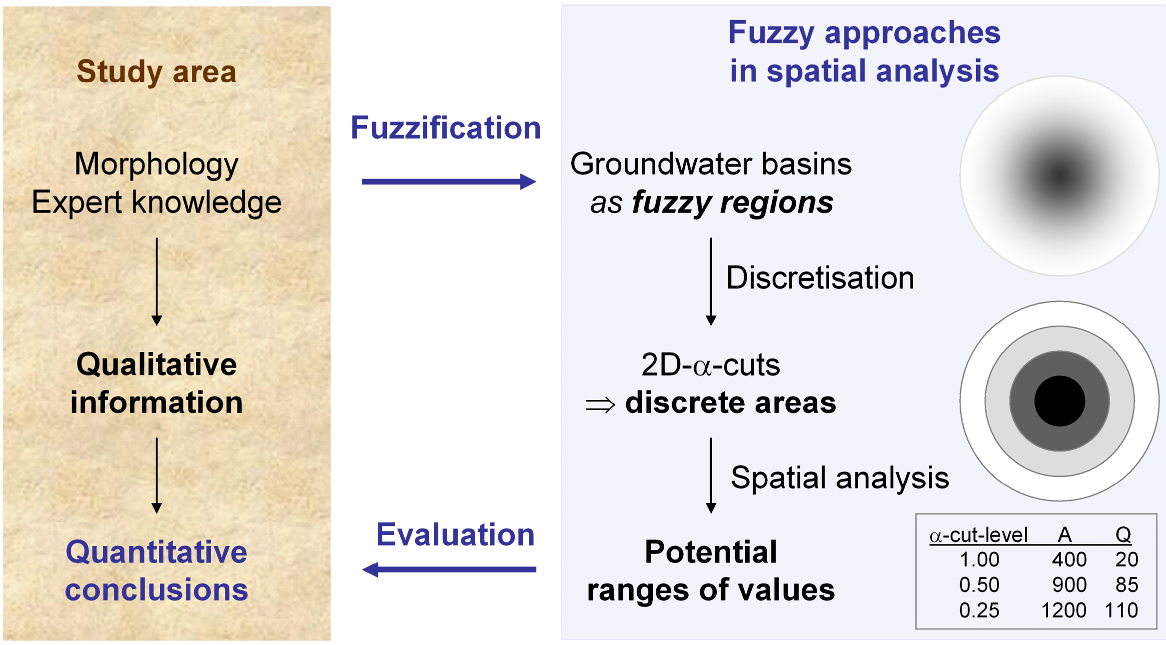


Figure 5.1: The concept of the Fuzzy Recharge Areas (modified after Gerner et al., 2012)

Fuzzy Recharge Areas are fuzzy regions (FR), i.e. raster surfaces with membership degrees $\mu_{A1}(x,y)$ between 0 and 1. Raster cells with $\mu_{A1}(x,y) = 1$ are certainly draining to the considered underground catchment A1. However, for raster cells with $\mu_{A1}(x,y) < 1$, the subsurface drainage to an adjacent basin A2 is possible as well. The concept includes the following steps:

1) Expert knowledge

- Gathering of information - e. g. geological model of the study area, results of tracer or isotope studies, quality and quantity of the spring water, groundwater isoline maps etc.
- Data analysis and hypothesis generation about recharge areas and flow systems

2) Fuzzification

- Definition of outer boundaries (maximum extent of the Fuzzy Recharge Areas)
- Definition of inner boundaries (assumptions on membership degrees at certain sites)
- Data processing, i.e. translation of outer and inner boundaries (discrete data) into a continuous surface, referred to as Fuzzy Recharge Areas

3) Consideration of adjacent areas

- Fulfilment of the complementarity constraint in regard to the consideration of adjacent areas according to section 5.1.2.

4) Evaluation

- Discretisation: Processing of 2D α-cuts by selection of raster cells with degree of membership equal or above the considered α-cut levels. As the case may be, adjacent areas are considered according to section 5.1.2.
- Spatial analysis: Hydrological analyses referring to α-cuts of the spatial extent

The approach results in potential extents of balance areas FR(α) as a fundamental basis for water balance assessment. Thus, it provides a quantitative measure of uncertainty with respect to the spatial extent of the considered basin. From the viewpoint of hydrologic modelling, the α-cut level of a certain extent can also be seen as a model parameter. An exemplary application is presented in section 7.

#### *5.1.2 Consideration of adjacent basins*

A thematic layer 'groundwater basins' may consist of two adjacent Fuzzy Recharge Areas A1 (referred to as first order) and A2 (referred to as neighbour) as subsets. By definition, the degree of membership $\mu_{\overline{FRA}}(x,y)$ of the complement $\overline{FRA}$ of the fuzzy region $FRA$ can be written as $\mu_{\overline{FRA}}(x,y) = 1 - \mu_{FRA}(x,y)$.

Within this context, it has to be considered, that

- the neighbour A2 may have membership degrees $\mu_{A2}(x,y) \le \mu_{\overline{A1}}(x,y)$ (e.g. in regions outside of the overlapping part of FRA1 and FRA2)
- more than two adjacent basins may be considered. Therefore, a subsequent consideration of complements may be necessary.

For this reason, a slightly different approach than the formal complement seems to be appropriate:

In the first instance, fuzzy regions for each basin can be processed independently. During evaluation, conditional fuzzy regions $FR_{A2}(\alpha_{A1})$ can be considered as correspondent to the $\alpha$-cut level of the first-order $\alpha_{A1.}$ Thus, the following steps are necessary, exemplarily illustrated in Figure 5.2:

1) Provision of fuzzy regions for the first-order (A1) and the (first) neighbour (A2) (see Figure 5.2-a and c)

2) Processing of an $\alpha$-cut $A1(\alpha_{FRA1})$ for the first-order area (Figure 5.2-b)

3) Processing of the complement to the first-order $\alpha$-cut $F\overline{A1}(\alpha_{A1})$ (Figure 5.2-d)

4) Intersection of $\overline{A1}(\alpha_{A1})$ and neighbour A2, resulting in a conditional fuzzy region $A2(\alpha_{A1})$ for the neighbour (Figure 5.2-e)

5) Processing of conditional $\alpha$-cuts for the neighbour $A2(\alpha_{A1,}\alpha_{A2})$ (Figure 5.2-f).

(a) first-order A1

| | | | | |
|---|---|---|---|---|
| 0.8 | 0.8 | 0.5 | 0.2 | 0.0 |
| 1.0 | 0.8 | 0.6 | 0.3 | 0.0 |
| 1.0 | 0.9 | 0.8 | 0.5 | 0.1 |
| 1.0 | 0.9 | 0.7 | 0.4 | 0.0 |
| 0.9 | 0.8 | 0.5 | 0.1 | 0.0 |

(b) $\alpha$-cut A1(0.7)

| | | | | |
|---|---|---|---|---|
| 1 | 1 | 0 | 0 | 0 |
| 1 | 1 | 0 | 0 | 0 |
| 1 | 1 | 1 | 0 | 0 |
| 1 | 1 | 1 | 0 | 0 |
| 1 | 1 | 0 | 0 | 0 |

(c) neighbour A2

| | | | | |
|---|---|---|---|---|
| 0.2 | 0.2 | 0.5 | 0.9 | 1.0 |
| 0.0 | 0.3 | 0.4 | 0.9 | 1.0 |
| 0.1 | 0.2 | 0.5 | 0.7 | 1.0 |
| 0.1 | 0.1 | 0.3 | 0.8 | 1.0 |
| 0.2 | 0.2 | 0.5 | 1.0 | 1.0 |

(d) complement of first-order $\overline{FA1}$(0.7)

| | | | | |
|---|---|---|---|---|
| 0 | 0 | 1 | 1 | 1 |
| 0 | 0 | 1 | 1 | 1 |
| 0 | 0 | 0 | 1 | 1 |
| 0 | 0 | 0 | 1 | 1 |
| 0 | 0 | 1 | 1 | 1 |

(e) conditional neighbour $A2(\alpha_{A1}=0.7)$

| | | | | |
|---|---|---|---|---|
| 0.0 | 0.0 | 0.5 | 0.9 | 1.0 |
| 0.0 | 0.0 | 0.4 | 0.9 | 1.0 |
| 0.0 | 0.0 | 0.0 | 0.7 | 1.0 |
| 0.0 | 0.0 | 0.0 | 0.8 | 1.0 |
| 0.0 | 0.0 | 0.5 | 1.0 | 1.0 |

(f) conditional $\alpha$-cut $A2(\alpha_{A1}=0.7,\ \alpha_{A2}=0.8)$

| | | | | |
|---|---|---|---|---|
| 0 | 0 | 0 | 1 | 1 |
| 0 | 0 | 0 | 1 | 1 |
| 0 | 0 | 0 | 0 | 1 |
| 0 | 0 | 0 | 1 | 1 |
| 0 | 0 | 0 | 1 | 1 |

Figure 5.2: Complementary consideration of adjacent fuzzy regions

## 5.2 Water balance assessment based on fuzzy arithmetic

### *5.2.1 Outline of the calculation procedure*

The following procedure aims at the water balance assessment based on fuzzy numbers of spatially distributed rainfall, recharge as portion of rainfall, water use and additional water balance variables. In contrast to crisp considerations, a measure of uncertainty is included in the model. Thus, variants based on different parameter sets to describe a confidence range are not necessary.

The considered balance area in an individual case is equal to a selected subset (α-cut) of the respective *Fuzzy Recharge Area* (see section 5.1). Figure 5.3 shows a flowchart of the calculation procedure. It includes recharge estimates for each raster cell and the cumulation of the yield per raster cell over the respective response unit and, over the whole balance area. Finally, the balance of cumulated yield and cumulated water use in the balance area is calculated. The schedule represents a single arbitrary time step. In the first instance, the approach aims at long-term average considerations. Smaller time steps are principally feasible, as far as reasonable approaches for the prevailing conditions in the respective time steps can be provided.

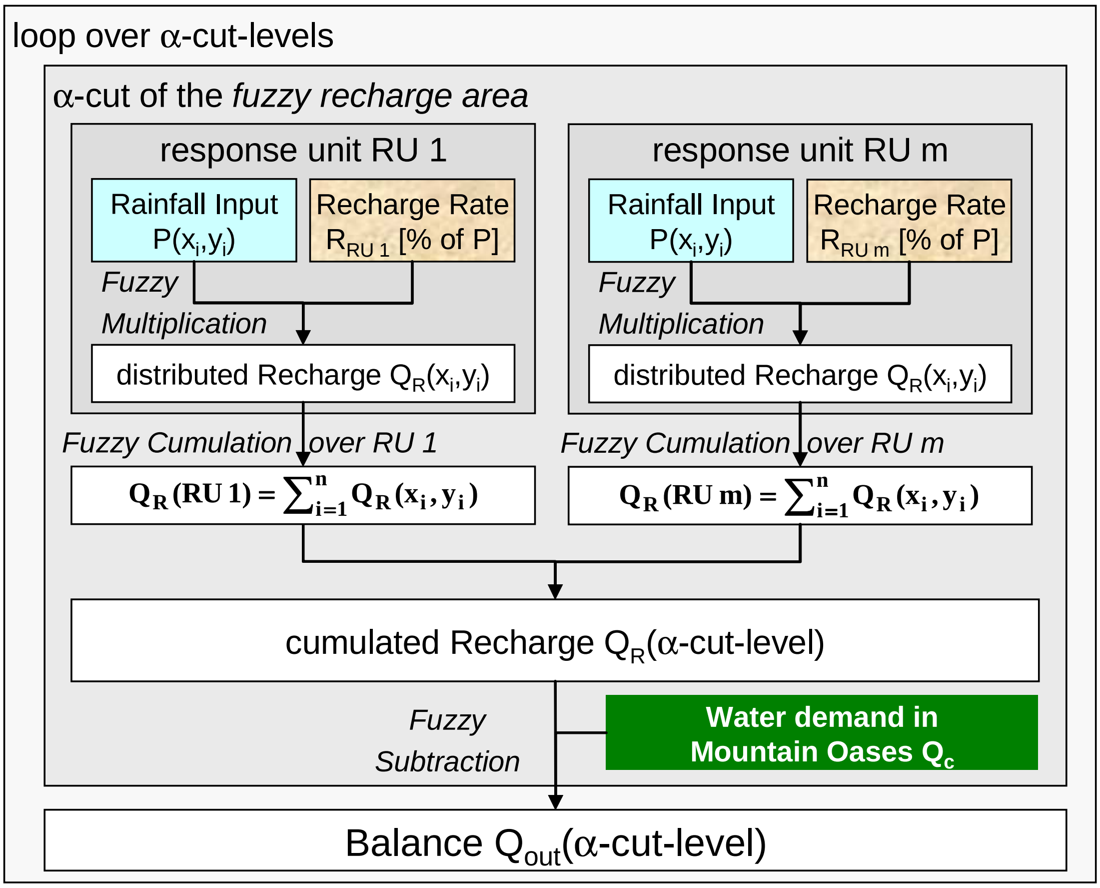


Figure 5.3: Water balance assessment based on fuzzy arithmetic

The calculation procedure requires distributed rainfall input, recharge rates for each defined response unit, as well as water use estimates. In the frame of this approach, a trapezoidal or triangular representation of fuzzy numbers is supposed to be reasonable. They can be defined by each three or four points as explained in section 3.2. As far as necessary or reasonable, other shapes are possible as well.

Fuzziness in rainfall input is useful, for example to consider measurement errors. The implementation is based on crisp regionalised rainfall and a fuzzy correction factor which can be either spatially distributed or related to defined sub-areas. If the considered rainfall is the result of a stochastic simulation, fuzzy numbers can follow the shape of the resulting probability distributions.

Fuzzy numbers of recharge rates as portion of rainfall can be provided according to availability based on any available approach. For example, they can represent rough estimates based on expert knowledge or inter-site comparison. As an example for a regionalisation approach, the implementation of the APLIS approach (Andreo et al., 2008) is presented in section 5.2.3.

Water use is basically the product of cropped area $A_c$ and crop water use $ET_c$. According to the reliability of data on cropped areas, this variable can be considered either as crisp or as fuzzy. A fuzzy representation of crop water use is reasonable with regard to the uncertainties in assessing this variable.

### *5.2.2 Implementation of the fuzzy arithmetic operators*

The basics of fuzzy arithmetic are presented in section 3.2. The implementation of the fuzzy arithmetic operators addition, subtraction, multiplication and division is based on the respective MatLab-function *fuzarith* (MathWorks, 2008). Thus, it refers to a universe X. The accuracy of the operations depends on the resolution of the universe X. The domain of X is predefined by the orders of magnitude of operands and output values. Large domains are demanding in terms of storage and, thus, computation time. Fuzzy cumulation denotes the successive execution of the basic operators keeping an interim result– e.g. to cumulate the elements of a raster or for each response unit within a balance area. Thus, values of different orders of magnitudes have to be dealt with.

For this reason, an individual fitting of the universe X for each operation, depending on the respective operator, was implemented to ensure both a minimal necessary domain and an adequate resolution with regard to accurate arithmetic operations.

### 5.2.3 *Implementation of the regionalisation approach APLIS*

The APLIS method (Andreo et al., 2008) allows for estimation of recharge in carbonate aquifers, expressed as a percentage of annual precipitation using the five variables *Altitude* (A), *Slope* (P), *Lithology* (L), preferential *Infiltration landforms* (I) and *Soil type* (S). After classifying these variables according to Table 5.1, recharge rates are calculated using the following equation:

$$R = (A + P + 3 * L + 2 * I + S) / 0.9 \qquad (5.1)$$

*Altitude* and *Slope* can clearly be classified based on a digital elevation model (DEM). The classification of *Lithology* and *Soils*, however, and even more the one of *Infiltration landforms* (which both represent the occurrence of karst features) depends highly on the available data base. Thus, in the case of data scarcity, a fuzzy representation is highly recommendable. *Altitude* and *Slope* are hence included as crisp numbers. The soil class is optionally crisp or fuzzy. *Lithology* and *Infiltration landforms* are definitely considered to be fuzzy variables. However, they can be defined in two ways:

- user defined fuzzy numbers or
- derivation of fuzzy numbers using a Fuzzy Inference System (FIS).

Table 5.1: Ratings for the variables: *Altitude, Slope, Lithology, Infiltration landforms* and *Soil type* (Andreo et al., 2008); the data range is expressed as, for example "(300–600]", meaning that the value of 300 is not included in this class whilst 600 is included

<table>
<tr><th>Rating (APLIS)</th><th>A: Altitude [m]</th><th>P: Slope [%]</th><th>L: Lithology</th><th>I: Inf. landforms</th><th>S: Soil</th></tr>
<tr><td>10</td><td>≤ 300</td><td>≤ 3</td><td rowspan="2">Limestones and dolostones karstified</td><td>many</td><td>Leptosols</td></tr>
<tr><td>9</td><td>(300 – 600]</td><td>(3 – 8]</td><td></td><td>Arenosols and xerosols</td></tr>
<tr><td>8</td><td>(600 – 900]</td><td>(8 – 16]</td><td rowspan="2">Limestones and dolostones fracturated, slightly karstified</td><td></td><td>Calcareous regosols and fluvisols</td></tr>
<tr><td>7</td><td>(900 – 1.200]</td><td>(16 – 21]</td><td></td><td>Euthric regosols and solonchaks</td></tr>
<tr><td>6</td><td>(1.200 – 1.500]</td><td></td><td rowspan="2">Limestones and dolostones fissured</td><td></td><td>Cambisols</td></tr>
<tr><td>5</td><td>(1.500 – 1.800]</td><td>(21 – 31]</td><td></td><td>Euthric cambisols</td></tr>
<tr><td>4</td><td>(1.800 – 2.100]</td><td>(31 – 46]</td><td>Gravels and sands</td><td></td><td>Histosols and luvisols</td></tr>
<tr><td>3</td><td>(2.100 – 2.400]</td><td>(46 – 76]</td><td>Conglomerates</td><td></td><td>Chromic luvisols</td></tr>
<tr><td>2</td><td>(2.400 – 2.700]</td><td>(76 – 100]</td><td>Plutonic and metamorphic rocks</td><td></td><td>Planosols</td></tr>
<tr><td>1</td><td>> 2.700</td><td>> 100</td><td>Shales, silts, clays</td><td>scarce</td><td>Vertisols</td></tr>
</table>

The degree of karstification (*Lithology*) and occurrence of karst features (*Infiltration landforms*) are, among other factors, functions of slope and climatic factors. The latter are, in turn, functions of altitude. Qualitatively, a high rating of *Lithology* and *Infiltration landforms* according to Table 5.1 corresponds to high elevation values (variable *Altitude*) and low slopes (variable *Slope*). According to section 3.3, this is a typical application of a FIS, therefore such systems were included (see Figure 5.4). They estimate the two variables *Lithology* and *Infiltration landforms* based on the APLIS ratings of altitude and slope. In the case of the *Infiltration landforms*, *Lithology* is considered as an additional variable.

In fact, the authors of the APLIS approach point out, that the resulting rates should not be considered as exact values. They therefore classify the result into intervals of $\Delta R = 20\ \%$. However, for an application within the presented framework, spatially distributed fuzzy numbers aside from these predefined intervals appear more reasonable than up to 5 clusters with uniform intervals of recharge rates.

The crisp result of a FIS is the outcome of a defined defuzzification method. To include a certain degree of fuzziness, different defuzzification methods were applied. In detail, it was the centroid of area, bisector of area, mean value of maximum, smallest and largest (absolute) value of maximum. Subsequently, minimum, median and maximum of the 5 defuzzification methods mentioned above were considered as basis for fuzzy operands for the calculation of the APLIS-recharge rates.

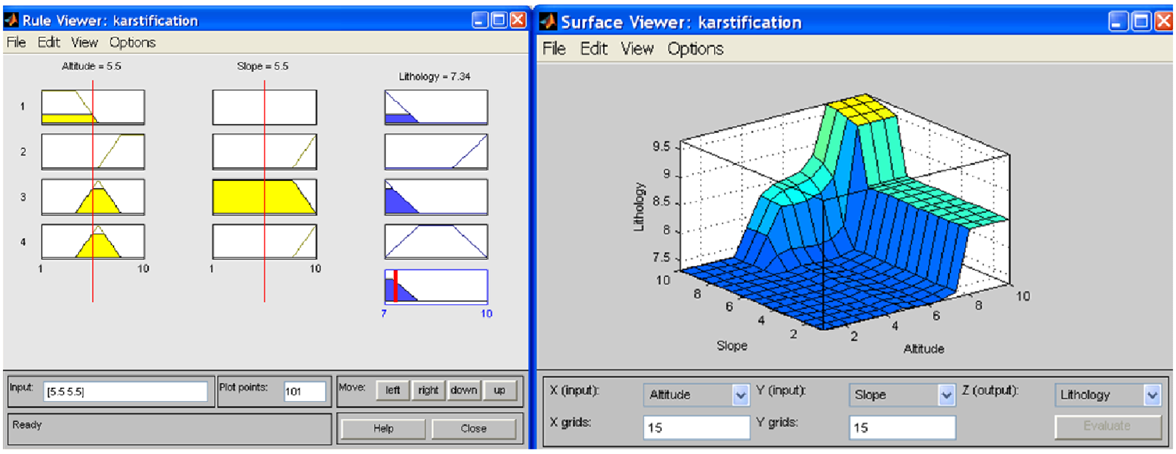


Figure 5.4: Fuzzy Inference System to classify *Lithology* as a function of *Slope* and *Altitude* with regard to the application of the APLIS approach

# 6 A conceptual hydrologic model to assess mountain-front recharge

## 6.1 Basic idea

According to section 2.3, water balance assessment in arid mountain catchments is subject to limitations, either due to an inadequate process representation or due to a lack of an adequate data base for largely process based approaches. Consequently, process knowledge is necessary to provide time dependent rainfall based approaches. However, a minimal necessary model complexity is worthwhile with regard to limited data availability.

In the following concept, groundwater recharge is a non-linear function of actual spatially distributed monthly rainfall. The derivation of the response function (see section 6.4.1) considers the key processes according to the subdivision of precipitation based recharge as illustrated in Figure 2.3. Thereby, the following simplifications are made:

- In deriving the response functions, initial losses and maximum infiltration per time step as well as the soil moisture deficit are represented by integral variables instead of submodules with a more or less detailed process description.
- The amount of indirect recharge induced by site specific rainfall is assessed in a conceptual way. The approach does not consider the actual location where indirect recharge takes place. It rather aims at the cumulative volume over the considered area for the respective time step.

## 6.2 Model structure

The model structure (see Figure 6.1) is distributed with regard to rainfall input. The considered catchment area in an individual case is equal to a selected subset (α-cut) of the respective Fuzzy Recharge Area (see section 3.1). Optionally, it is subdivided into distinct hydrogeologic response units (HGRUs). These represent an area with uniform response characteristics to site-specific rainfall according to the respective geomorphology and climate conditions. Consequently, they are an analogue to hydrologic response units (HRU) in hydrologic modelling, but aiming at subsurface flow components rather than at the best possible description of surface runoff.

For every case, i.e. a combination of season and HGRU, a non-linear relationship between rainfall input and recharge rate as percentage of rainfall per time step has to be defined. In this context, a season represents a defined series of calendar months. Analogue to the empirical linear approach of (Bredenkamp, 1990) there is no response up to a certain rainfall threshold (in the following termed sill). Above that sill, however, there are non-linear relationships which result in different relative responses for different rainfall depths per considered time step. These represent varying portions of direct and indirect recharge according to the hydrologic characteristics of the respective response unit. Therefore, the approach provides a sort of unit or long-term mean response to a certain rainfall input for a considered season and response unit. It covers the variability in time (actual monthly rainfall input and seasonality of the response function representing mean seasonal antecedent moisture) and space (regionalised rainfall input and optional distinction of response units).

For each time step, the response of the single raster cells is cumulated over the respective response unit. This cumulated recharge volume is routed via two-reservoir aquifer storage models (see section 6.5). The balance of cumulated outflow from available aquifer models and cumulated water use is equal to mountain-front recharge for the respective time step.

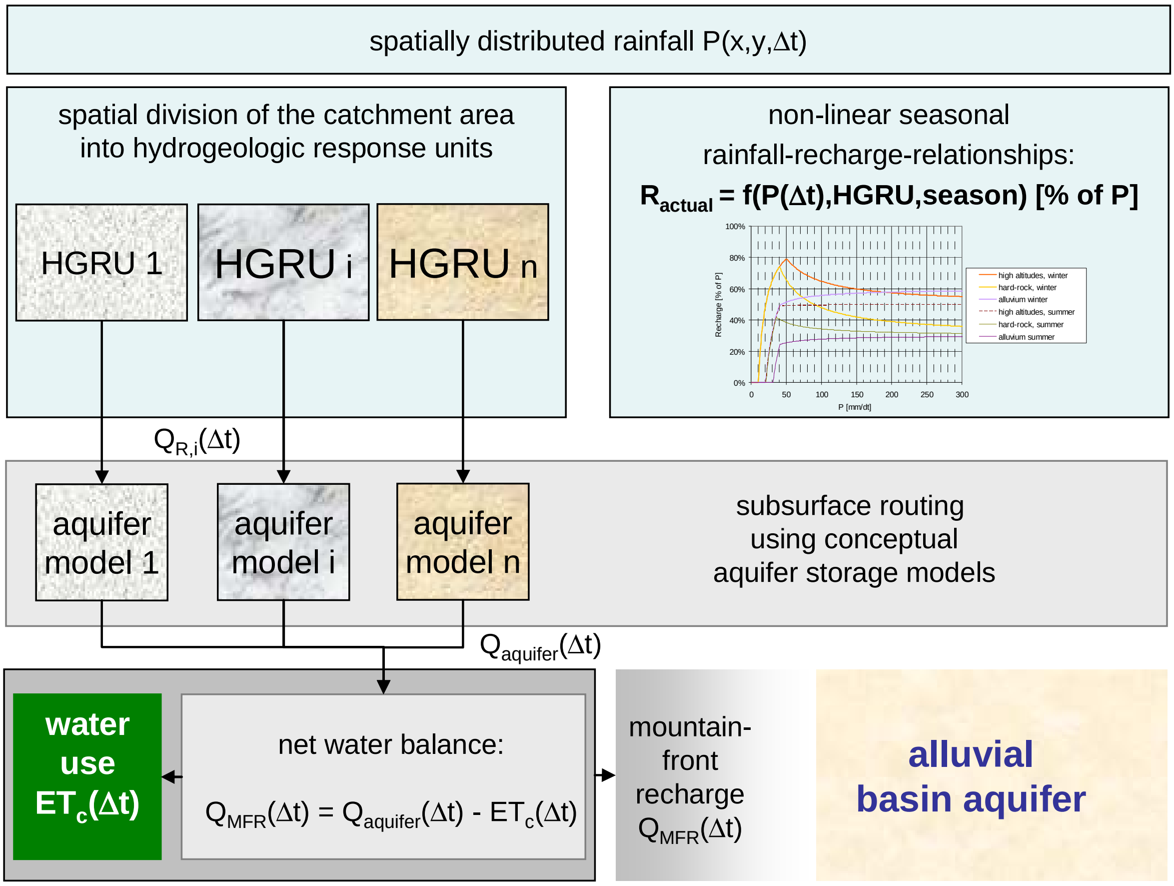


Figure 6.1: A conceptual hydrologic model for time dependent estimates of mountain-front recharge

## 6.3 Calculation procedure using histograms of rainfall depths

In the first instance, the calculations are performed on a monthly basis. As a second step, these values are aggregated to long-term average annual values (LTAs), each separately for every case and over the total of all cases. While the monthly results provide the sought output, the LTAs provide reference values for cross comparison with available reference data to calibrate or validate the rainfall-recharge relationships.

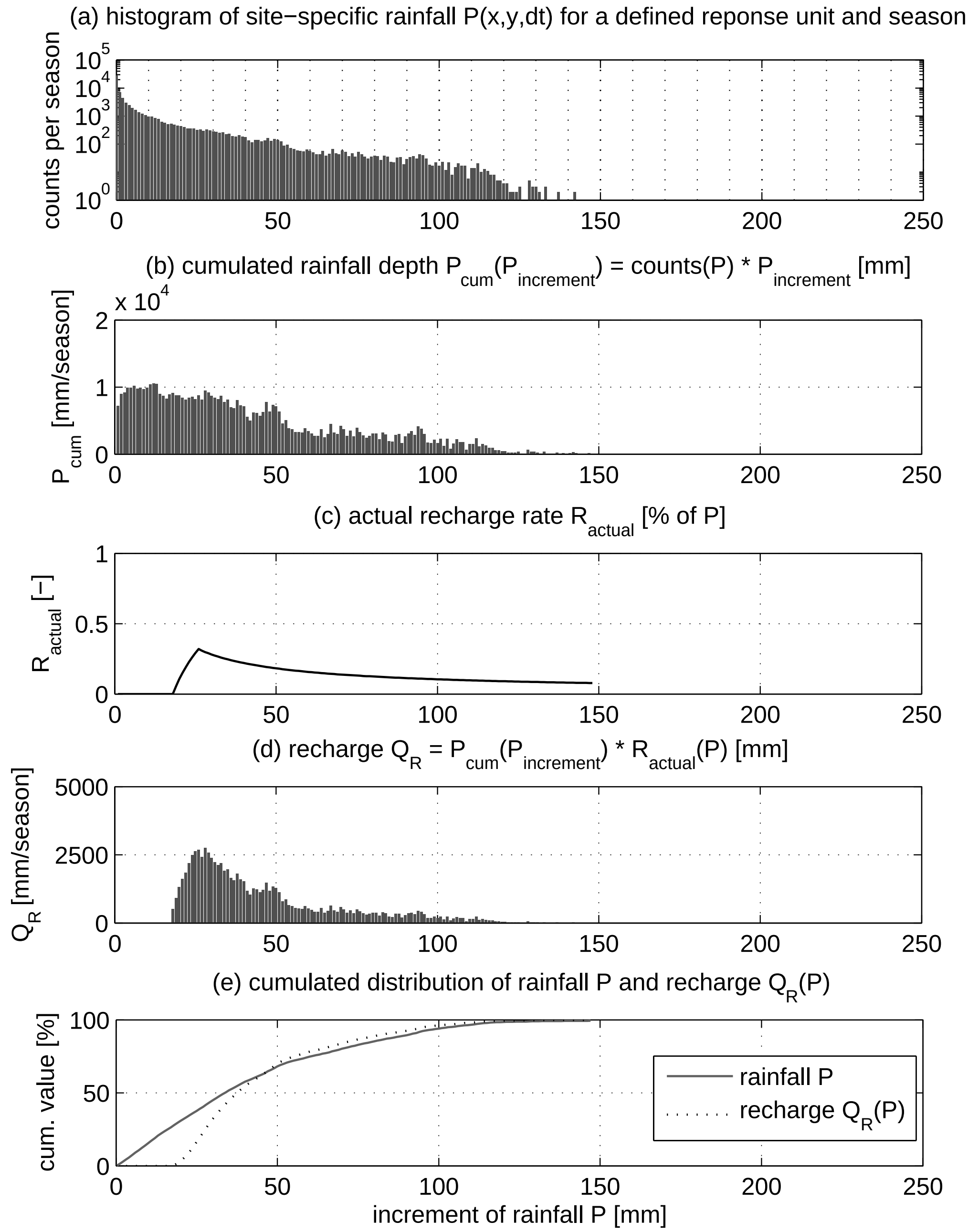


Figure 6.2: Histogram based calculation of recharge as portion of rainfall

The calculation is based on rainfall histograms for the considered spatial and temporal unit. Figure 6.2 shows the histogram based approach for a single case in an exemplary way. The top diagram shows the histogram, i.e. the decreasing counts of each rainfall depth within the respective season and response unit. The following cumulated depth, i.e. the product of rainfall depth and according counts shows, that a lower number of time steps with median rainfall depths (e.g. 50 mm) result, over the whole period, in a similar yield than a huge number of very low rainfall depths per time step. The product of cumulated yield (counts * P) and response function R(P) results, finally, in the estimated amount of recharge per rainfall depth class.

## 6.4 Non-linear seasonal rainfall-recharge relationships

### *6.4.1 Derivation of the rainfall-recharge relationships*

Provided the availability of reference values for the model output, rainfall-recharge relationships can, in principle, be derived empirically. For this purpose, an analytical description of the relationship is necessary. Basically, there are three important components:

sill: a rainfall value $P_{sill}$ below which there is no response at all ($R_{sill} = 0$)

rising limb: the section of the function where the ordinate is rising from $R_{sill}(P_{sill}) = 0$ to a break-point ($P_{break}$, $R_{break}$), where, in general, the sharp rise turns into a more moderate course.

tailing: the further course of the relationship which can be, in principle, a level off, a further rise or a tailing off.

According to section 2.3, an appropriate data base for this approach is rather an exception. Thus, the relationships are derived based on water balance considerations according to the subdivision of precipitation based recharge in Figure 2.3, resulting in the following water balance equation 6.1. In contrast to Figure 2.3, this water balance equation does not distinguish between localised recharge (during runoff concentration) and indirect recharge (during channel routing).

$$P = ET_{surface} + SMR + Q_{R,\,direct} + SMR_{alluvium} + Q_{R,\,indirect} + Q_{wadi} \tag{6.1}$$

| | | | |
|---|---|---|---|
| where | $P$ | = rainfall | [mm/Δt] |
| | $ET_{surface}$ | = surface wetting loss | [mm/Δt] |
| | $SMR$ | = soil moisture replenishment | [mm/Δt] |
| | $Q_{R,\,direct}$ | = direct recharge | [mm/Δt] |
| | $SMR_{alluvium}$ | = soil moisture replenishment in alluvial valleys | [mm/Δt] |
| | $Q_{R,\,indirect}$ | = indirect and localized recharge | [mm/Δt] |
| | $Q_{wadi}$ | = surface runoff at catchments outlet | [mm/Δt] |

Table 6.1 gives information on the physical interpretation of the single balance variables and names approaches for assessment of their potential, i.e. maximal values. The actual values are the result of a water balance accounting scheme according to the respective rainfall input.

Table 6.1: Assessment of water balance components for derivation of non-linear seasonal rainfall-recharge relationships according to Equation 6.1

| Water Balance Component | Physical interpretation | Assessment |
|---|---|---|
| $ET_{surface}$ | surface wetting losses | • potential value initial $loss_{max}$:<br>The surface wetting loss depends especially on surface characteristics; thus, assessment may be based on a literature review on initial losses. Besides, the mean number of events per time step can be considered.<br>• actual value:<br>Min ($P(\Delta t)$, initial $loss_{max}$) |
| *auxiliarily :* Infiltration | water entering the unsaturated zone | • potential value $Inf_{max}$:<br>integral variable based on infiltration rates [mm/h] and rainfall characteristics like (cumulated) event duration and rainfall intensities; infiltration rates can be based on literature review; rainfall characteristics can be estimated based on literature or evaluated based on available data<br>• actual value:<br>$\min(P(\Delta t)\text{-ETsurface}(\Delta t), Inf_{max}(\Delta t))$ |
| SMR | soil moisture replenishment | • potential value SMD (soil moisture deficit):<br>SMD ≤ field capacity FC; SMD is primarily a function of antecedent rainfall and evapotranspiration. Additional factors are soil storage characteristics and vegetation cover<br>• actual value:<br>$\min(\text{Infiltration}(\Delta t); \text{SMD}(\Delta t))$ |
| $Q_{R,\ direct}$ | direct recharge (or effective infiltration) | Balance: $\text{Infiltration}(\Delta t) - \text{SMD}(\Delta t)$ |
| *auxiliarily :* $P_{eff}$ | effective rainfall | Balance: $P(\Delta t) - ET_{surface}(\Delta t) - Q_{R,direct}(\Delta t)$ |
| *auxiliarily :* transm. losses | transmission losses or potential indirect recharge, respectively | n-th root of effective rainfall $P_{eff}(\Delta t)$ |
| $SMR_{alluvium}$ | soil moisture replenishment in alluvial valleys | n-th root of transmission loss |
| $Q_{R,indirect}$ | actual indirect recharge | Balance: transm. losses – $SMR_{alluvium}$ |
| $Q_{wadi}$ | surface runoff | Remainder of the balance equation |

Potential values for initial losses (initial $loss_{max}$) and infiltration ($Inf_{max}$) per time step as well as the soil moisture deficit (SMD) are integral variables representing the long-term average conditions regarding the actual processes in a considered season and response unit. SMD is a surrogate for the actual soil moisture status (antecedent rainfall and evapotranspiration) under given soil characteristics and vegetation cover. Initial losses and infiltration do not only represent morphological characteristics, but also rainfall characteristics like average occurrence, duration and intensity in the respective time step.

This wide-ranging simplification compared to the actual processes is due to the lack of data which would allow the expectation of a gain in accuracy in applying more complex modelling concepts.

In a way, these integral variables are comparable to, for example, the Manning coefficient. In channel hydraulics, this value is often used to cover both, channel roughness and also local head losses between different stations. Eventually, it is an empirical value. In addition, it depends on the actual discharge level. Analogously, the variables mentioned above are related to distinct rainfall characteristics and climatic conditions.

After the estimation of the parameters mentioned in Figure 6.3, a balance for every value of rainfall depth P per time step can be calculated resulting in the total response

$$Q_R = Q_{R,\,direct} + Q_{R,\,indirect} \qquad (6.2)$$

The recharge rate as function of rainfall R(P) [% of P] equals to $Q_R(P)/P$.

The components which are related to runoff generation (initial $loss_{max}$, $Inf_{max}$ and SMD) can be, to a certain degree, substantiated by literature values and evaluation of available rainfall and climate data.

The absolute values of transmission losses are increasing with increasing rainfall. The relative fraction, however, decreases from close to 100 % to low amounts of effective rainfall to rather low portions for erratic high rainfall events. Thus, transmission losses are assumed to be the n-th root of effective rainfall. In the following, this n-value is termed as $n_{transm\ loss}$. Analogously, soil moisture replenishment of alluvial storages is expressed as n-th root of transmission losses. In distinction to $n_{transm\ loss}$, this n-value is termed as $n_{SMR\ alluvium}$.

The water balance considerations are limited to the actual time step. It should not be confused with a continuous soil moisture accounting scheme. An extension to a continuous soil moisture accounting would require an adequate soil moisture module and hence a corresponding number of additional model parameters. This goes beyond the basic idea of this approach, which aims at a minimal number of calibration parameters.

Per default, a time step $\Delta t$ = 1 mon is used. Figure 6.3 shows an example of a non-linear rainfall-recharge-relationship based on a set of parameters (initial $loss_{max}$, $Inf_{max}$, SMD, $n_{transm\ loss}$, $n_{SMR\ alluvium}$).

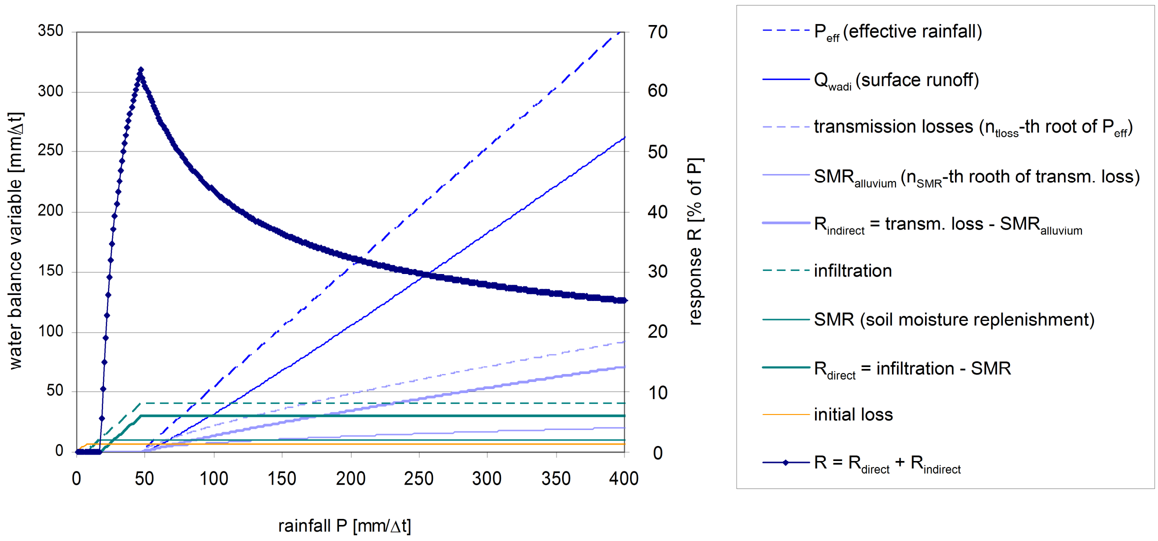


Figure 6.3: Non-linear rainfall-recharge relationship based on water balance considerations ($n_{tloss} = n_{transm\ loss}$; $n_{SMR} = n_{SMR\ alluvium}$)

### *6.4.2 Sensitivity analysis*

With regard to the sensitivity of each variable in this water balance approach, a sensitivity analysis was conducted. It was based on a default value for each variable, resulting in a median response based on the rainfall sample used in the case study application in section 7. Table 6.2 gives an overview on requested variables, their default values and the range of values considered in the frame of the sensitivity analysis.

For evaluation or comparison of the resulting response functions, the following criteria were considered:

- rainfall threshold $P_{sill}$ [mm]: maximum rainfall depth with zero response – indicates impact of low rainfall
- break point: end of the rising limb
    - o rainfall depth of break-point $P_{break}$ [mm]
    - o response at break-point $R_{break}$ [-] - mostly identical with maximal response
- response of maximal considered rainfall depth $R(P_{max})$ [-] – indicating the response for extreme rainfall events
- integral of response function over P $\sum_{P=0}^{P\max} R(P)[-]$ - for (non-weighted) comparison of response functions

- long-term average recharge $R_{LTA}$ [% of P], i.e. response to an actual rainfall sample, weighted according to the histogram of the rainfall sample
  - $R_{LTA}$(whole sample) without consideration of seasons
  - $R_{LTA}$(winter) winter season
  - $R_{LTA}$(summer) summer season

Table 6.2: Parameters for calculation of the response function – default values and considered ranges of values

| parameter | unit | note | default | Range |
|---|---|---|---|---|
| init $loss_{max}$ | mm/Δt | under consideration of literature values on initial losses per event and mean number of rainy days per Δt | 7 | $2 \leq x \leq 12$ |
| $Inf_{max}$ | mm/Δt | under consideration of (final) infiltration rates ($5 \leq x \leq 50$ mm/h), estimated cumulated event duration per Δt and median rainfall intensities | 30<br><br>(variation of SMD: both 30 and 60) | $5 \leq x \leq 115$ |
| SMD | mm | estimates for scattered vegetation on bare rock or shallow soils, respectively | 10 | $0 \leq x \leq 30$ |
| $n_{transm\ loss}$ | [-] | | 1.3 | $1.05 \leq x \leq 1.75$ |
| $n_{SMR\ alluvium}$ | [-] | | 1.5 | $1.00 \leq x \leq 2.25$ |

Appendix A shows different response functions and selected evaluation criteria under variation of the different model parameters. An evaluation in tabular form is part of Table 6.3. Therein, the gradients of the evaluation criteria from lowest to highest value of the actually varied variable were classified according to a statistical evaluation of the 6 gradients for 5 considered parameters. The classes ‘constant’, ‘below median’ and ‘median’ (i.e. arithmetic mean $\leq$ criterion $\leq$ median or reversely) indicate a minor impact of the variable on the respective criterion. The classes ‘above median’ and ‘maximum’, however, show a relatively weighty impact. The red colour in Table 6.3 indicates a decrease of the criterion from lowest to highest value for each considered variable.

Table 6.3: Gradients of different evaluation criteria – based on variation of different variables

| criterion | Δcriterion = criterion(max of parameter) - criterion(min of parameter) | | | | | |
|---|---|---|---|---|---|---|
| | initial loss | infiltration | SMD | | transm. losses | $SMR_{alluvium}$ |
| | | | inf. 30 mm | inf. 60 mm | | |
| $P_{sill}$ | median | < median | **maximum** | **> median** | Constant | |
| $P_{break}$ | > median | **maximum** | constant | | | |
| $R_{break}$ | < median | > median | **maximum** | **> median** | | |
| $R(P_{max})$ | constant | > median | < median | | **maximum** | **> median** |
| integral response | < median | > median | median | < median | **maximum** | < median |
| **$R_{LTA}$** | < median | **> median** | **maximum** | **> median** | < median | < median |

Among all considered criteria, the long-term average response $R_{LTA}$ is considered to be the most important indicator. The variation of SMD results in the widest range of values for $R_{LTA}$. The sensitivity of infiltration is similar to that of SMD. In contrast, it has an impact on the sill value and therefore on the contribution of low rainfall. Infiltration is the one parameter which features a considerable seasonality. $R_{LTA}$ for the winter period is considerably higher than in the summer period due to the different rainfall characteristics. Thus, the model reflects the main drivers of mountain-front recharge (MFR) as mentioned in section 2.1.

The initial losses show a considerably lower impact on $R_{LTA}$. The impact of transmission losses and, last but not least, the storage replenishment in alluvial valleys is even smaller. Their relatively low impact on $R_{LTA}$ is due to the fact, that months with cumulated rainfall above 100 mm are relatively rare in the considered rainfall sample. Thus, the impact of erratic high rainfall events (with often limited spatial extent) on the long-term water balance as a whole is considerably lower compared to prevalent low or median rainfall.

The evaluation criteria show, that transmission losses and $SMR_{alluvium}$ do only influence the tailing of the response function and, consequently, the integral of the response R over rainfall P. Initial losses, infiltration and SMD, however, influence the sill value and the break point. Finally, they influence the shape of the rising limb and consequently the sensitivity to low and median rainfall events. This approach for derivation of the response functions is hence considered to be physically reasonable.

### *6.4.3 Response functions based on extreme parameter sets*

With regard to the robustness or plausibility of the water balance approach for derivation of response functions, worst cases were derived based on rather extreme parameter values. Table 6.4 gives an overview of the investigated assumptions. For clarification, the low sensitive parameter $n_{SMR\ alluvium}$ for soil moisture replenishment in alluvial valleys was set to the default value 1.5.

Table 6.4: Assumptions for Response functions based on extreme parameter sets

| Parameter | extremely low | | extremely high | |
|---|---|---|---|---|
| | assumption | value | assumption | value |
| init $loss_{max}$ | low value per event \| 1 event per month | 3 | high value per event \| > 1 events per month | 15 |
| $Inf_{max}$ | low infiltration rates \| short duration events | 10 | high infiltration rates \| rather long-lasting than short duration events | 100 |
| SMD | low storage capacity \| high antecedent moisture \| hardly any vegetation | 5 | higher storage capacity \| low antecedent moisture \| vegetation perceptible | 50 |
| $n_{transm\ loss}$ | low (i.e. transmission losses relatively high) | 1.10 | high (i.e. transmission losses relatively low) | 1.75 |
| $n_{SMR\ alluvium}$ | low sensitivity, therefore out of consideration; default value 1.5 | | | |

The resulting response functions are shown in Figure 6.4. Values for each resulting long-term average response $R_{LTA}$ for the considered rainfall sample are given in the legends. The upper Figure 6.4 (graph a, functions 1 – 4) is based on a parameterisation, where evaporation losses and infiltration are very low. This is a reasonable scenario for solid, non-fissured rocks or cemented soils. Direct recharge is very low in this case. Thus, surface runoff is high and total recharge highly depends on indirect recharge and, consequently, on hydraulic properties of the alluvial valleys. Even for high relative transmission losses and extremely low soil moisture deficit (SMD), the long-term average response $R_{LTA}$ is below 40 %.

Functions 5 and 6 (graph b) show a low SMD, but very high potential infiltration. This results in high values for $R_{LTA}$ for the rainfall threshold, where P(sill) is very low and the response is very high even to low or median rainfall. It is a reasonable scenario for karst regions or other highly permeable surfaces during the winter season. In this case, the impact of indirect recharge during high rainfall events is secondary compared to high direct recharge based on frequent low or median rainfall. Functions 7 and 8 are based on extremely high infiltration rates and, coincidently, extremely high SMD. This combination can be considered for selected, more developed soils and is therefore outside of the scope of the present study.

The graphs c and d show a very high rainfall threshold P(sill) due to very high initial losses. Consequently, there is hardly any direct recharge based on low rainfall. In the case of low infiltration (graph c), $R_{LTA}$ is below 25 %. Similar to graph a, transmission losses show a high sensitivity. If infiltration is high and SMD is low (functions 13 and 14), there is a considerable response to median rainfall values resulting in $R_{LTA}$ of more than 40 %. It is concluded, that this value is a reasonable lower limit for highly fractured or karstified terrain with less developed or even absent soils.

Similar to functions 7 and 8, the functions 15 and 16 show high infiltration and high soil moisture deficit. Thus, they are outside of the scope of this approach.

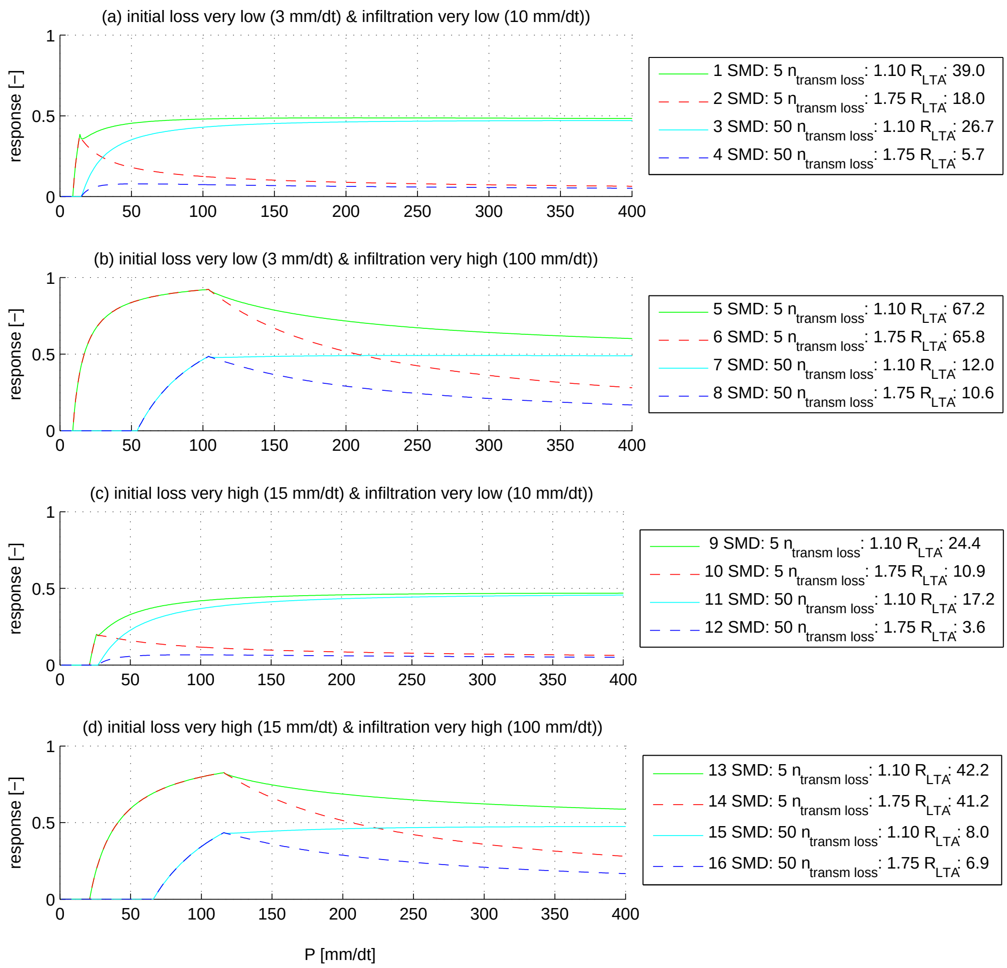


Figure 6.4: Response function based on extreme parameter sets

Table 6.5 summarizes the findings discussed. It may serve as a rough guideline for the practical application of this approach. In general, the water balance approach for derivation of the response functions provides physically plausible results, even for extreme cases. The combination of high infiltration and high soil storage is beyond the scope of this approach. In this case, an appropriate continuous soil moisture accounting is indicated.

Table 6.5: Parametrisation of response functions for distinct conditions based on evaluation of extreme parameter sets

| Hydrogeological setting | | Parameters | | | |
|---|---|---|---|---|---|
| Geo-morphology | rainfall | initial loss | infiltration | soil moisture deficit SMD | transmission losses |
| solid rock or cemented alluvium | short duration | default | very low | secondary | according to actual characteristics and antecedent conditions |
| | lasting | increased | | | |
| high infiltration | short duration | default | increasing with rainfall duration | low to median, according to soil storage characteristics and antecedent moisture conditions | secondary |
| (karst, highly fractured rock) | lasting | increased | | | |
| well-developed soils (out of consideration) | secondary | secondary | high | high | secondary |

## 6.5 Subsurface routing based on linear reservoir models

Based on the approaches discussed in section 2.4, the following models were implemented:

- the serial karst aquifer model according to Király (2002) (see Figure 6.5, right),
- a parallel two-reservoir model, likewise with storages Sl and Sh as well as the distribution factor Rl
- a parallel 2+1 reservoir model similar to Schwarze et al. (1999) with a split-up of the low permeability storage Sl into two parallel storages Sl1 and Sl2. In contrast to Schwarze et al. (1999), distribution of recharge is defined by the factor Rl instead of a constant maximum recharge (see Figure 6.5, left).

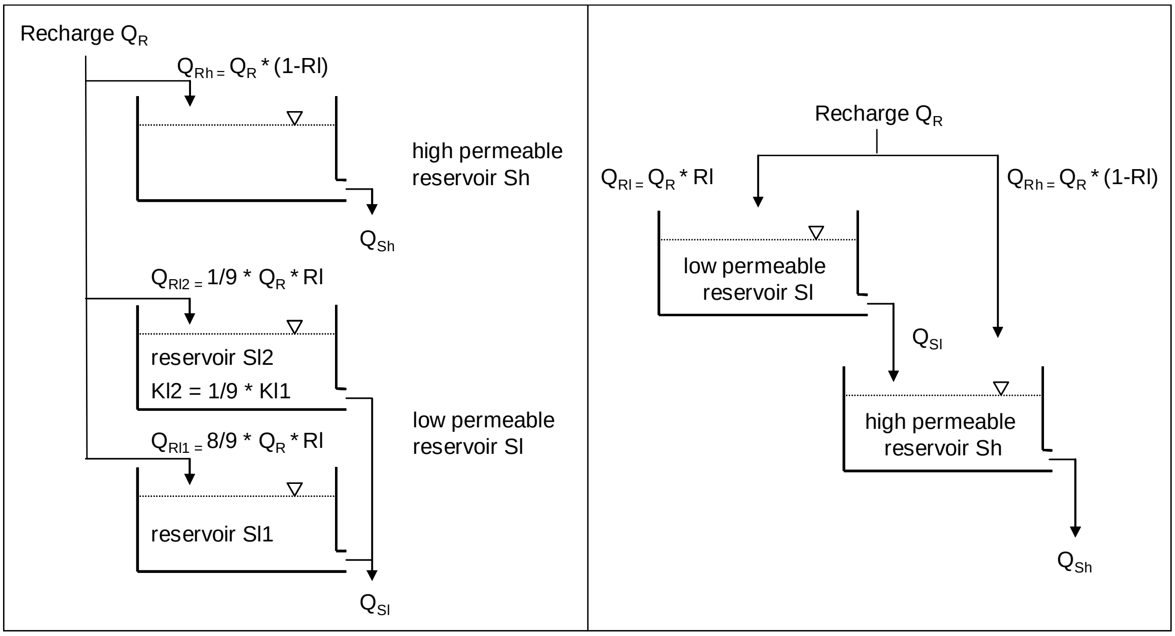


Figure 6.5: Reservoir models for hard rock or karst aquifers; left figure: 2+1 reservoir model similar to Schwarze et al. (1999); right figure: two-reservoir model for karst aquifers acc. to Király (2002)

With regard to the behaviour of the three different approaches or the sensitivity of its parameters, respectively, a sensitivity analysis was conducted based on a synthetical percolation time series. To summarise, it can be stated that for meso scale water balance assessment and a monthly time step, the reservoir constant Kl of the low permeable storage is supposed to be the most important parameter. Although originally proposed especially for karst aquifers, the model of Király (2002) is considered to be a reasonable conceptual model for subsurface routing in karst and other hard rock aquifers in the given context. Consequently, this approach was included in the conceptual hydrologic model as a whole. For the application to lithology classes besides karst, the parameterisation can be based on reference values of Schwarze et al. (1999) or Schwarze (2004).

# 7 Case Study: Groundwater recharge assessment for the Barka Region (Oman)

The eastern Batinah coastal plain is the most densely populated, cultivated and industrialized area in the Sultanate of Oman. Agriculture plays an important role in this region. Most of the farms are located near the coastline and take their water from groundwater resources, such as numerous decentralized and often uncontrolled wells. Thus, high water demands of agriculture require more than 90% of the water resources (Al-Hattaly and Al-Kindy, 2008).

The transition to pumped wells in the 70's and the agricultural expansion since the 70's resulted in a wide-spread salinization due to groundwater depletion along the Batinah coast. This led to landward migration of agricultural zones and accompanying social problems. Consequently, there is an urgent need for a long term perspective in conservation and water management. Weyhenmeyer et al. (2002) point out, that those water management studies conducted in the 80's and 90's did not direct their attention to the interconnection between the groundwater recharge areas in the adjacent mountains and the groundwater abstraction sites in the coastal zone. Only in the end of the 90's, extensive investigations based on geochemistry and isotopy gave a detailed qualitative picture of recharge mechanisms in this system (see section 7.1.5). Moreover, the actually available groundwater resources on the Batinah plain are to a considerable part fossil water which has precipitated during the Pleistocene (Weyhenmeyer et al., 2000).

Although these isotope studies provided detailed qualitative knowledge on recharge source areas and flow paths, even in 2004 an (unpublished) 'Integrated Catchment Management Project' was conducted, where groundwater recharge was linked to the rainfall monitoring stations within the groundwater model domain, i.e. on the coastal plain, far downstream to the source areas of the main portion of recharge to the alluvial aquifer. Consequently, the pressing need for a really Integrated Water Resources Management (IWRM) considering the system in all its complexity is, more than ever, topical. Consequently, a respective approach was proposed by Grundmann et al. (2012). It comprises water resources assessment (WRA), assessment and optimisation of agricultural water use and, finally, an optimal management of the coupled groundwater-agriculture system including consideration of climate change scenarios.

For groundwater management in the coastal zone, a 3D density-dependent model for this task was recently set up by Walther et al. (2012), featuring a relatively high spatial resolution. The assessment of inflow boundary conditions, however, extends over an area of roughly about 1500 km² (see section 5.1). The recharge inducing rainfall-runoff-processes display a fast response to rainfall events, while groundwater recharge in the mountain catchment is subject to storage in the mountain aquifer. Observed spring hydrographs, for example, generally show a response time to rainfall events of about 3 to 6 months. Precipitation, in turn, is subject to cycles with several periods of up to 17-20 years (see section 7.1.4). Thus, water resources assessment has to consider different temporal and spatial scales.

As a basis for water resources assessment within this setting, Figure 7.1 shows a conceptualisation of the water resources system as a whole. In the following, the focus lies on the assessment of mountain-front recharge. Indirect and artificial recharge as well as direct recharge due to precipitation on the plain is addressed in section 7.1.

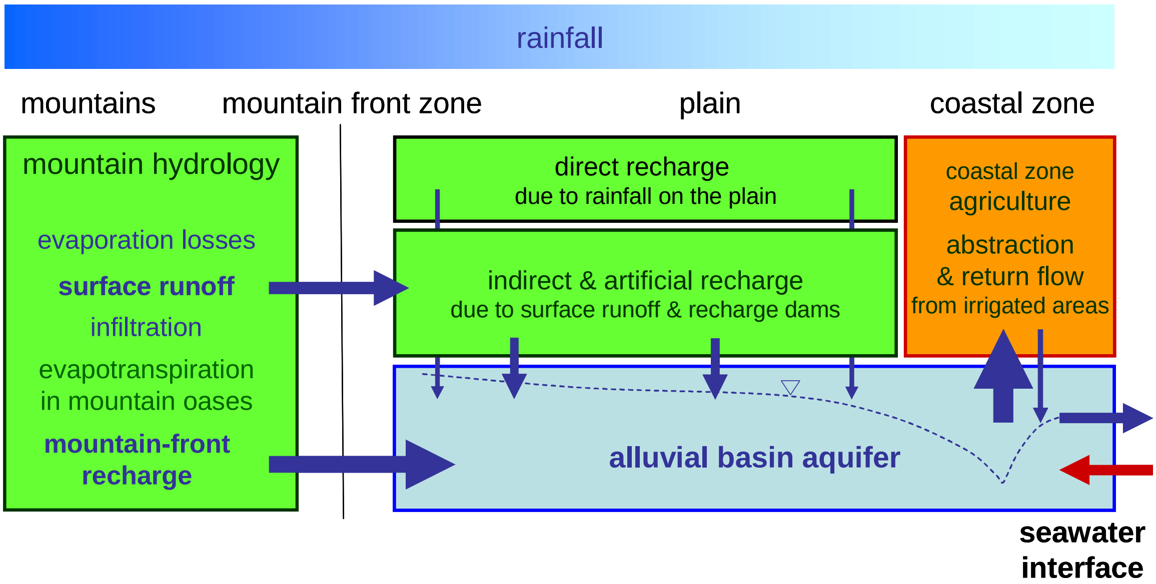


Figure 7.1: Conceptualisation of the water resources system in the study area

Based on the introduction to the study area in section 7.1 and the discussion above, the following conclusions can be drawn with regard to water resources assessment in this setting:

- Portrayal of salinization in the coastal area under temporally varying groundwater abstraction implies the need for transient groundwater management. Groundwater recharge including its temporal and spatial distribution is an important boundary condition.
- Assessment of groundwater recharge has to consider a variety of interacting hydrological processes on different temporal and spatial scales.
- Consideration of climate change scenarios requires prognostic tools to assess groundwater recharge for varying input. Thus, in addition to approaches based on groundwater data which integrate over time and space, reliable, rainfall based estimates are desirable.

Additionally, the study area features data scarcity regarding

- a limited spatial and temporal resolution of available rainfall data compared to the tempo-spatial variability of rainfall-runoff-processes,
- field survey in the mountain catchment (e. g. infiltration characteristics, degree of karstification, storage capacity of the unsaturated zone etc.)
- hydrogeologic survey in the mountain front zone and further downstream towards the groundwater model domain on a flow distance of about 5 km.

## 7.1 Study area

### *7.1.1 Topography*

The case study area is situated in the north of the Sultanate of Oman in the Al-Batinah region. Al-Batinah is a densely populated, roughly 30 km broad coastal plain which extends over 250 km along the coast of the gulf of Oman north-westward of the capital Muscat. The Hajar mountain range (also termed as Oman Mountains) borders to Al-Batinah from the south with peaks up to a height of 3000 m a.s.l.

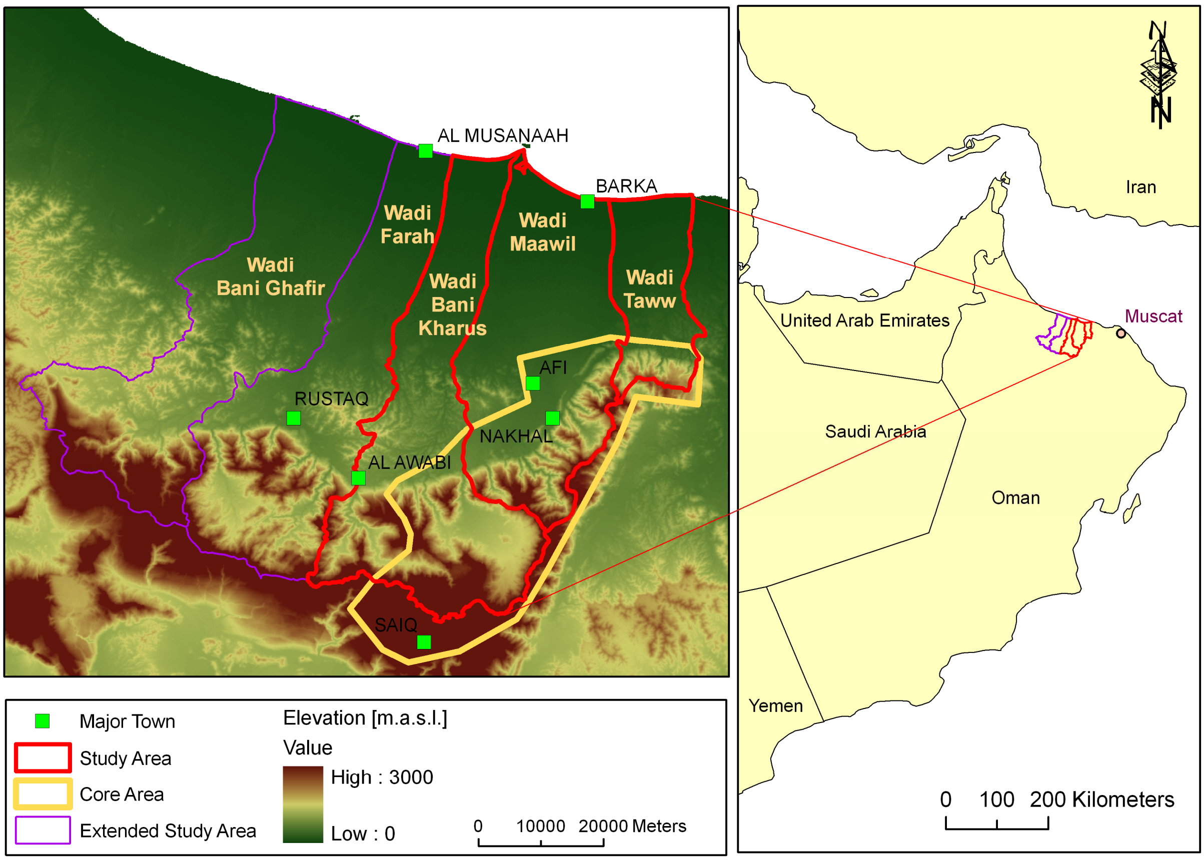


Figure 7.2: The study area

The Barka region itself is located in the south-eastern part of Al-Batinah. Its centre, the city of Barka, is situated approximately 80 km to the west of Muscat. From east to west, it covers the three Wadi catchments Wadi Taww, Wadi Maawil and Wadi Bani Kharus. Their drainage basins (see Figure 7.2) comprise an area of about 2640 km². This area divides up into the plain (about 1500 km²) and the mountainous part. The latter is a part of the Jebel Akhdar mountain chain, which in turn belongs to the central Hajar Mountains.

With regard to the assessment of mountain front recharge, the groundwater basin in the mountainous part is the most relevant entity. Its easternmost limit is clearly defined by a change of the major geological units. The delimitation to the westerly Wadi Farah, however, is not clearly defined. An extended area covering the whole east-west extent of the

Jebel Akhdar area includes in addition the headwaters of Wadi Farah and the most western Wadi Bani Ghafir. Its further division is a matter of investigation. Additionally, the areas south to the drainage divide have to be considered (see section 7.1.5). Thus, as a first approximation, the relevant basin in the mountainous part covers an area of about 1500 km². In the following, it is termed as the core area (see Figure 7.2).

### *7.1.2 Climate*

A subtropical desert climate is prevalent throughout the Sultanate of Oman. It is classified as arid or, in parts, extremely arid (MWR, 1995). Despite the general aridity, greater rainfall in cooler, high altitudes of the study area results in numerous springs and occasional surface water at lower altitudes. Both, natural and irrigated vegetation is present at several locations. Therefore, the mountain chain is termed as Jebel Akhdar, the 'Green Mountain'. Following the classification of MEIGS, Warner (2004) classifies the Hajar mountains as semi-arid.

The Hajar Mountains and the Batinah are encircled in the inter-tropical convergence zone (ITCZ) and the subtropical anticyclonic belt. Both of them cross the northern Oman with seasonal periodicity. As a consequence *‚the 'normal' climatic features are clear, bright skies, light winds, pleasantly warm dry winters and oppressively hot dry summers'* (Stanger, 1986). On the other hand, these circulation patterns result in distinct seasons with regard to prevalent weather systems in different parts of Oman. The up-welling of cold coastal water and cyclones are additional influences to the climate in Oman.

According to MWR (1995), the winter season covers the period from November to April. It is characterised by the *seif* rainfall in the northern part of Oman. This is based on eastward-moving depressions originating over the North Atlantic or the Mediterranean Sea. Additionally, advection of a deep layer of cold air from central Asia to Oman across the Persian Gulf can also bring rainfall in winter, spring and autumn. Often, this is particularly heavy rainfall.

At any time of the year, rainfall can occur as a result of convective rainstorms. Maximum amounts are observed in July and August. Finally, tropical cyclones moving from the Arabian Sea can bring heavy rainfall, especially to the southern and eastern coasts. They have been observed in all months from May to December. At Muscat, this occurs once in ten years on average (MWR, 1995). Recent examples were the extreme events Gonu in June 2007 and Phet in June 2010.

In the study area, the mean annual rainfall varies from 50 – 100 mm in the coastal zone to over 300 mm in the Northern Oman Mountains with wide year-on-year variations. Sustained periods of above-average and below-average rainfall are observed. Consequently, persistence of dry years is considered to be one of the major challenges for effective water resources management (Brook and Sheen, 2000). A further discussion of rainfall characteristics in the study area based on available monitoring data is following in section 7.1.4.

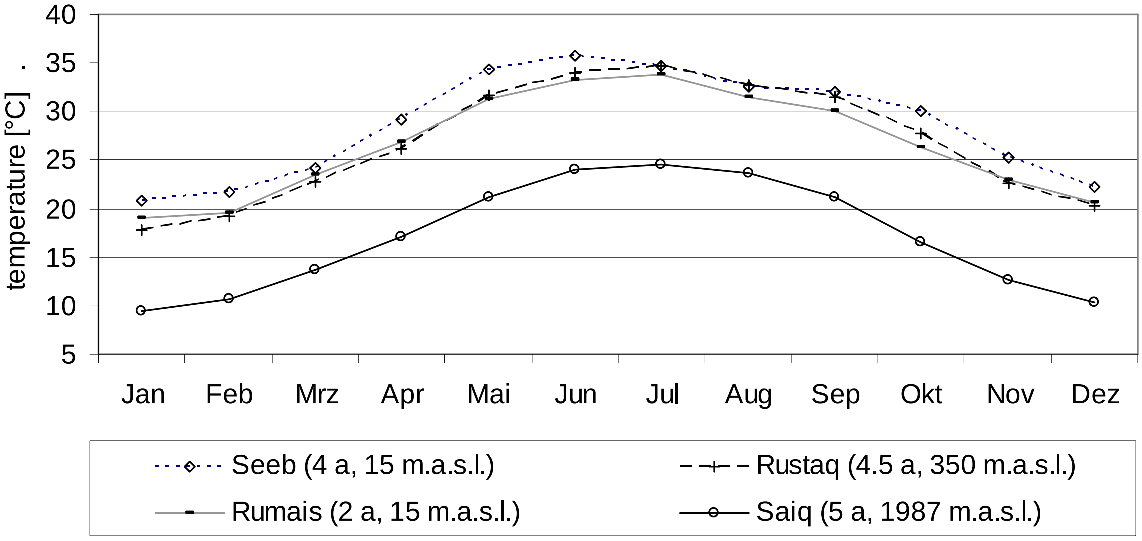


Figure 7.3: Mean monthly temperatures of selected stations in the study area according to Stanger (1986); in brackets: length of observation period and altitude of the station

Mean annual temperatures in the lowlands are typically between 26 °C and 29 °C. The mean diurnal range is between 12 and 15 °C (Stanger, 1986). Figure 7.3 shows mean monthly temperatures for three stations in the study area and the station Seeb about 80 km west to the study area. The length of the observation period and altitude are given in brackets. Despite the difference in altitude, the values of Rustaq (350 m a.s.l.) and the two stations at the coast are similar, which may be due to the higher humidity at the coast. In contrast, the station at Saiq (1950 m a.s.l.) shows a temperature gradient of around 10 °C compared to Rumais. There, a minimum temperature of -3,6 °C was recorded (MAF, 1990). On the Jebel Shams (above 3000 m a.s.l.), snow sometimes occur in winter months (MWR, 1995). Maximum air temperature seldom exceeds 45 °C in the shade. Nevertheless, rock surface temperatures regularly exceed 50 °C during the summer months (Stanger, 1986).

Average relative humidity (R.H.) is about 60 % in the north of Oman with 50 – 90 % in coastal areas (MAF, 1990; MWR, 1995). R.H. is a highly variable climatic parameter with large diurnal variations (Stanger, 1986).

### *7.1.3 Evapotranspiration*

According to MWR (1995), 2100 mm/a is a fist value for the potential evapotranspiration (ETP) in the Al Batinah region with reduced values at the coast due to higher humidity. In the interior region, ETP is supposed to reach values of 3000 mm/a (MWR, 1995). Stanger (1986) addresses the large range of potential values for pan evaporation according to the geographical site and, not least, to the exposure (see Figure 7.4).

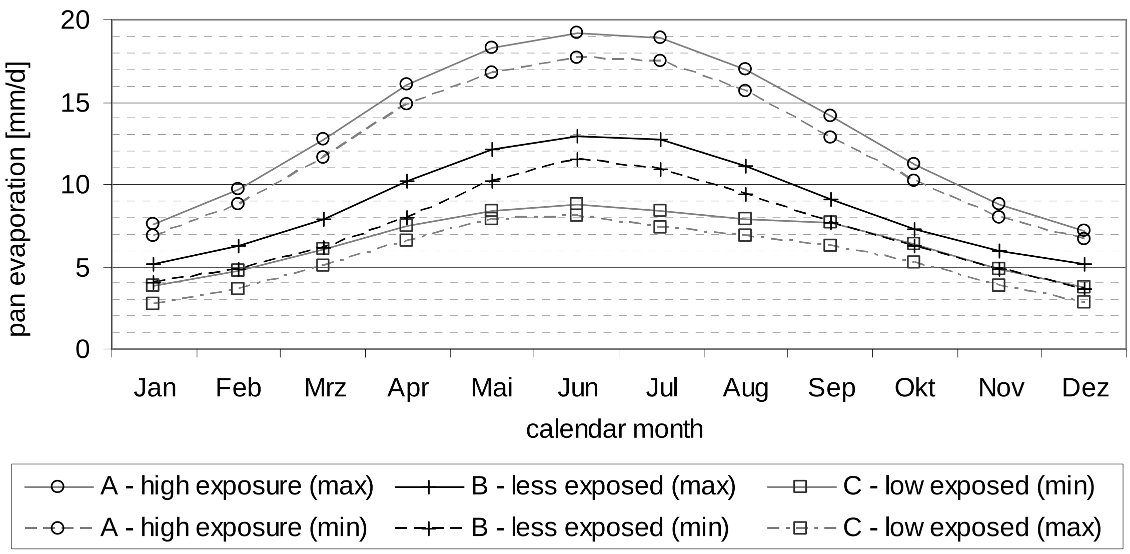


Figure 7.4: Comparative open pan evaporation from different environments in Oman after Stanger (1986); A: high exposure (foothills, coastal and interior plains); B: less exposed low altitude mountain and coastal areas; C: foothill cultivated areas of low exposure and high altitude mountains (above 2000 m a.s.l.)

Siebert et al. (2007) collected climate data over a period of 2 years in the Mountain Oases at Balad Seet (996 m a.s.l.). Based on the Penman-Monteith approach, they estimated the reference evapotranspiration $ET_0$ as a basis to assess crop water use. Table 7.1 provides a compilation of values for different locations in the study area. Apparently, the values at Balad Seet are below those of Saiq, although the oasis lies around 800 m lower than Saiq. This can be due to the different influences in addition to air temperature as a function of altitude like insolation, wind, humidity etc. In order to check the plausibility of the values in Table 7.1, they were compared with the pan evaporation given in Figure 7.4, which was multiplied by the pan coefficient $K_P$. The latter depends on pan site and environment as well as the levels of mean relative humidity and wind speed (Allen et al., 1998). Accordingly, the annual sum for Balad Seet is corresponding to a cropped site in a less exposed altitude area (class B). The higher value for Saiq indicates a higher exposure (between class A and B) which can be due to the unshielded location on a plateau. Rustaq, located at the foothills, can be classified into class A (high exposure) assuming a medium humidity. In summary, the values in Table 7.1 give reasonable estimates for potential evapotranspiration in the mountainous part of the study area.

Table 7.1: Reference evapotranspiration ET0 at different sites in the study area

| calendar month | Saiq (1950 m a.s.l) (MWR, 1996) | Balad Seet (996 m a.s.l) (Siebert et al., 2007) | Rustaq (340 m a.s.l) (MWR, 1996) |
|---|---|---|---|
| Jan | 86 | 88 | 108 |
| Feb | 95 | 101 | 123 |
| Mrz | 142 | 137 | 195 |
| Apr | 194 | 170 | 231 |
| Mai | 222 | 202 | 274 |
| Jun | 217 | 208 | 271 |
| Jul | 221 | 200 | 262 |
| Aug | 220 | 189 | 270 |
| Sep | 193 | 157 | 266 |
| Okt | 161 | 141 | 192 |
| Nov | 106 | 99 | 149 |
| Dez | 90 | 84 | 126 |
| Mean annual sum | **1947** | **1776** | **2466** |

### *7.1.4 Rainfall characteristics*

Rainfall observations in Oman started in 1884 at Muscat (Kwarteng et al., 2009). In the South Batinah, records are available since 1974 (station at Rustaq). From this time onwards, the monitoring network has been extended successively (see Figure 7.5). The mean density in the core area is currently around 1 station per 60 km². The monitoring stations are designed according to the World Meteorological Organization (WMO) standards for an arid region. Over time, standard daily gauges were replaced by automatic recorders.

The maintenance of the monitoring network in the mountainous terrain is challenging. For example, between 2001 and 2007, three stations at altitudes around 2000 m a.s.l. where mostly out of service due to a lack of maintenance. So, both the network and the records of available stations exhibit considerable gaps in the mountainous part of the study area.

Additionally, there is a lack of stations in the altitude range 1000 to 2000 m a.s.l. and 2200 to 3000 m a.s.l. This affects especially the slopes of the mountain range and the consideration of physiographic factors of rainfall occurrence like gradient, aspect, exposure and, above all, position relative to upwind higher relief ("barrier effect").

The significance of often used altitude-rainfall relationships is limited for this reason. Stanger (1986) assumed, that they are not necessarily linear, but that there is a maximum on summer dominated rainfall data at about 1500 m a.s.l. and one which is based on winter dominated rainfall data at ca. 2000 to 2200 m a.s.l. In order to check this assumption, the correlation between altitude and recharge was investigated again in the frame of this work, based on a meanwhile extended data base. For this purpose, 53 stations over the whole Jebel Akhdar mountain range including available stations in the high altitudes south to the drainage divide were considered in the period from 1984 to 2007. With regard to different rainfall mechanisms in distinct seasons, it was distinguished between annual and seasonal values in deriving altitude-rainfall relationships (see Figure 7.6).

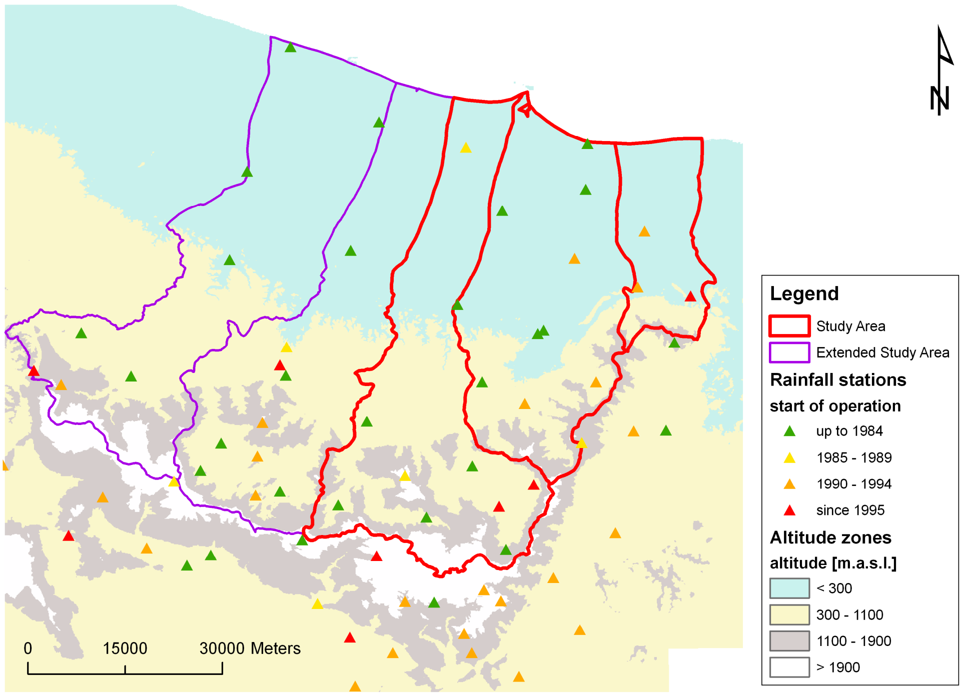


Figure 7.5: Rainfall monitoring network – classified according to start of operation

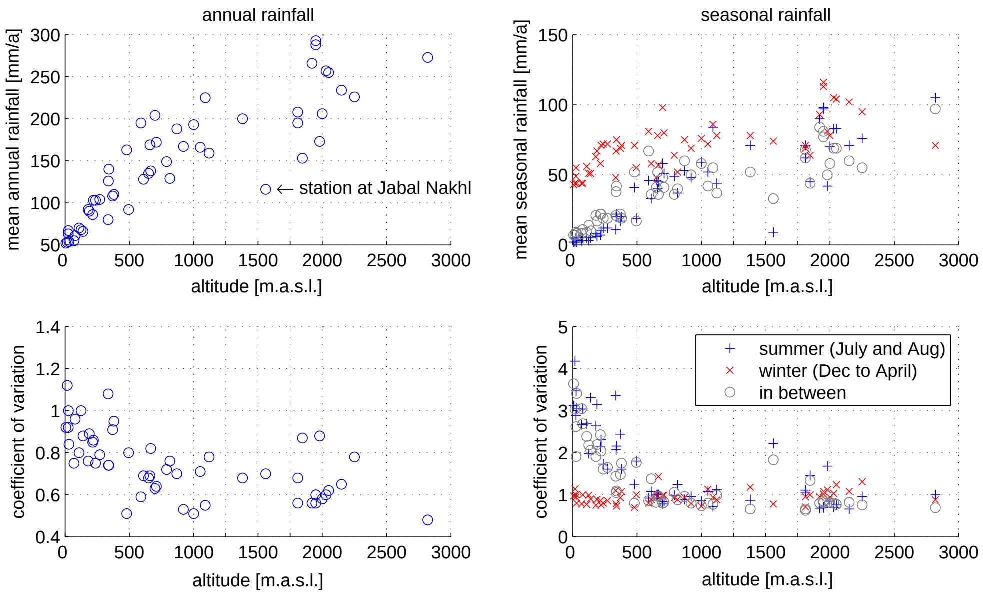


Figure 7.6: Altitude-rainfall relationships based on available monitoring data (period 1984 –2007); left side: mean annual rainfall; right side: mean seasonal rainfall; upper row: rainfall values; lower row: coefficient of variation

The winter season covers the *seif* rain season from December to April, while the summer season is limited to July and August. The consideration of the periods outside of the summer and winter season is an attempt to investigate, in how far the tropical cyclones find expression in the altitude-rainfall-relationship. In the following, this period is termed in-between season. Though, tropical cyclones can also occur in the winter or summer season.

The station at Jabal Nakhl (1560 m a.s.l.) appears to be an outlier. This is obvious in the annual data (upper left graph) and even more clear in the data for the summer season (upper right diagram). Indeed, the available time series features zero values in periods, where considerable rainfall was observed at adjacent stations. A similar case is the winter season for the station at Jebel Shams (2820 m a.s.l.). In this case, the time series features a zero value for an extreme event in March 1997 with more than 300 mm at adjacent stations.

Obviously, the altitude-rainfall relationships of summer and in-between season feature a more or less similar shape. The plot for the winter season, however, differs considerably. While a significant rise of average rainfall with altitude can be observed for the summer season, originating in very low amounts at sea level, the relationship in the winter season is more equable. Between 500 and 1500 m.a.s.l, there is a more or less constant long-term average value of around 80 mm. Only in altitudes of 2000 to 2250 m a.s.l., there are considerably higher values at a number of stations. While the latter confirms the maximum of winter rainfall described by Stanger (1986), the assumption of a summer dominated rainfall at about 1500 m a.s.l. cannot be confirmed based on the presented data.

Similar to the rainfall amounts, the coefficient of variation is low for the winter season. Thus, winter rainfall is relatively stable both in occurrence and amounts. Summer rainfall, however, shows a high variability, especially in the low altitudes. Here, no or very low rainfall is the normal case. Only occasionally, tropical cyclones cause severe rainfall. In the mid and high altitudes, the coefficient of variation is lower due to more frequent convective rainstorms.

Long-term mean annual rainfall in the core area is about 162 mm/a (period from 1984 to 2007). Saiq (1950 m a.s.l.) shows a maximum value of 330 mm/a. The maximum observed annual value at this station was 871 mm in 1997. 386 mm were recorded in March alone. The yearly average of the station Barka (near Barka), is only around 54 mm (in 1984-2004).

Table 7.2 shows the number of rainy days and their seasonal distribution for 53 stations mentioned above in the extended study area. With regard to the assessment approach presented in section 4, not only the whole period was evaluated, but also subsets under exclusion of months without any observed rainfall. Here, the number of rainy days per month is roughly twice of the whole period of time. It is concluded, that the mean number of rainy days over the whole area is similar in the winter and summer season. Though, the variability among the different stations is 2 to 3 times higher in summer than in winter. The station at Jebel Shams (2820 m a.s.l.), for example, shows a maximum value of 5 rainy days on average during July and August compared to a mean value of 1.6 (July) or 1.8 (August). In March, there are 3 rainy days compared to an overall mean of stations of 1.6 days. Moreover, the relationship between altitude and mean number of rainy days (Figure 7.7) shows the same characteristics as the relationship between altitude and rainfall amounts and their coefficient of variation (Figure 7.6). Thus, in winter, independent of altitude a number of rainy days between one and two days (or 2 to 4 days in months where rainfall occurs actually) is a suitable assumption over the whole study area. In summer, however, this number is increasing considerably with altitude.

Table 7.2: Number of rainy days based on 53 rainfall stations in the extended study area (period 1984 - 2007)

| calendar month | | 1 | **2** | **3** | 4 | 5 | 6 | **7** | **8** | 9 | 10 | 11 | 12 |
|---|---|---|---|---|---|---|---|---|---|---|---|---|---|
| whole period | mean value | 1.0 | **1.5** | **1.6** | 1.2 | 0.7 | 1.0 | **1.8** | **1.6** | 1.0 | 0.7 | 0.6 | 1.0 |
| | standard dev. | 0.4 | **0.5** | **0.5** | 0.6 | 0.6 | 0.8 | **1.4** | **1.6** | 1.0 | 0.5 | 0.3 | 0.4 |
| | Maximum | 1.9 | **2.6** | **3.0** | 2.7 | 2.2 | 3.0 | **5.0** | **5.2** | 3.0 | 1.9 | 1.3 | 2.4 |
| months with observed rainfall only | mean value | 2.4 | **3.0** | **2.7** | 2.2 | 1.5 | 1.8 | **2.8** | **2.5** | 1.6 | 2.1 | 2.0 | 2.1 |
| | standard dev. | 0.7 | **0.7** | **0.7** | 0.6 | 0.9 | 0.9 | **1.3** | **1.6** | 1.1 | 0.8 | 0.7 | 0.4 |
| | Maximum | 4.3 | **5.0** | **5.1** | 3.7 | 3.5 | 3.3 | **5.3** | **6.0** | 3.8 | 4.0 | 3.8 | 3.0 |

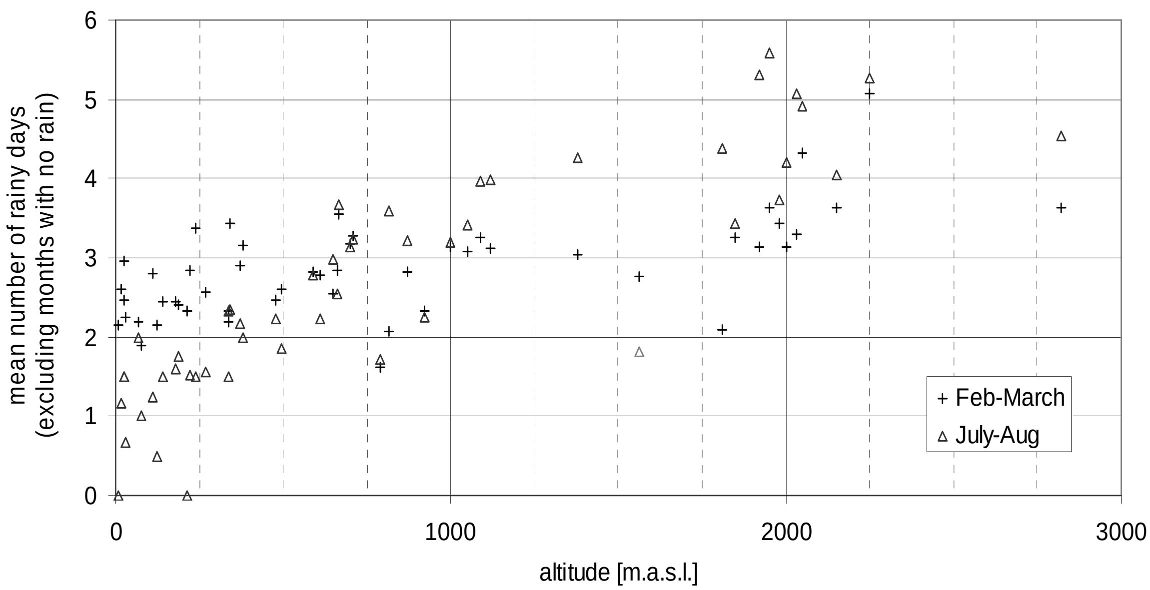


Figure 7.7: Relationships between altitude and number of rainy days (February-March compared to July-August)

Duration and temporal distribution of rainstorms in the study area was investigated by Al-Rawas and Valeo (2009) based on 2042 rainstorms at different stations. It has to be mentioned, that stations above an altitude of 1800 m a.s.l. were not included. Table 7.3 shows rainfall duration classes and their relative proportion of the total number of events. In general, all storm events showed a very high intensity at the beginning of the storm. Mountainous region and plain did not show differences in duration or temporal distribution of rainstorms.

Table 7.3: Typical duration of rainstorms according to Al-Rawas and Valeo (2009)

| duration | ≤ 2 h | 2 to 6 h | 6 to 24 h | 24 – 48 h |
|---|---|---|---|---|
| relative proportion of total number of events | 30 % | 19 % | 25 % | 26 % |
| rainfall mechanism | predominantly convective rainstorms | | various | |

Figure 7.8 shows mean monthly rainfall amounts for the core area. They correspond to 80 mm for the winter months (November to April) and 81.7 mm for the summer months (May to October). Histograms based on a 1 x 1 km raster for winter and summer half years are presented in Figure 7.9. They are based on regionalised monthly data. External drift kriging (EDK) according to Bárdossy (1997) has been used to regionalise station data. In winter and summer, 75 % of the rainfall yield is based on rainfall depths up to 75 mm per month. Extremely high rainfall occasionally occurred in March (in 1997), in the month of June (e.g. tropical cyclone Gonu in 2007) and in July.

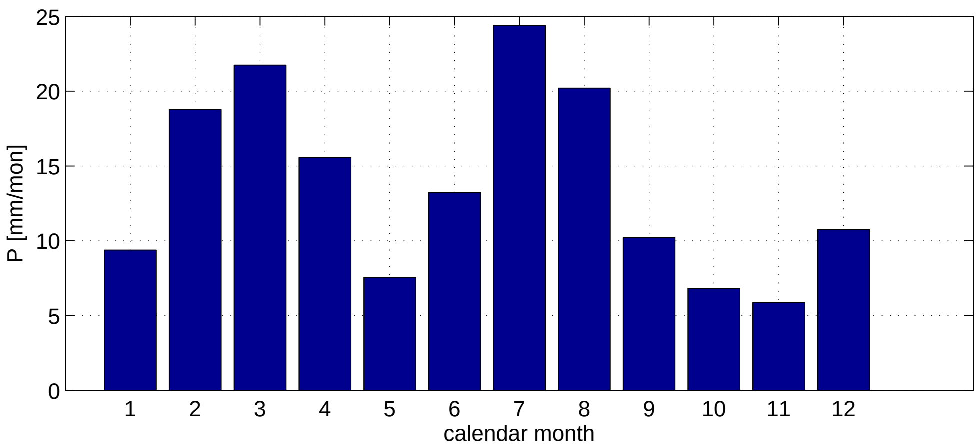


Figure 7.8: Mean monthly rainfall for the core area (1984 –2007) derived from regionalised data

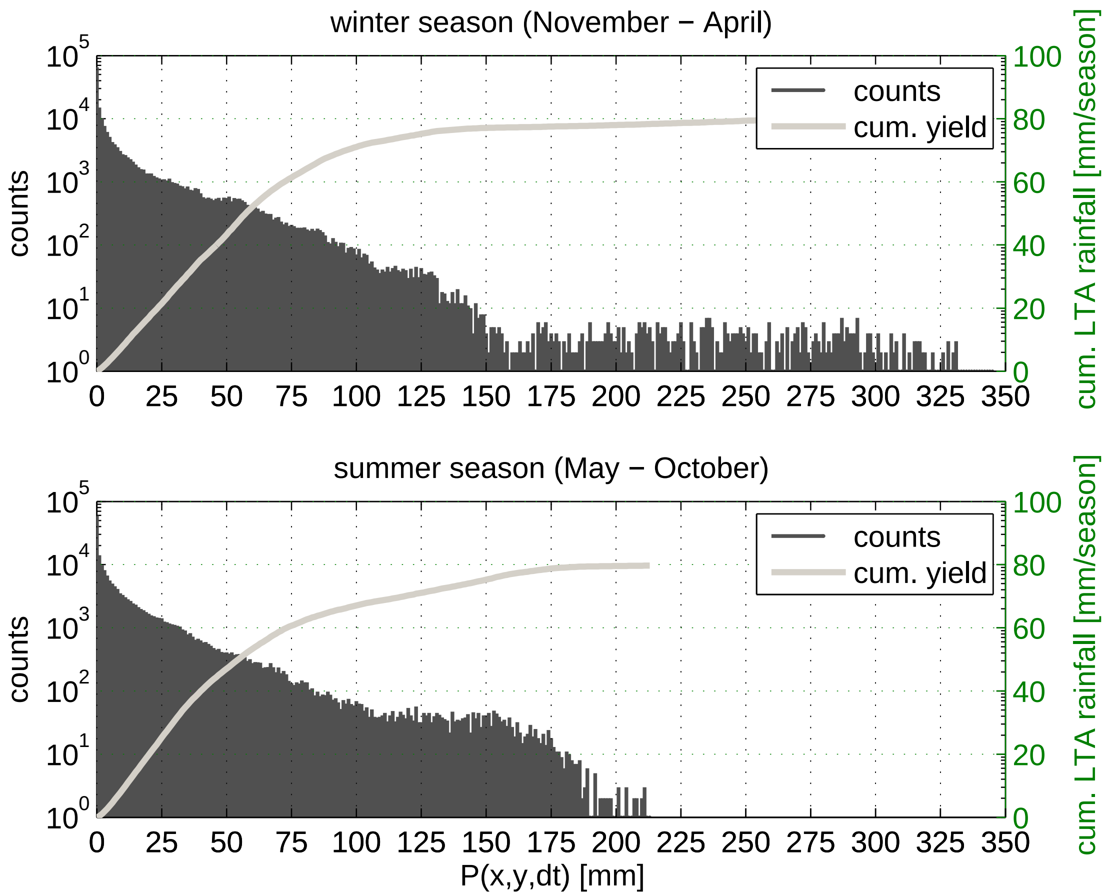


Figure 7.9: Histograms of regionalised monthly rainfall (cell size 1 x 1 km) for the core area (period 1984 - 2007)

Based on the isotopy of rainfall samples collected between 1995 and 1998, Weyhenmeyer et al. (2002) derived two local meteoric water lines. The northern/northwestern vapour source (LMWL-N) represents Mediterranean frontal systems and orographic rainfall. The southern/southeastern source (LMWL-S) indicates Indian Ocean cyclones and tropical depressions. The latter is similar to the global meteoric water line (GMWL), while the first is similar to those which were derived for Bahrain and Southwest of Israel. Compared to the GMWL, they feature a reduced slope which is typical for arid zones.

Brook and Sheen (2000) investigated cyclicity of rainfall. For the station at Muscat (1895-1995), they detected a 5-year cycle which explains 15.6 % of the variance, a 17.7 year cycle (12.2 %), a 6.3 year cycle(6.7 %) and a 10.2 year cycle (3.1 %). The 17.7 year and the 6.3 year cycles are correlated with the Southern Oscillation (SO). Accordingly, Figure 7.10 shows annual values for the mountainous part of the study area as well as an analytical approximation based on harmonic analysis. The analytical function is based on unsmoothed annual values from 1974 to 2009. For gap filling before 1984, a linear regression between the average of little available station data and areal precipitation based on regionalised data for the core area has been used. The analytical function is based on the following equation:

$$
\begin{aligned}
y &= a0 + a1 * \cos(2 * \Pi * \frac{x}{c1}) + b1 * \sin(2 * \Pi * \frac{x}{c1}) \\
&........ + a2 * \cos(2 * \Pi * \frac{x}{c2}) + b2 * \sin(2 * \Pi * \frac{x}{c2}) \\
&........ + a3 * \cos(2 * \Pi * \frac{x}{c3}) + b3 * \sin(2 * \Pi * \frac{x}{c3}) \\
&........ + a4 * \cos(2 * \Pi * \frac{x}{c4}) + b4 * \sin(2 * \Pi * \frac{x}{c4})
\end{aligned} \tag{7.1}
$$

Approximated periods were c1 = 5 a, c2 = 7.3 a, c3 = 9.7 a and c4 = 18.7 a (with $R^2 = 0.658$ and a RMSE of 69.1). An approximation of monthly values (moving average over 23 months) resulted in similar characteristics (c1 = 2.5 a, c2 = 7.4 a, c3 = 9.6 a and c4 = 18.9 a with $R^2 = 0.752$ and a RMSE of 3.34). In this case, however, the fit of the monthly data includes not a 5 year cycle but a 2.5 year cycle instead.

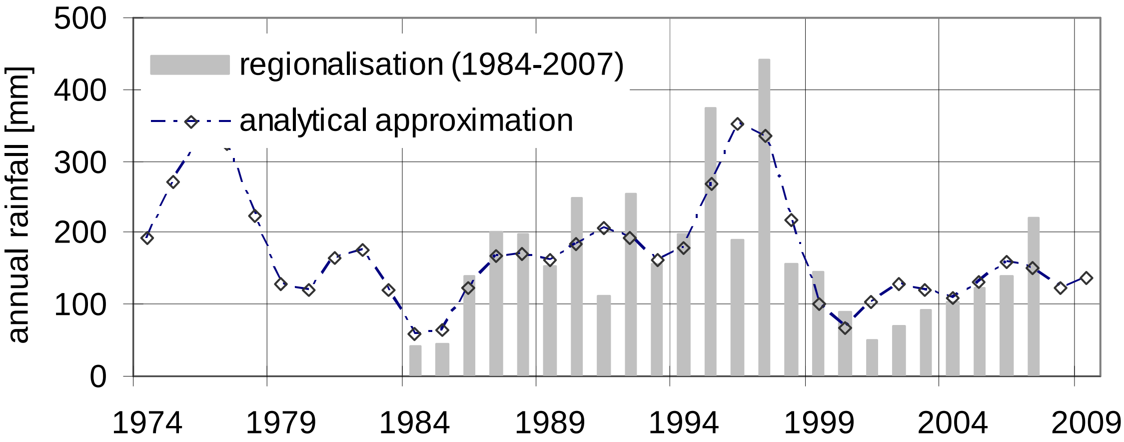


Figure 7.10: Annual rainfall in the core area based on regionalised data and analytical approximation based on harmonic analysis

The area wide assessment of rainfall measurement errors is limited by availability of necessary climate data and detailed information on exposure or surrounding of monitoring stations. Based on selected climate stations and sensitivity analyses, Gebremichael (2010) concluded that bias adjustment increased the gauge-measured rainfall in the study area as a whole by less than 10%. The gauge measured annual rainfall increased 3.5 - 14% of the gauge measured yearly totals.

### *7.1.5 Geology and Hydrogeology*

The geology of the Hajar Mountains was extensively investigated by Glennie (1974). Additional information can be found in (MWR, 1996; Stanger, 1986; Weyhenmeyer et al., 2000). Figure 7.11 shows the prevalent geological units in the study area. They can be also regarded as hydrostratigraphic units.

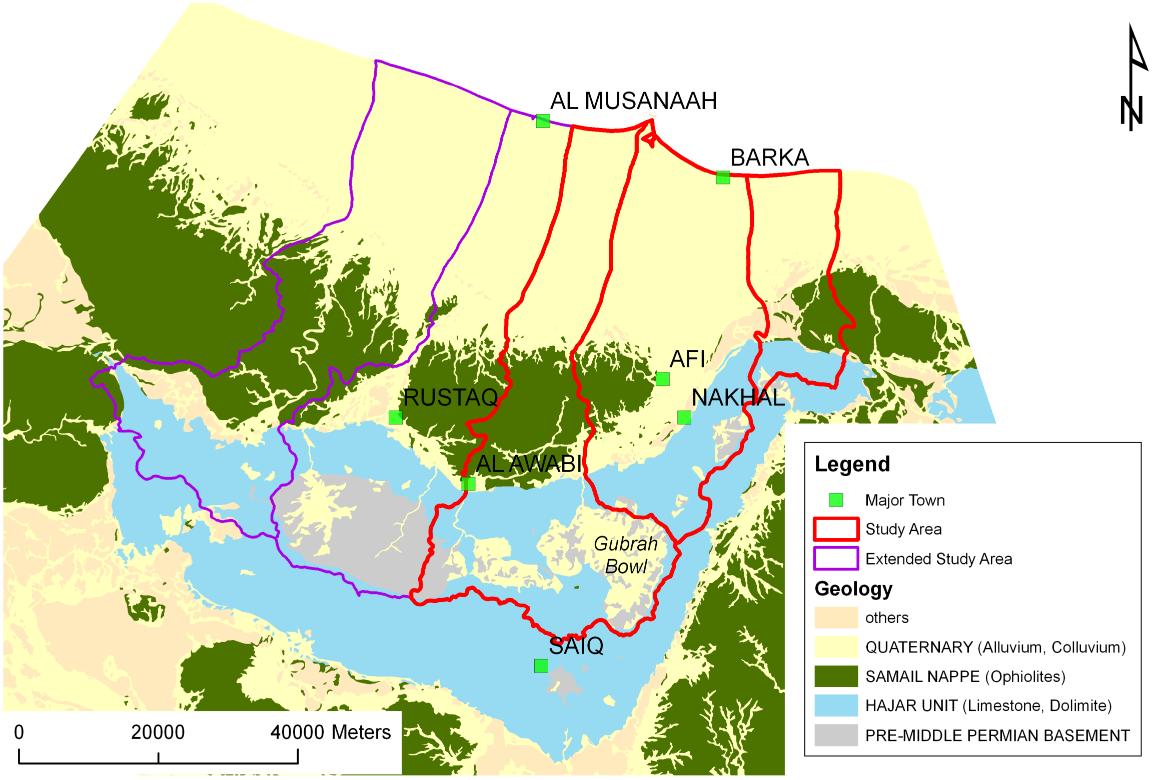


Figure 7.11: Prevalent geological units based on the Geological Map 1:250.000 (sheet NF4003-Seeb)

The extent of the Jebel Akhdar is more or less equal to the spreading of the Hajar Unit. It consists of a large anticline rising up to 3000 m. Its eastern extremity is termed as the Jebel Nakhl, according to the nearby town of the same name. The highest peak, the Jebel Shams, lies within Wadi Bani Ghafir in the western part of the mountain chain. A schematic section of the anticline is provided in Figure 7.12.

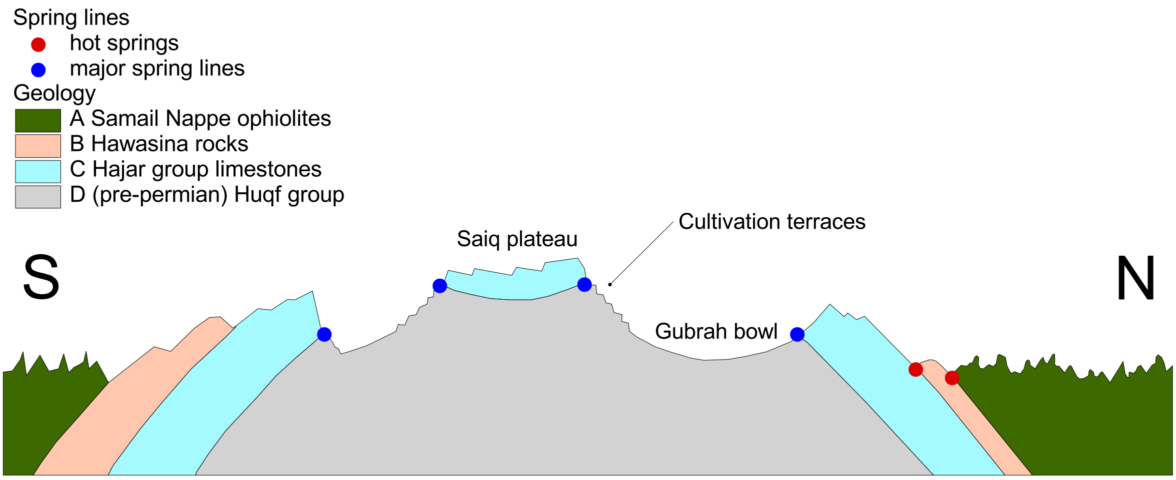


Figure 7.12: Spring lines of the Jebel Akhdar, modified after MWR (1995) (not to scale)

The core of the anticline consists mainly of highly fractured and faulted pre-Permian silt-stone and limestone formations (phyllite, shales, calcite and dolomite) and thin sandstone layers. It is exposed around several topographically low bowls or tectonic windows. To some extent, alluvial deposits cover the pre-Permian formations. An example is the Gubrah Bowl (Wadi Mistal), between the cities of Saiq and Nakhal. According to Stanger (1986), the occurrence of springs along the contact between the pre-Permian unit and the overlying Hajar unit and the absence of springs with significant discharge within the per-Permian unit indicate a lower permeability and restricted aquifer capabilities of these rocks.

The Hajar Unit, which forms the limb of the anticline, is dominated by limestone and dolomite. These carbonates are highly fractured and karst features are found throughout most sequences. Numerous springs indicate significant, well constraint groundwater circulation (Weyhenmeyer et al., 2000). Figure 7.12 shows the major spring lines in the study area. The piedmont springs (in Figure 7.12 indicated as hot springs) occur at relatively low altitude but at a high stratigraphic horizon. They are sparsely distributed, often thermal and yield generally in large, stable discharges. Examples are Rustaq Hammam (82 ± 20 l/s) or Nakhl Thowara (40 l/s). The high level springs, however, show a low stratigraphic level, invariably cold water temperatures of about 25 °C, and low discharges. Spring discharges exceed values of 10 l/s only for short periods after rainfall (Stanger, 1986).

Weyhenmeyer (2000) refers to the large regional differences in the groundwater table of several hundred meters, suggesting that the productive fracture zones are not effectively hydraulically connected. The heterogeneity of the aquifer is also mentioned by MWR (1996). Stanger (1986) points out the widespread immature karstic development, which results, for example, in the locally impervious nature of the more massive beds. Weyhenmeyer et al. (2002), however, state that wells and springs along the piedmont towards the northern Batinah plain show tritium activities close to rainwater values which suggest rapid infiltration and groundwater circulation through the karstified pre-Permian and Mesozoic limestone and dolomite formations to the base of the Jebel Akhdar mountain.

North to the Hajar unit, between Rustaq in the west and Afi in the east, the so called Frontal Mountains stretch out. This low-lying mountain range is composed of the Samail Nappe Ophiolites, a sequence of mid-Cretaceous ophiolitic rocks. According to Glennie (1974), these rocks are one of the world’s largest and best exposed examples of an oceanic crustal and upper mantle sequence. Until recent years, the Ophiolite was assumed to be an aquitard and groundwater flow was believed to be confined to the thin (< 30 m) alluvial deposits overlying the ophilite (Stanger, 1986). Based on strontium isotope ratios, Weyhenmeyer (2000) concluded that groundwater circulation takes place in the magnesite and calcite lined fractures found throughout the Samail Ophiolite.

Besides the adjacent alluvial aquifer on the Batinah plain, quarternary alluvium appears in often narrow valley floors, for example in Wadi Bani Kharus upstream to the city of Al Awabi. Moreover, more widespread alluvial deposits crop out within the spreading of the pre-Permian formations (see above) and in Wadi Maawil easterly to the ophiolitic Frontal Mountains, around the cities of Nakhl and Afi. According to Stanger (1986), erosion products from the Hajar Super Group massifs make a major contribution to the mostly coarse grained piedmont wadi systems.

Relatively little substantial information is available on the properties of these alluvial deposits. The Ministry of Water Resources and Rural Municipalities (MRMWR) provided data on the thickness of the alluvium at around 10 available scattered boreholes. In some cases (e.g. south to Al Awabi), relatively thick deposits (> 45 m below surface), which are partly close to rather shallow ones (< 27 m.b.s.) make it difficult to derive reliable and representative conclusions. The occurrence of base flow over several months at the gauge near Afi after wet periods, implies a considerable local groundwater storage capacity in this area.

Shifting channels due to sporadic changes in the balance between erosion and deposition and other morphological processes resulted in an unusual configuration in which surface flow from Wadi Mistal breaks to the ophiolites merging with the main Wadi Bani Kharus, while subsurface flow appears to drain through the former alluvial fan into the Wadi Maawil (Stanger, 1986).

The Batinah plain is by far the most important aquifer of the region (Macumber, 2003; Stanger, 1985; Stanger, 1986). It consists of adjacent, but differentiable alluvial fans. Due to the coalescence of tributaries, the lateral catchment divides are indistinct. Wadi Al Farah and Wadi Maawil are the two major wadis draining the Jebel Akhdar.

(Macumber, 2003; Weyhenmeyer et al., 2002) pointed out, that groundwater recharged in the Jebel Akhdar is diverted by the less permeable Frontal Mountains. In fact, it follows two major flow paths passing through gaps in the Ophiolites near Nakhl (eastern ‘Maawil plume’) and Rustaq (western ‘Farah plume’) and is then stretching across the coastal plain to the sea. With a thickness of the alluvial channel of more than 70 m, the western flow-path is more deeply incised than the piedmont area of Wadi Maawil with relatively shallow alluvium (max. thickness < 40 m). Following this line, the quaternary alluvial aquifer increases in its vertical extent and has the largest thickness within the so called ‘‘Maawil trough’’. Subsequently, it thins out northwards (Macumber, 2003). Grain sizes decrease continuously from the mountainous region towards the coast.

Isotope studies (Macumber, 1998; Weyhenmeyer et al., 2002) revealed, that around 80 to 90% of the groundwater resources of the coastal plain within the range of the Maawil-plume are based on precipitation in high altitudes. Based on the altitude effect, Weyhenmeyer et al. (2002) deduced an average recharge altitude of approximately 1700 m a.s.l. Similar findings were stated related to the Farah plume.

Based on the analysis of tritium from observation wells on the Batinah plain, it was concluded that the portion of recent recharge in the area of the Maawil and Farah ‘plumes’ is secondary. In contrast, the area between those two plumes, shielded by the Frontal Mountains, displays a higher proportion of recent recharge.

In an isotope cross plot, $\delta^2H$ and $\delta^{18}O$ values of all the samples within the catchment of the Maawil plume lie between the above mentioned local meteoric water lines (LMWL-N and LMWL-S) – but more or less parallel to the LMWL-N. It was suggested, that this is due to a mixture of northern/north-western and southern/south-eastern vapour sources. The contribution of the southern source was assessed at about 50 %. Though of lower frequency, this south-eastern source shows high intense events of long duration. According to Weyhenmeyer et al. (2002), a more detailed quantitative assessment of the relative contribution of the two vapour sources to modern day groundwater recharge requires a continuous long-term isotope database for precipitation and rainfall chemistry. Similarly, considerations of a long-term evaporation rate for the whole area based on chloride and sodium measurements in rainfall samples resulted in an upper limit of 80 %. Due to the lack of data on dry chloride deposition, it was emphasized that this number can possibly be significantly lower.

Although the results of the mentioned isotopic and geochemical studies provided well-founded qualitative information on groundwater flow paths, uncertainties remain with regard to the actual extent of the groundwater basins of the two groundwater plumes mentioned above. For example, there is evidence that groundwater flow from the Wadi Mistal does not follow the (surface) drainage divides, but is discharging to the ‘Maawil plume’. Macumber (2003) concluded that there must be a subsurface inflow from recharge areas lying to the south of the east-west divide including the Saiq plateau.

Available groundwater hydrographs of selected groundwater stations in the alluvial aquifer on the Batinah plain reflect the hydrological processes in the corresponding basin. Unfortunately, the availability of observation wells is limited to the central and coastal part of the plain and, thus, at least about 5 km downstream to the mountain front zone. The hydrographs with the lowest distance to the piedmont zone reflect the mid-term cycles which are apparent in rainfall (see section 7.1.4). Further downstream towards the coast, the influence of the upper boundary decreases. In the coastal zone, the hydrographs feature seasonal fluctuations due to extractions for irrigated agriculture. In addition, long-term negative trends indicate the continuously increasing water demand in the recent decades.

### *7.1.6 Soils*

The soil map in Figure 7.13 shows the predominant soil classes, focusing on the soils which appear in the mountainous part and the mountain front zone, including the alluvial valley in Wadi Maawil as transition to the northern plain. Table 7.4 provides further details for these soil classes.

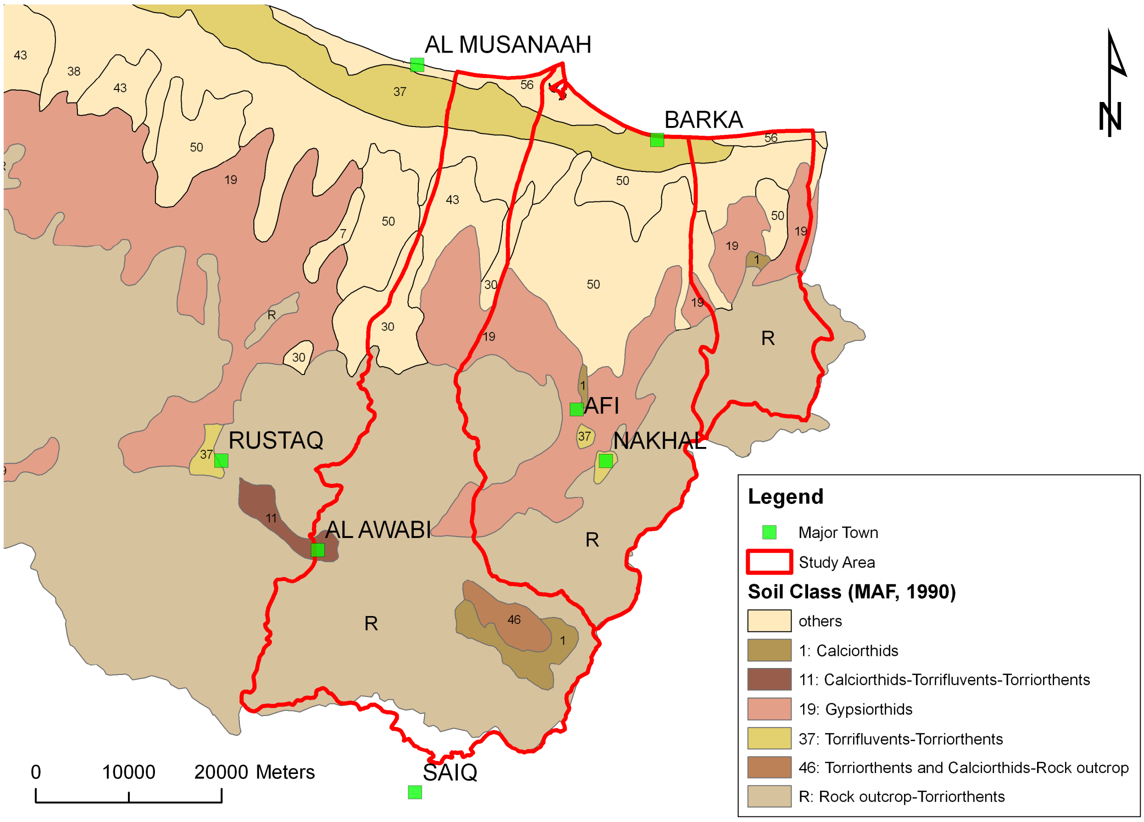


Figure 7.13: Soil map (MAF, 1990)

Table 7.4: Prevalent soil classes (MAF, 1990)

| ID | soil class | grain size | depth | slope | note |
|---|---|---|---|---|---|
| 1 | Calciorthids | loamy to loamy-skeletal | deep to mode-rately deep | 0-5% | |
| 11 | Calciorthids-Torrifluvents-Torriorthents | loamy sand & sandy skeletal | deep | 0-3% | moderately flooded |
| 19 | Gypsiorthids | loamy, loamy-skeletal & sandy-skeletal | deep to mode-rately deep | 0-15% | saline soils with gypsum pan on slightly to strongly dis-sected alluvial terraces & fans |
| 37 | Torrifluvents-Torriorthents | sandy & loamy | deep | 0-3% | slightly to moderately flooded |
| 46 | Torriorthents & Calciorthids-Rock outcrop | loamy & loamy-skeletal | shallow & moderately deep | 0-15% | soils & rock outcrop |
| R | Rock outcrop-Torriorthents | loamy-skeletal to sandy-skeletal | shallow | 0-100% | mountains & strongly dis-sected rocky plateaus |

In the mountains, the shallow Rock outcrop-Torriorthents (class R) are prevalent. This map unit is about 70 % rock outcrop, 20 % Torriorthents and 10 % minor soils. Mountains and hills are dominated by rock outcrops. The Torriorthents, however, cover Piedmont slopes, footslopes and channels. Very gravelly, loamy to sandy and shallow to deep soils are present, with high vertical hydraulic conductivity. The soil atlas does not contain further information on characteristics of these rock outcrops.

Apart from the Torrifluvent-Torriorthents on agricultural land close to Rustaq, Afi and Nakhl, only the Gubrah Bowl (southeast of Wadi Bani Kharus) and the alluvial valley in Wadi Maawil contain different soils.

The low sloped areas in the Gubrah Bowl are characterised by deep to moderately deep Calciorthids (class 1). In the gently sloping areas the shallow to moderately deep Torriorthents & Calciorthids-Rock outcrop (class 46) are prevalent. According to MAF (1990), both soils feature a moderate vertical hydraulic conductivity.

Gypsiorthids (class 19) are predominant in the alluvial valley of Wadi Maawil. In contrast to the Calciorthids they are saline soils. Vertical hydraulic conductivity is moderate and water retention is low. Typically, a layer cemented by crystalline gypsum is underlying.

### 7.1.7 *Runoff characteristics*

Figure 7.14 shows the four gauged catchments in the study area. The drainage basins display considerable differences in their characteristics (see Table 7.5). The catchment of the gauge Al Awabi shows the highest slope and the lowest portion of alluvium which implies a high predisposition to flash flood runoff generation. In contrast, the catchment of the gauge Sabt shows a lower slope and a rather high proportion of quaternary deposits. Containing the two catchments mentioned above, the catchment of the gauge at Al Abyadh (Wadi Bani Kharus) is by far the largest one (763 km²). The Wadi Maawil (gauge near Afi) comprises an area of 313 km². The morphologic variables are, on average, similar to in the drainage basin of gauge Al Abyadh.

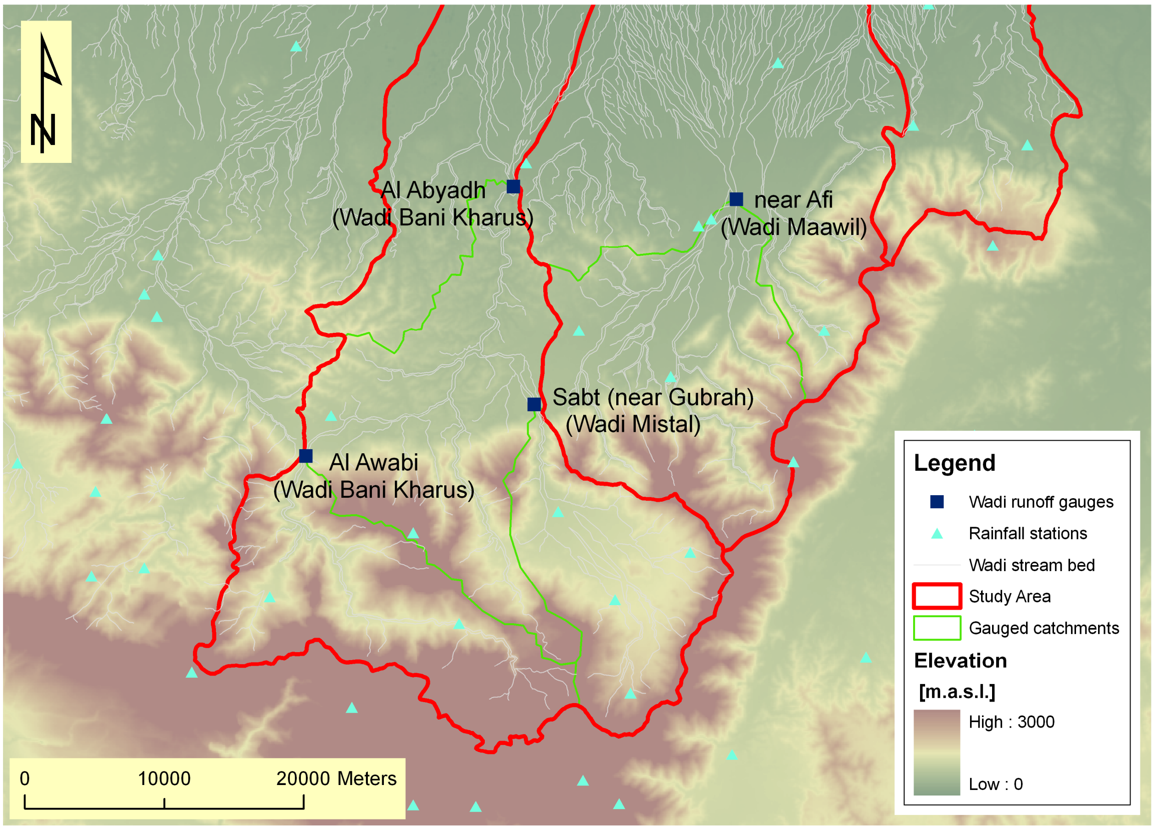


Figure 7.14: Gauged drainage basins in the study area

Table 7.5: Morphological characteristics of the four gauged surface catchments (modified after Giese (2011))

| variable | unit | gauge | | | |
|---|---|---|---|---|---|
| | | Sabt | Al Awabi | Al Abyadh | Afi |
| area | km² | 202 | 254 | 763 | 313 |
| gauge height | m a.s.l. | 420 | 600 | 200 | 225 |
| mean slope | % | 33,7 | 46,0 | 35,4 | 35,3 |
| proportion of quarternary deposits (alluvium, slope colluvium) | % | 60 | 21 | 31 | 36 |

Based on available monitoring data, Giese (2011) investigated rainfall-runoff processes in above mentioned basins. Daily data on gauged runoff for the four gauges is available since 1984. The relative number of days with observed discharge in proportion to the total number of observed days is shown in Table 7.6. With a value of 15 %, the gauge at Afi shows by far the highest portion of days with observed surface runoff. An explanation therefore is the intermittent occurrence of baseflow (see below). Based on the daily data, events, i.e. consecutive days with observed surface runoff, were selected. The headwaters Sabt and Al Awabi show generally short event durations with a mean value of 2.5 days (Al Awabi) or below (Sabt). At Al Abaydh, longer events occur from time to time with a maximum duration of 44 days in the summer of 1997. Only at gauge Afi, baseflow over several months is observed occasionally, which is fed by the local alluvial aquifer.

Only at Al Awabi summer events predominate, while Afi shows the highest number of winter events. A possible explanation could be the differences in altitude-rainfall relationships between the summer and winter season (see section 7.1.4), where summer rainfall is supposed to be less important in the lower elevated catchment of the gauge at Afi.

Table 7.6: Overview on observed runoff events after Giese (2011)

| | unit | gauge | | | |
|---|---|---|---|---|---|
| | | Sabt | Al Awabi | Al Abyadh | Afi |
| days with observed Q in proportion to obs. period | % | 3 | 5 | 4 | 15 |
| proportion of occurrence summer / winter | % | 46/54 | 56/44 | 39/61 | 30/70 |
| rainfall-runoff events selected for further evaluation (basis: daily data) | counts | 70 | 80 | 59 | 70 |
| availability of events in high temporal resolution (rainfall & runoff ) | counts | 9 | 7 | 5 | 8 |

The available hydrographs of Al Awabi show sharp rising peaks, which are typical for flash floods in arid zones. At the other gauges, recession is less steep. Hydrographs at Al Abyadh and Afi often show a tailing over several days or weeks as well as consecutive peaks within one or two days. In this regard, the available data reflects the differences in geomorphology regarding slope and geology between the different catchments.

The availability of rainfall-runoff events in high temporal resolution was limited (see Table 7.6). So, rainfall-runoff events were selected and analyzed based on daily data as a step towards prognostic rainfall-runoff relationships – aware that daily data is a substitute with limited force of expression in this context due to the temporal dynamic of rainfall-runoff-events. Table 7.6 shows the number of runoff events based on daily data which were selected for further evaluation.

Apparently, a major limitation in evaluation of rainfall-runoff processes in the study area is the limited density of the rainfall monitoring network of one station per 60 $km^2$ on average. Gaps in the network were already mentioned in section 7.1.4. According to this, a large range of altitudes is not represented in the rainfall monitoring network. In rainfall-runoff analysis, this becomes apparent through implausibly high runoff coefficients if areal precipitation is underestimated. Consequently, events with implausible runoff coefficients were sorted out.

In addition, the use of daily data results in a systematic overestimation of areal precipitation related to events, for the runoff inducing short duration rainfall event is often followed by another event on the same day. Therefore, the considerable scattering of the resulting empirical rainfall-runoff relationships is, among other factors, due to the uncertainties in assessing the correspondent areal precipitation to an observed runoff. This is in accordance with the scientific literature as for example discussed in section 2.2.1.

The mean annual runoff at the gauge Afi is 3.14 mio $m^3/a$ and 3.8 mio $m^3/a$ at Al Abyadh for the period from 1984 to 2007. These average values are strongly influenced by the extreme values in 2007, 1997 and 1995. Within that period, the highest peaks at both gauges were observed during the Gonu event in June 2007 with 881 $m^3/s$ at Afi and 777 $m^3/s$ at Al Abyadh.

### *7.1.8 Vegetation and irrigated agriculture in mountain oases*

The mountainous terrain is mainly characterised by bare rocks with little or no vegetation. In cooler high altitudes with more rainfall, scattered vegetation is prospering. In some places, trees grow in alluvial channels indicating perennial subsurface flow.

Irrigated agriculture occurs in mountain oases. The cultures comprise perennial crops (predominantly date palms) and various seasonal crops (fruits, vegetables, grains). It is based on the so called *falaj* systems (plural: *aflaj*). These are surface or underground channels which distribute available water from alluvial channels, springs or mountain aquifers which are tapped by dug channels similar to the *qanat* systems in Iran. According to Stanger (1986), the term *falaj* is derived from an ancient semitic root meaning “to divide” and refers to the system of water allocation. The traditional agriculture has evolved to cope with fluctuating groundwater supply.

The National Aflaj Inventory Project (MRMWR, 2001) provides an extensive data base on cropped areas, water quality and, to a certain extent, water quantities of aflaj systems. An evaluation of cropped areas and water use estimates is presented in section 6.3.3.

## 7.2 Recharge mechanisms in the study area

Based on section 7.1, recharge mechanisms and influencing variables are summarized in the following. For this purpose, selected features are illustrated in Figure 7.15 and Figure 7.16.

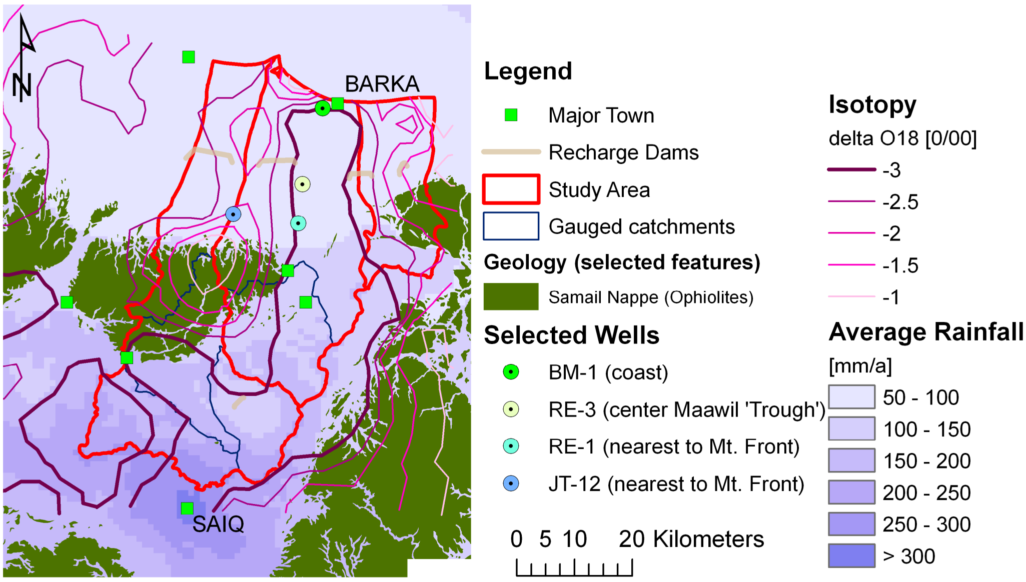


Figure 7.15: Recharge mechanisms (I): Topography, mean annual rainfall and isotopy; isolines of $\delta^{18}O$ according to Weyhenmeyer et al. (2002)

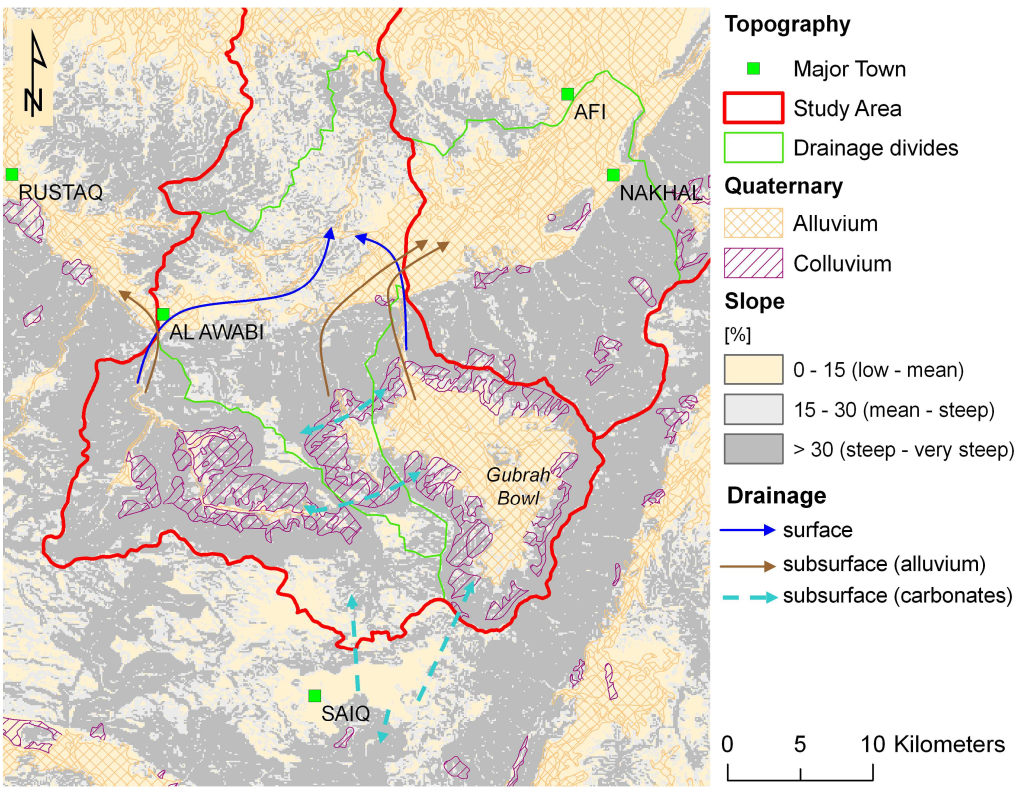


Figure 7.16: Recharge mechanisms (II): Slope and spreading of alluvium in the mountain region

Rainfall:

Mean annual rainfall is increasing with altitude (see Figure 7.15). Summer and winter seasons show about the same amounts of rainfall. However, rainfall occurrence is more variable in summer. Additionally, the amount and occurrence of rainfall are increasing significantly with altitude in summer. In winter, it is more equable up to altitudes of 2000 m a.s.l. The altitudes between 2000 and 2200 m a.s.l. (Saiq plateau) show a rainfall maximum, both in summer and winter. (Rather advective) winter rainfall is supposed to be less intense and more wide-spread than summer rainfall. Thus, winter rainfall is supposed to induce proportionally more direct recharge and less indirect recharge compared to summer rainfall.

Tropical cyclones have been observed in every month from May to December. They occur on average about once in ten years. If they do occur, they bring heavy rainfall, which induces a large proportion of surface runoff and, not least, discharge to the sea.

Potential Evapotranspiration:

According to the hypsometry of the study area, there is a temperature difference in the study area of about 10 °C from the Batinah plain to the high altitudes of the Jebel Akhdar. In addition to temperature, the potential evapotranspiration (ETP) is also a function of exposure. Thus, a distinction of ETP only according to altitude is not useful.

Geology and Soils:

In a simplified way, one may differentiate between more or less fractured and karstified carbonates outcropping at the slopes and in the high altitudes and alluvial material in the valleys in the lower altitude zones with low to median slope. A transition zone is present in the area covered by slope colluvium. It corresponds with medium to steep, sometimes even very steep, slopes. Outside cultivated areas, soils are in general less developed. A large portion of the area consists of rock outcrops.

Slope:

Considerable areas with low or maximally medium slope appear in the high altitudes (Saiq plateau) as well as in the Gubrah bowl and in the alluvial valley of Wadi Maawil (see Figure 7.16). Therefore, direct recharge at the site is more promoted than surface runoff and indirect recharge. The slopes of the mountain range, however, show steep to very steep gradients. These areas are prone to flash flood runoff generation, and subsequent indirect recharge in alluvial valleys. In these areas, direct or localized recharge depends on the occurrence of fractures or karst features.

Isotopy:

Wells in the high altitudes of the study area but also the in the so called Maawil ‘plume’ on the Batinah plain show $\delta^{18}$O-values below -3.0 ‰ (Figure 7.15). Macumber (2003) even includes a -3.5 ‰ isoline within the Maawil ‘plume’. This indicates that the groundwater resources in the Maawil ‘plume’ have precipitated mainly in the high altitudes. It has to be mentioned that the wells in the westerly Farah ‘plume’ feature only $\delta^{18}$O-values above -3.0 ‰. Accordingly, in the study of Matter et al. (2005) for the area south to the study area, no $\delta^{18}$O-values below -3.1 ‰ were detected in the mid and low altitudes. Water which has recharged in the highest parts of the study area is supposed to drain rather to the Maawil ‘plume’ than to the westerly Farah ‘plume’ or to the southern limb of the Jebel Akhdar.

Flow paths under consideration of principal recharge mechanisms

The three principal recharge mechanisms direct, localized and indirect recharge also correspond to distinct flow paths (see Table 7.7). Accordingly, a main distinction can be made between direct recharge and routing in the mountain aquifer after (deep) percolation and indirect recharge and routing in alluvial valleys. The table outlines general conclusions about areas, which may contribute preferably to the respective recharge mechanisms.

In the low sloped areas of the high altitudes, the portion of direct and localized recharge subsequent to low or medium rainfall is supposed to be more important than indirect recharge after heavy rainstorms. Consequently, drainage via the mountain aquifer is supposed to be the primary flow path.

Due to the geomorphology of the study area, the downstream flow of indirect recharge via alluvial valleys is not necessarily identical to the surface drainage direction (see Figure 7.16). For example, the surface runoff generated in Wadi Mistal, the south-eastern tributary to Wadi Bani Kharus, flows northeast of Al Awabi into the Wadi Bani Kharus towards Al Abyadh. The subsurface or near-surface flow in the valley alluvium, however, is supposed to follow the sub-recent alluvium towards the easterly Wadi Maawil (Stanger, 1986). Considering the geology, a similar situation occurs at Al Awabi. The surface runoff component is routed in the channel of Wadi Bani Kharus towards Al Abyadh. The sub- or near-surface component, however, is supposed to follow rather the sub-recent alluvium to the west than the narrow recent channel towards Al Abyadh.

Basically, the total subsurface flow in the headwaters of Wadi Bani Kharus is diverted by the ophiolitic Frontal Mountains into the eastern Maawil ‘plume’ and the western Farah ‘plume’. The actual route of the east-west divide is considered to be a source of uncertainty in water resources assessment. Accordingly, the groundwater divide between the Batinah Region in the north and the adjacent catchment in the south is subject to uncertainties.

Table 7.7: Principal recharge mechanisms and corresponding flow paths

| Recharge mechanism | drainage to alluvial basin aquifer | | catchment area |
|---|---|---|---|
| | via fissures, fractures, karst features (after deep percolation) | via alluvial valleys | |
| direct recharge | primarily | cannot be ruled out | according to hydro-stratigraphic and hydro-structural features |
| localised recharge (during runoff concentration) | according to local hydraulic conditions | according to local hydraulic conditions | |
| indirect recharge (during channel routing after runoff concentration) | cannot be ruled out | primarily | headwaters: according to surface catchment divides<br>downstream: according to spreading of alluvial valleys (can diverge from surface drainage direction) |
| inter-aquifer flow / interface mountain block – alluvial basin | not necessarily lateral along alluvial valleys only; upward flow from carbonatic footwall north to the mountain front possible (see Figure 7.17) | lateral inflow at the mountain front | |

Temporal dynamics:

Surface runoff shows an immediate response to rainfall events. Accordingly, indirect and artificial recharge on the Batinah plain takes place within hours, days or weeks after rainfall. Aflaj hydrographs within the Jebel Akhdar or in the piedmont zone indicate a response time to rainfall events of 3 to 6 months.

A visual interpretation of available groundwater hydrographs compared to rainfall time series imply, that there is a time lag between rainfall events in the mountains and groundwater response (changes in groundwater levels) at observed locations of at least 2.5 years at JT-12. This station lies around 5 km downstream to the mountain front (see Figure 7.15). Due to hysteresis, this value cannot be considered as constant, but as a lower limit. Based on Walther et al. (2012), the mean flow velocity in the aquifer around the groundwater station mentioned above is supposed to be between $1*10^{-5}$ and $3*10^{-5}$ m/s which is equal to a flow distance of about 1 to 2.5 km in 2.5 years. Thus, a causal relation between rainfall and observed changes in groundwater levels seems to be plausible, assuming that there is an inter-aquifer flow from the tertiary limestone aquifer to the alluvial aquifer on the Batinah plain besides an upstream inflow to the basin aquifer along the mountain front. Figure 7.17 implies that such a connection between mountain aquifer and alluvial basin aquifer exists.

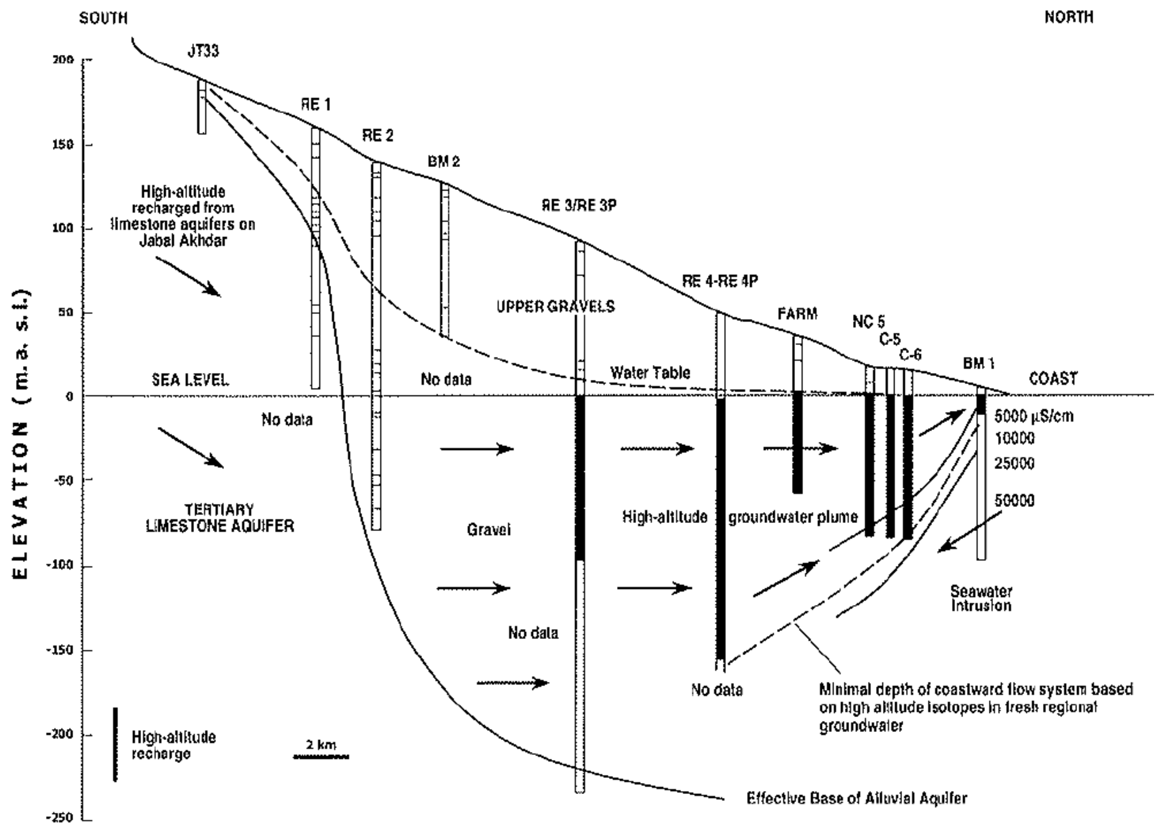


Figure 7.17: Occurrence and flow of isotopically depleted groundwater along the Maawil trough (Macumber, 2003)

<u>Indirect and artificial recharge on the plain:</u>

The upstream boundary to assess indirect recharge on the Batinah plain is the surface run-off at the mountain front. Respective runoff characteristics in the study area were addressed in section 5.7. Sophisticated tools to assess indirect recharge and artificial recharge downstream to the recharge dams were recently set up by Philipp and Grundmann (2013). This work contains appropriate hydrodynamic models to describe flash flood routing in ephemeral rivers including consideration of transmission losses. In addition, a dam module assesses the retention in recharge dams.

Presuming the operation of recharge dams, transmission losses or potential indirect recharge downstream to the respective wadi runoff gauges near Afi (Wadi Maawil) and Al Abyadh (Wadi Bani Kharus) range from some ten percent for occasional extreme events (e.g. Gonu in June 2007) with considerable discharge to the sea up to more than 90 % for more frequent runoff events with low or median magnitude. Since recharge dams have been in operation, runoff to the sea has not been observed any more in the latter case (Philipp, pers. comm., January 17, 2013).

Mountain-front recharge vs. indirect recharge: zones of influence and temporal dynamics

The ‘plume’ area is recharged via subsurface inflow from upstream. According to the location of the recharge dams on the Batinah plain (see Figure 7.15), the recent course of the wadi channels is outside of the ‘plume’. Weyhenmeyer et al. (2002) point out, that there is evidence of tritium occurrence in these areas. Thus, the zones along the wadi courses receive water, which has infiltrated through the channel alluvium. While the subsurface inflow underlies a considerable attenuation during routing from recharge areas to the alluvial basin aquifer, indirect recharge shows a short term response to rainfall events in the mountains. In general, recharge dams are empty within 10 days after onset of the flash flood events.

Direct recharge on the plain:

Considering high potential evapotranspiration and relatively low rainfall amounts on the Batinah plain (section 5), it is assumed, that direct recharge due to precipitation on the plain is rather low, compared to balance components in the considered study area mentioned above. Exceptions can be the occasional tropical cyclones, which are accompanied with severe rainfall. Grundmann (pers. comm., January 17, 2013) reported soil moisture observations in the frame of irrigation experiments at the agricultural research station near Barka. Accordingly, hardly any change in soil moisture was observed after a rainfall event of 23 mm. In contrast, intense watering with a high water amount (above 100 mm) to leach the soil, resulted in a change in soil moisture, even in greater depths. It is concluded that rare, extreme rainfall events contribute to (direct) groundwater recharge while the frequent low or medium events can be neglected.

## 7.3 Assessment of mountain-front recharge - Methodology

In the following, the flux comprising mountain-front recharge is denoted as $Q_{MFR}$ . The reference cross section for assessment of MFR is the (assumed) mountain front line. The spatial references or balance areas for its assessment are defined α-cuts of the Fuzzy Recharge Areas for the Maawil ‘plume’ (see section 7.3.1). Especially for the application of the conceptual hydrologic model (see 7.3.5), but also for the long-term average approach, response units with distinct parameterisation have to be determined (see section 7.3.2). In addition to the actual recharge in the mountain catchment, water use in mountain oases has to be considered (see section 7.3.3).

Based on steady state groundwater modelling, an upstream inflow to the groundwater model domain on the Batinah plain $Q_{GWM}$ of 68 mio m³/a was computed (Walther et al., 2012). This can be considered as a reference value for long-term average $Q_{MFR}$.

### *7.3.1 Data Processing of Fuzzy Recharge Areas*

In the following, the procedure to derive Fuzzy Recharge Areas as outlined in section 5.1 is applied to the potential groundwater basin of the Maawil ‘plume’. Based on the discussion of recharge mechanisms in section 7.1, Figure 7.18 shows the data base to derive the Fuzzy Recharge Areas for the Maawil ‘plume’.

The outer boundary shows the assumed maximum extent of the underground catchments, both for the eastern Maawil ‘plume’, and the western Farah ‘plume’. Together, they represent that part of the Jebel Akhdar of which the subsurface water potentially drains northward to the Batinah plain. In the north, this area is either limited by an assumed mountain front line or outcrops of the Samail Nappe ophiolites, which are supposed to be secondary in this context. To the east and south, the area is limited by the border of the Hajar Unit. In general, a degree of membership of $\mu(x,y) = 0$ is assumed for the outer boundary. A value of $\mu(x,y) = 1$ was only assigned to the mountain front line in the alluvial valley around Afi, the opening towards the alluvial basin aquifer.

The portions of the (surface) drainage basins of Wadi Taww and Wadi Maawil outside of the ophiolites are assumed to drain completely to the Maawil ‘plume’ ($\mu(x,y) = 1$), while the drainage basin of Wadi Farah is assumed not to contribute at all ($\mu(x,y) = 0$).

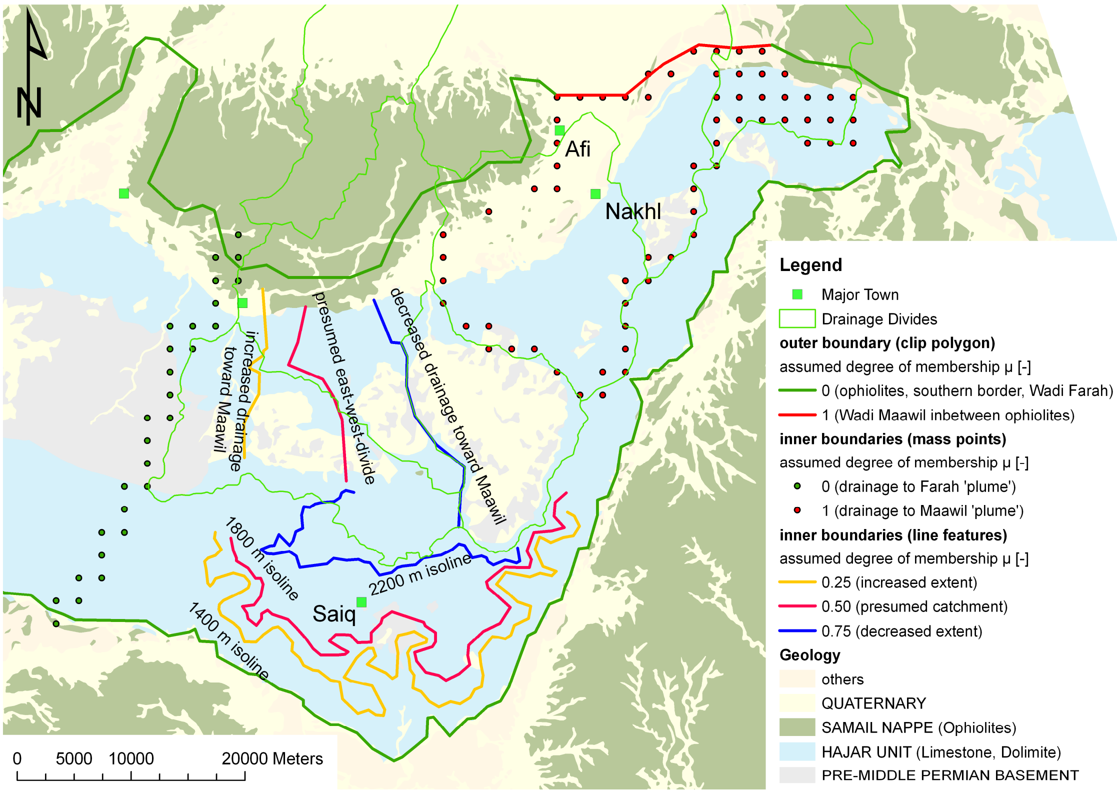


Figure 7.18: Outer and inner boundaries for derivation of Fuzzy Recharge Areas

The northern end of the presumed east-west divide (with $\mu(x,y) = 0.5$) south to the Frontal Mountains lies between the two areas, covered with sub-recent alluvium, which spreads either further to the west or to the east. To the south, it follows in first instance the (local) drainage divides. Finally, its southern end reaches into the Saiq plateau. Here, it is assumed, that direct recharge and subsurface drainage to the Maawil 'plume' predominate compared to drainage according to the surface drainage network. Although they follow to some degree the topography, the supporting lines for 'increased' or 'decreased drainage toward Maawil' are quite subjectively which has to be considered in evaluation of the resulting water yields. This corresponds to the statement of Jacobs (2007), whereupon fuzzification is quantification at the same time. On the Saiq plateau, the inner boundaries are assumed to follow distinct isolines to describe the potential extent of the groundwater basin, which is related to certain $\alpha$-cuts. Based on isotopic evidence, the contribution of the areas above 2200 m a.s.l. to the Maawil 'plume' is quite solid. The 1800-isoline ('presumed divide' with $\mu(x,y) = 0.5$') is completely within the low sloped plateau area, which shows the highest $\delta^{18}$O-values. Thus, it is assumed, that this area contributes mainly to the Maawil 'plume'. Beyond that line, however, the steep southern slopes are starting – where surface runoff and, thus, indirect recharge is supposed to dominate and subsurface drainage to the north is more and more unlikely.

Based on these outer and inner boundaries, a Triangulated Irregular Network (TIN) was interpolated. Finally, this TIN was converted to an ascii raster file with a spatial resolution of 1 x 1 km². It is illustrated in Figure 7.19. With regard to water balance assessment for different α-cuts, the location of oases were included.

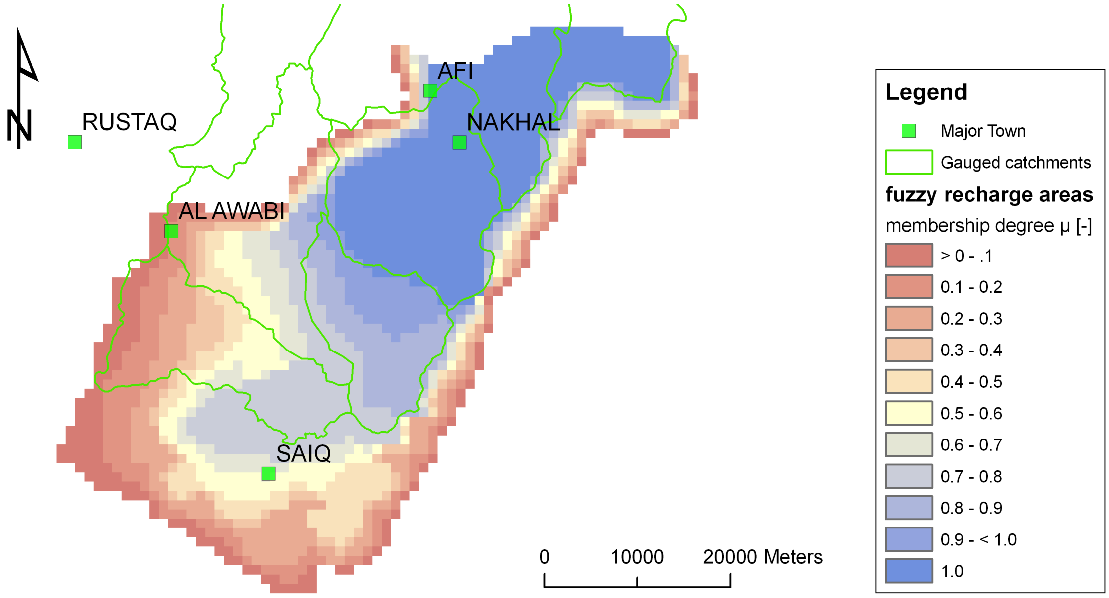


Figure 7.19: Fuzzy Recharge Areas of the Maawil 'plume'

### *7.3.2 Determining response units*

The raster based framework (section 2) allows defining hydrogeologic response units (HGRU) to distinguish zones with distinct response functions (for the conceptual hydrologic model) or assumptions on recharge rates (for the long-term average considerations).

Especially with regard to the conceptual hydrologic model, the primary goal is to delineate zones with distinct characteristics regarding recharge mechanisms and recharge flow paths. The degree of distinction depends on available data or expert knowledge of the catchment characteristics and reference data for calibration. An increasing number of response units are beneficial as long as they are accompanied by an increase of reliable information. In this case study, detailed field surveys, like, for example, carried out extensively by Lange (1999) in a similar context are lacking. Observed hydrographs of *aflaj* do not represent the total catchment area, but only unknown sub-catchments. Available reference data is limited to a single long-term average value (see above). Thus, a low number of 3 response units was defined. In addition to their names, Table 7.8 shows criteria for their delineation based on available geo data. The highlighted criteria were finally used for data processing.

In the case of the alluvial valleys, the spreading of (recent and sub-recent) alluvium corresponds well with slopes ≤ 15 %. Slope colluvium is corresponding with higher slopes, but the hydrologic characteristics are more similar to the alluvial valleys than to the steep slopes with outcrop of rocks (see section 7.3.5 including Table 7.13). Thus, the prevalent geology is finally used as a classification criterion instead of the slope. The 'slopes' are the remainder, i.e. those raster cells, which do not belong to the other classes with clear selection criteria.

Table 7.8: Definition of response units

| ID | Name | slope | altitude | prevalent geology |
|---|---|---|---|---|
| 1 | quaternary | low to mean (≤ 15 %) | < 1800 m a.s.l. | **Quaternary (sub-recent and recent alluvium or slope colluvium)** |
| 2 | slopes | steep to very steep (> 30 %) | arbitrary | limestone and dolostone |
| 3 | high altitudes | **low to steep (≤ 30 %)** | **≥ 1800 m.a.s.l** | |

Considering an α-cut $FRA_{0.50}$ of the Fuzzy Recharge Areas, 'quaternary' covers 31 % of the total basin. The 'slopes' represent 53 % and the relative portion of the high altitudes amounts to 16 %.

### *7.3.3 Water use in mountain oases*

Crop evapotranspiration $ET_c$ is the product of reference evapotranspiration $ET_0$ and the crop coefficient $k_c$. Integrated over the total cropped area within the considered balance area, it results in the total crop water demand $Q_c$. For the actual crop water use depends on the actual water availability, $Q_c$ is a potential value which may not be used up completely in selected periods.

Thus, cropped areas of mountain oases according to MRMWR (2001) were used to assess water use according to the respective extent of the balance area. In addition to the standard extent, MRMWR (2001) contains also the so called 'uncropped area', which can be optionally used for farming, e.g. in particularly wet periods. Uniformly, the latter is a third of the value for the 'cropped area'.

The crop coefficient $k_c$ depends on the culture as well as on the growing stage. According to Allen et al. (1998), $k_c$ is mostly below 1 in the initial state and between 0.40 and 1.25 in the mid state, depending on the crop. For date palms, the most important perennial culture in the study area, $k_c$ is between 0.90 and 0.95. Cropping patterns, i.e. a distinction of different crops within the cropped area, are not available. Thus, a unit value $k_c \sim 1$ over the whole year is assumed. Consequently, crop water requirement corresponds to the assumed value of $ET_0$.

Table 7.1 shows average monthly values of $ET_0$ at different sites of the study area. For the oases actually covering different altitudes and exposures, the median values in this table with an annual sum of 1946 mm at Saiq (MWR, 1996) is considered to be a reasonable estimate. The other two other stations (1776 mm/a and 2466 mm/a) can be regarded as upper and lower limit. In the National Aflaj Inventory (MRMWR, 2001), a unit reference value of 2700 mm/a was assumed. This can be considered appropriate for the coastal zone. For the mountainous part of the study area, this value is considered to be too high. Table 7.9 shows cropped areas and mean annual values of the crop water demand $Q_c$.

Table 7.9: Estimates of mean annual crop water demand Qc

| cropped area | cumulated crop water demand Qc [mio m³/a] | | |
|---|---|---|---|
| $A_c$ [m²] | $ET_{c\ min}$ | $ET_{c\ median}$ | $ET_{c\ max}$ |
| $9.79 * 10^6$ | 17.39 | 19.06 | 24.14 |

### *7.3.4 Long-term average considerations based on fuzzy arithmetic*

The following considerations are based on the approach outlined in section 5.2. Response units are defined according to section 7.3.2.

An option to estimate spatially distributed recharge to carbonate aquifers as fraction of mean annual rainfall is the APLIS regionalisation approach (Andreo et al., 2008). Its implementation is discussed in section 5.2.3. Alternatively, usually used, crude estimates for hard rock in northern Oman are $15\ \% \leq R \leq 35\ \%$ and $5\ \% \leq R \leq 20\ \%$ for soft rock (Al Shaqsi, 2004). It is assumed that the APLIS approach is appropriate for the 'slopes' and for the 'high altitudes'. For the 'quaternary', where relatively high evaporation losses due to soil moisture storage are supposed, the crude estimates for soft rock are applied instead. Table 7.10 shows the different assumptions on recharge rates for the respective response units. Fuzzy numbers are written as set of ordered pairs. In deriving the fuzzy numbers, a slight transition was assumed around the crisp interval limits.

Table 7.10: Assumptions on recharge rates R [% of mean annual precipitation] for distinct response units

| response unit | quaternary | slopes | high altitudes |
|---|---|---|---|
| approach / assumption | crude estimates: $R=\left\{\frac{0}{3},\frac{1}{7},\frac{1}{18},\frac{0}{22}\right\}$ | APLIS | APLIS |

According to section 5.2, rainfall is the product of the regionalised value P(x,y) and an optional correction factor $P_{corr}$ to consider measurement errors or uncertainties in regionalisation, for example. Similarly, for the cropped areas the standard value can be considered but also an extended area which is cropped in selected years only. Likewise, $ET_0$ can be considered as crisp value, or minimum and maximum values can be included. With regard to the comparison of the total outcomes of fuzzy arithmetic approach, conceptual model and the reference value based on groundwater modelling, two variants are distinguished:

In variant A, recharge rates and the spatial extent of the basin are the only considered sources of uncertainty. This is the basis for a comparison with available reference values in section 7.4.1. In variant B, rainfall correction factor $P_{corr}$, $A_{crop}$ and $ET_0$ are considered as fuzzy numbers. The confidence ranges of $A_{crop}$ and $ET_0$ were discussed in section 7.3.3. Rainfall measurement errors were addressed in section 7.1.4. The correspondent fuzzy numbers are shown in Table 7.11.

Table 7.11: Assumptions on fuzziness in rainfall, cropped areas and reference evapotranspiration

| | rainfall P(x,y) | $A_c$($\alpha$-cut level) | $ET_0$ |
|---|---|---|---|
| variant A | crisp (regionalisation) | crisp (standard value) | Crisp<br>($ET_{0\ median}$ = 1946 mm/a) |
| variant B | $P(x,y)*P_{corr}$<br>$P_{corr} = \left\{\frac{0}{.97}, \frac{1}{1.03}, \frac{1}{1.08}, \frac{1}{1.13}\right\}$ | $A_{crop}*A_{corr}$<br>$A_{corr} = \left\{\frac{0}{1.0}, \frac{1}{1.1}, \frac{1}{1.2}, \frac{1}{1.3}\right\}$ | $ET_0 = \left\{\frac{0}{1776}, \frac{1}{1900}, \frac{1}{2000}, \frac{0}{2466}\right\}$ |

### *7.3.5 Time-dependent assessment using the conceptual hydrologic model*

According to section 4, the main steps for the setup of this water balance model are

- determination of response units (see section 7.3.2),
- determination of seasons,
- parameterisation and calculation of the seasonal response functions
- parameterisation of the aquifer models for each response unit.

Determining Seasons:

The primary concern regarding the seasons is the option to consider average seasonal climate characteristics in derivation of the response functions. Comparable to the response units, it is worthwhile to aim for an appropriate number of seasons.

Rainfall mechanisms play an important role in this context. The most important ones are the *seif* rain in winter (December to April with focus on February and March) and the summer rain season in July and August. The tropical cyclones occur occasionally in all months from May to December. They are supposed to show different process dynamics with regard to groundwater recharge generation due to high intensities over a longer duration than usual convective storms. Additionally, they have a considerable impact on mean values due to their magnitudes. As far as they occur within the calendar months of winter and summer rain seasons, they cannot be distinguished in this modelling approach. A distinct 'in between season' (May to June and September to November) is an attempt to assess the long-term average yield of these events at least to a certain degree.

According to Table 7.1, potential evapotranspiration (ETP) is considerably higher in March and, even more, in April compared to January and February. However, a sensitivity analysis regarding this problem revealed, that a distinction of the winter season according to ETP does hardly influence the long-term average result. Consequently, a winter rain season (December to April), a summer rain season (July and August) and an 'in between season' (May to June and September to November) is considered.

Definition of response functions for each case:

According to section 6.2, a case denotes the combination of a distinct response unit and season. For each case, a parameter set has to be defined and a correspondent response function is calculated. The parameters depend on catchment characteristics like infiltration characteristics or soil storage capacity on the one hand, and rainfall characteristics like occurrence, duration, and intensity on the other hand. Thus, available information is compiled in the following section. Table 7.12 shows rainfall characteristics according to response units based on section 7.1.4. It is an indication for estimating cumulated initial losses or infiltration. In the tailing phase of the temporal distribution of rainfall events, intensity is assumed to be considerably lower than potential infiltration rates.

Table 7.12: Rainfall characteristics according to response units and seasons

| HGRU | 1 – quaternary | 2 – slopes | 3 – high altitudes |
|---|---|---|---|
| | rainfall occurrence[1)] [d/month] | | |
| summer | 2.0 | 3.5 | 4.5 |
| in between | 2.0 | 3.5 | 4.5 |
| winter[2)] | 2.5 | 3.0 | 3.5 |
| | expected rainfall duration [h/event] | | |
| summer | ≤ 2 | ≤ 2 | ≤ 2 |
| in between | 2.0 | 3.5 | 4.5 |
| winter[2)] | > 2 (up to 48) | > 2 (up to 48) | > 2 (up to 48) |

1) Occurrence per month refers to months in which rainfall actually occurred.
2) Winter rainfall is supposed to be less intense but of longer duration.

Table 7.13 shows available literature values on initial losses and infiltration rates. Accordingly, even on steep slopes considerable infiltration can occur, as far as they are covered by colluvium. On steep slopes with outcrops of rocks, which are represented by the response unit 'slopes' in this study, initial losses and infiltration is assumed to be similarly low than in the limestone plateaus in Table 7.13.

Table 7.13: Literature values on relevant catchment characteristics according to Lange et al. (1999)

| terrain types | initial loss [mm/event][1)] | final infiltration rate [mm/h] |
|---|---|---|
| range over all types in the respective study | 4.5 to 11 | 5 to 50 |
| limestone plateau; (non-diss.; dissected) | 4.5; 7 | 5; 15 |
| steep active slope (colluvium) | 10 | 30 |
| sandy plain (crusted) | 9 | 15 |
| sandy plain (vegetated) | 11 | 50 |

The model approach is based on a monthly time step. Thus, the number of rainy days has to be considered in assessing the maximum initial loss. However, as the histograms in Figure 7.9 show, rainfall amounts below the minimal possible initial losses do occur. Similarly, the estimation of the maximum infiltration has to integrate potential infiltration rates at site and rainfall characteristics.

In hard rock terrain, soil storage available for evapotranspiration by plants ranges from 30 to 150 mm (Ahmed et al., 2008). The major part of storage is in the weathered zone (porosity). Additionally, there is some storage in the weathered-fractured zone. The parameter SMD, which represents the soil moisture deficit in the presented approach, is a fraction of above mentioned maximum values. It can be assumed, that soil storage capacity and, thus, the parameter SMD, is very limited in the ‘high altitudes’ and within the ‘slopes’. In comparison, the response unit ‘quaternary’ is assumed to show a higher storage capacity. Thus, higher values of SMD are possible in this response unit. At last, SMD has to be considered as a calibration parameter.

Table 6.3 summarizes the sensitivity analysis in section 6.4.2. The most important conclusion with regard to model application is the fact, that $Inf_{max}$ and SMD are the most influential parameters. Additionally, they are interdependent.

Considering all expert knowledge, parameter sets for the relevant cases were compiled. To cover the potential range parameter values, a low yielding parameter set (aiming at a potential lower bound of results), a median and a high yielding parameter set (aiming a potential upper bound) were considered. For $Inf_{max}$ and SMD, additional steps in between were included. The results are shown in Table 7.14. Although the lithology within the ‘quaternary’ features the highest infiltration rates, the parameter $Inf_{max}$ is mostly higher in the other two response units, especially outside of the summer season. This reflects the differences in rainfall occurrence as function of altitude.

Table 7.14: Basic parameter sets aiming at minimum, median and maximum

| | HGRU | 1 – quaternary | | | | | 2 - slopes | | | | | 3 – high altitudes | | | | |
|---|---|---|---|---|---|---|---|---|---|---|---|---|---|---|---|---|
| | pot. yield | low | | med | | high | low | | med | | high | low | | med | | high |
| init loss$_{max}$ | summer | 11 | | 10 | | 9.0 | 10 | | 8.0 | | 6.0 | 13.0 | | 10 | | 7.0 |
| [mm/Δt] | in between | 11 | | 10 | | 9.0 | 10 | | 8.0 | | 6.0 | 13.0 | | 10 | | 7.0 |
| | winter | 14 | | 13 | | 11 | 8.0 | | 7.0 | | 5.0 | 10.0 | | 8.0 | | 6.0 |
| Inf$_{max}$ | summer | 8.0 | 15 | 20 | 30 | 35 | 4.0 | 13 | 17 | 26 | 30 | 8.0 | 25 | 32 | 45 | 50 |
| [mm/Δt] | in between | 15 | 35 | 40 | 50 | 120 | 13 | 40 | 47 | 60 | 105 | 24.0 | 60 | 90 | 150 | 203 |
| | winter | 28 | 35 | 40 | 50 | 150 | 11 | 35 | 40 | 50 | 90 | 18.0 | 50 | 78 | 130 | 158 |
| SMD | summer | 33 | 25 | 23 | 18 | 15 | 12 | 10 | 8.5 | 6.0 | 5.0 | 12.0 | 10 | 8.5 | 6.0 | 6.0 |
| [mm/Δt] | in between | 30 | 22 | 20 | 15 | 12 | 10 | 8.0 | 7.0 | 5.0 | 4.0 | 10.0 | 8.0 | 7.0 | 5.0 | 5.0 |
| | winter | 27 | 20 | 18 | 13 | 10 | 8.0 | 6.0 | 5.0 | 4.0 | 3.0 | 8.0 | 6.0 | 5.0 | 4.0 | 4.0 |
| $n_{transm\_loss}$ | summer | 1.75 | | 1.30 | | 1.10 | 1.75 | | 1.30 | | 1.10 | 1.75 | | 1.30 | | 1.10 |
| | in between | 1.75 | | 1.30 | | 1.10 | 1.75 | | 1.30 | | 1.10 | 1.75 | | 1.30 | | 1.10 |
| | winter | 1.75 | | 1.30 | | 1.10 | 1.75 | | 1.30 | | 1.10 | 1.75 | | 1.30 | | 1.10 |
| $n_{SMR\_channel}$ | summer | 1.10 | | 1.50 | | 1.75 | 1.10 | | 1.50 | | 1.75 | 1.10 | | 1.50 | | 1.75 |
| | in between | 1.10 | | 1.50 | | 1.75 | 1.10 | | 1.50 | | 1.75 | 1.10 | | 1.50 | | 1.75 |
| | winter | 1.10 | | 1.50 | | 1.75 | 1.10 | | 1.50 | | 1.75 | 1.10 | | 1.50 | | 1.75 |

According to section 6.4, the conceptual hydrologic model is able to capture the distinct characteristics of different environments. Though, due to its conceptual character and the scarce data base for parameterisation and calibration, the actual model application is necessarily subject to considerable uncertainties. In order to assess the reliability of the model outcome, not only the basic variants were considered, but a variety of combinations. For this purpose, the 3 basic variants for the less sensitive parameters were permuted with all 5 variants of both, Inf$_{max}$ and SMD. So, 75 parameter sets were considered to support the identification of the most suitable ones.

<u>Parameters (recession constants) for subsurface routing in the mountain aquifer:</u>

The bucket-type aquifer models (see section 4.5) represent the retention during subsurface drainage to the reference cross section, namely the mountain front. In addition, the translation has to be considered. Available *aflaj* hydrographs show a time lag of about 3 to 6 months.

As mentioned above, there is a lack of hydrogeologic survey and groundwater observations in the alluvial basin aquifer in close distance to the mountain front, as well as on the flow distance up to 5 km downstream to the mountain front. Consequently, neither the time-dependent results at the mountain front can be calibrated, nor a reasonable transfer function between mountain front and groundwater model domain can be established until further notice. Thus, the parameters in Table 7.15 are an initial estimate. It represents an aquifer which is slightly lower permeable than a limestone aquifer.

Table 7.15: Parameterisation of subsurface routing

| | |
|---|---|
| Kl (low permeable storage) [d] | 250 |
| Kh (high permeable storage) [d] | 15 |
| Distribution factor Rl [%] | 95 % |
| Time lag [mon] | 3 |

## 7.4 Assessment of mountain-front recharge – Results

As reference for presentation and discussion of the results, Table 7.16 shows the considered $\alpha$-cut levels of the Fuzzy Recharge Areas and related values of spatial extent, long-term mean annual rainfall and cropped area.

Table 7.16: $\alpha$-cuts of the Fuzzy Recharge Areas and related variables

| $\alpha$-cut level | spatial extent | long-term mean rainfall |
|---|---|---|
| $\alpha$ [-] | A [km²] | P [mm/a] |
| 0.40 | 1386 | 163.2 |
| 0.45 | 1334 | 162.2 |
| 0.50 | 1291 | 161.6 |
| 0.55 | 1160 | 155.5 |
| 0.60 | 1089 | 152.6 |

The averaged rainfall over the whole balance area is rising considerably from $\alpha$-cut level $\alpha = 0.55$ to $\alpha = 0.50$. This is due to comparatively very high values in the high altitudes. Their proportion is rising continuously from $\alpha$-cut level $\alpha = 0.60$ to $\alpha = 0.40$.

### *7.4.1 Long-term average considerations*

Conceptual Hydrologic model

For each considered spatial extent of the catchment ($\alpha$-cut) and each parameter set, the model returns a long-term mean annual subsurface outflow at the mountain front $Q_{MFR}$. It is the balance of cumulated groundwater recharge $Q_R$ and water demand of mountain oases Qc. Exemplarily for all $\alpha$-cuts of the Fuzzy Recharge Areas, Figure 7.20 (left graph) shows a histogram of the results of all 75 parameter sets for $\alpha$-cut level 0.5. The right graph shows a selection of results where long-term mean recharge rates in the different response units are within a reasonable range. The thresholds used for selection are shown in Table 7.17. They ensure that extreme results are included in further evaluation, but model runs with implausibly high or low recharge rates are excluded. Obviously, the model approach results in a left skewed distribution of $Q_{MFR}$ with a peak around of around 60 mio m³/a. The correspondent histograms for all 5 considered α-cuts are shown in Appendix A.

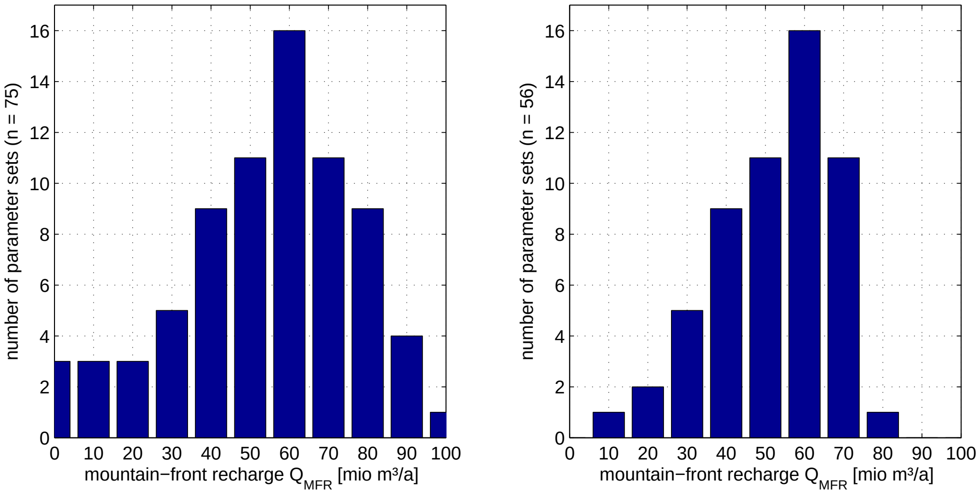


Figure 7.20: Histograms of calculated subsurface outflow at the mountain front $Q_{MFR}$ based on the conceptual hydrologic model (α-cut level 0.5); left: whole sample (n = 75); right: selected samples considering assumed thresholds of long-term mean recharge rate per response unit (n = 56)

Table 7.17: Thresholds for long-term mean recharge rates in distinct response units as plausibility check for parameter sets of the conceptual hydrologic model

| Response unit | lower threshold $R_{min}$ [%] | upper threshold $R_{max}$ [%] |
|---|---|---|
| 1 – quaternary | 5 | 40 |
| 2 – slopes | 15 | 50 |
| 3 – high altitudes | 20 | 60 |

To provide an overview on all considered α-cuts, Figure 7.21 shows empirical cumulated distribution functions of the model results based on model runs for the different considered α-cuts $FRA_{\alpha}$. The abscissa shows the probability of non-exceedence while the ordinate shows the outcome $Q_{MFR}$. Obviously, there is a considerable gap between the values for $\alpha = 0.50$ and $\alpha = 0.55$. Considering the differences in spatial extent of the catchments and high precipitation in the considered transition zone, this is plausible. The maximum value of the empirical distribution for the largest considered extent ($\alpha = 0.40$) is 83.3 mio m³/a.

As a basis to check the plausibility of the model and to compare it with complementary approaches to assess rainfall-recharge relationships, Table 7.18 shows long-term mean recharge rates in proportion to mean seasonal rainfall in the respective response units. It is based on 3 model runs and the α-cut $FRA_{0.50}$. The selected runs show a similar total long-term mean outcome $Q_{MFR}$ between 66 and 70 mio m³/a. In addition, rainfall P(season) shows the portion of rainfall in the respective season compared to the total rainfall in the considered response unit.

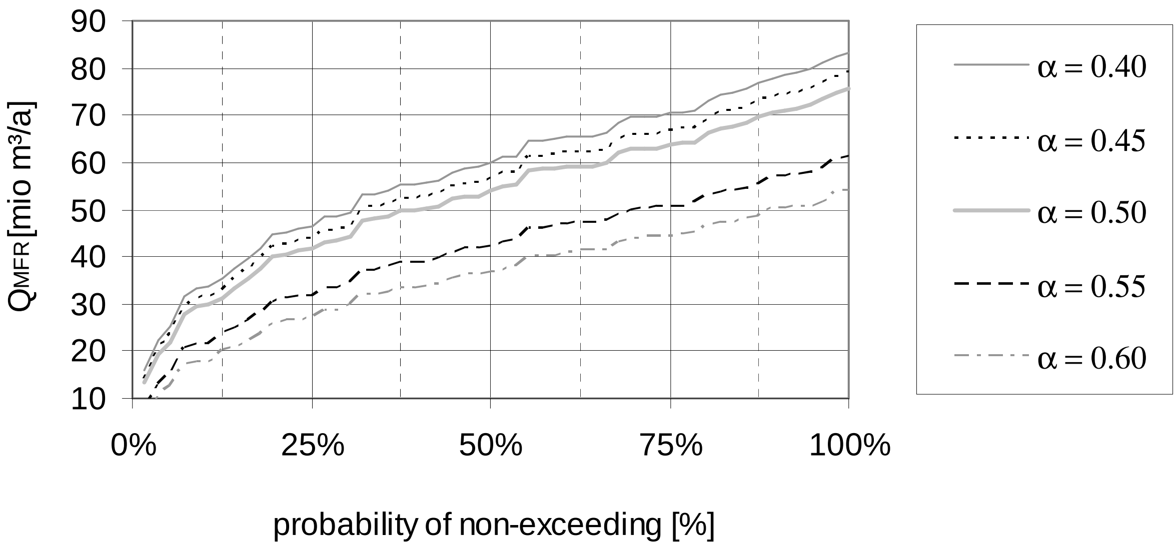


Figure 7.21: Empirical cumulated distribution functions for the model results of the different parameter sets and referred to different considered α-cuts $FRA_{\alpha}$

Table 7.18: Long-term mean rainfall P, recharge rates R and cumulated yield $Q_R$ according to response unit and season for selected model runs or parameter sets (α-cut FRA0.5)

| response unit: | parameter set ID: | 20 | 47 | 66 | 20 | 47 | 66 | 20 | 47 | 66 |
|---|---|---|---|---|---|---|---|---|---|---|
| | season | rainfall P(season) [% of P(HGRU)] | | | groundwater recharge R [% of P(season)] | | | cum. yield $Q_R$(season) [% of $Q_R$(HGRU)] | | |
| quaternary | summer | 22 | 22 | 22 | 15 | 11 | 12 | 13 | 11 | 17 |
| | in between | 24 | 24 | 24 | 18 | 20 | 13 | 18 | 22 | 19 |
| | winter | 54 | 54 | 54 | 32 | 27 | 19 | 69 | 66 | 64 |
| slopes | summer | 26 | 26 | 26 | 31 | 33 | 39 | 19 | 19 | 22 |
| | in between | 27 | 27 | 27 | 35 | 37 | 35 | 22 | 22 | 21 |
| | winter | 47 | 47 | 47 | 53 | 57 | 54 | 59 | 59 | 57 |
| high altitudes | summer | 33 | 33 | 33 | 43 | 46 | 50 | 28 | 29 | 31 |
| | in between | 28 | 28 | 28 | 42 | 42 | 44 | 24 | 23 | 23 |
| | winter | 39 | 39 | 39 | 61 | 63 | 64 | 48 | 48 | 47 |

Obviously, the winter season shows always the highest portion of rainfall. Summer and in-between season show similar orders of magnitude. It has to be mentioned, that summer comprises only the months of July and August while the in-between season represents 5 calendar months. The relative portion of winter rainfall is decreasing with increasing altitude. In contrast, the relative amount of summer rainfall is increasing with altitude.

The recharge rates show a general increase from the (lower lying) ‘quaternary’ unit over the ‘slopes’ to the ‘high altitudes’. The winter season shows always the highest rates with a considerable difference to the other seasons. In summer, recharge rates are generally lower in the response unit ‘quaternary’. The ‘in between season’ shows lower rates than the summer season in the ‘high altitudes’.

The cumulated recharge $Q_R$ shows an amplification of rainfall characteristics by similar patterns in long-term average recharge rates. In the ‘high altitudes’, the contribution of winter rainfall to the total yield is slightly lower than 50 %. Here, the portion of yield in the summer season is significantly higher (around 30 %) than in the response units ‘slopes’ (around 20 %) or quaternary (up to 17 % only). In comparison thereto, recharge induced by winter rainfall is around 60 % (‘slopes’) or even above (‘quaternary’).

Table 7.19: Proportions of cumulated yield $Q_R$ per response unit compared to the yield of the total area for selected model runs or parameter sets ($\alpha$-cut FRA0.5)

| HGRU | area (HGRU) [% of total area] | $Q_R$ (HGRU) [% of total yield] | | |
|---|---|---|---|---|
| | | Set ID = 20 | Set ID = 47 | Set ID = 66 |
| quaternary | 31 | 15 % | 13 % | 10 % |
| slopes | 53 | 55 % | 57 % | 58 % |
| high altitudes | 16 | 30 % | 30 % | 32 % |

Table 7.19 shows the relative contributions of single response units to the total yield of the considered balance area. According to Table 7.18, it is based on the model runs 20, 47 and 66 and the $\alpha$-cut $FRA_{0.50}$. For comparison, the area of each response unit relative to the total area is included. Accordingly, the ‘slopes’ represent 53 % of the balance area. With 55 to 58 %, their contribution to the total yield is slightly higher, but in the same order of magnitude. The ‘quaternary’ unit comprises 31 % of the total area but yields only up to 15 % of the total cumulated recharge $Q_R$. Reversely, 16 % of the total area in the ‘high altitudes’ contribute around 30 % to the cumulated yield. In addition to the rainfall distribution, these numbers reflect the high yield in the higher carbonatic units, or the higher losses from soil storage in the quaternary, respectively.

Fuzzy arithmetic approach

Figure 7.22 shows the balance of cumulated recharge $Q_R$ and crop water demand $Q_c$ which results in mountain front recharge $Q_{MFR}$ for variant B and the $\alpha$-cut $FRA_{0.50}$ of the Fuzzy Recharge Areas. In contrast to the ‘A-variant’ with crisp input, rainfall and crop water demand are considered as fuzzy numbers. The abscissa shows the values of the water balance variables. The membership degrees are plotted on the ordinate axis.

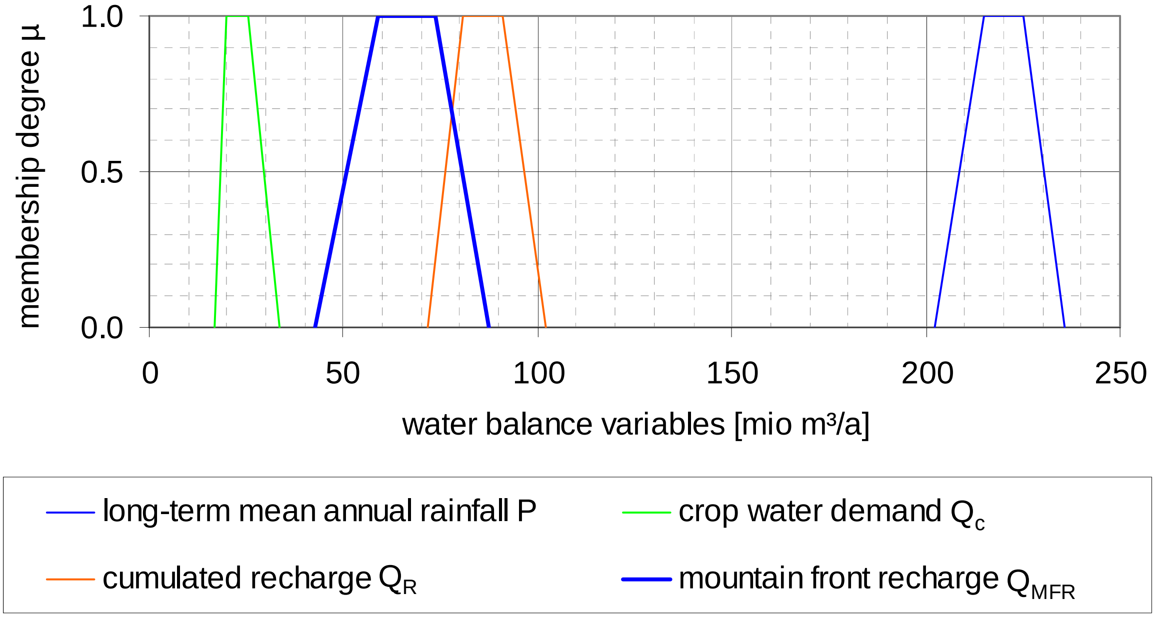


Figure 7.22: Results of the fuzzy arithmetic approach: Water balance for variant 1B ($\alpha$-cut $FRA_{0.5}$)

Figure 7.23 shows the outcome $Q_{MFR}$ for different $\alpha$-cuts $FRA_\alpha$ but each for the same variant A. The cores of the results for $\alpha$-cuts $FRA_{0.40}$, $FRA_{0.45}$ and $FRA_{0.50}$ are overlapping as well as for $FRA_{0.40}$ and $FRA_{0.45}$. Similar to the results of the conceptual hydrologic model, there is a considerable gap between the results for $\alpha = 0.55$ and $\alpha = 0.50$ due to the differences in spatial extent of the catchments and rainfall amounts in the transition zone.

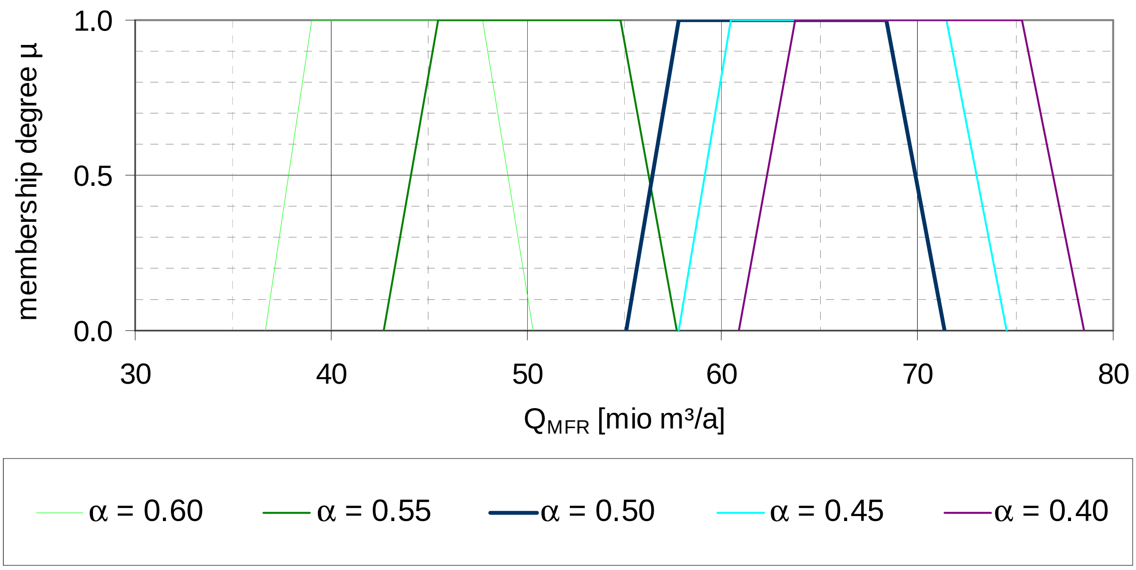


Figure 7.23: Results of the fuzzy arithmetic approach: $Q_{MFR}$ (variant A) for different $\alpha$-cuts of the Fuzzy Recharge Areas $FRA_\alpha$

Synopsis

In the following, the results of the two rainfall based approaches and the reference value based on steady state groundwater modelling are compared to each other. The results of the rainfall based approaches are compiled in Table 7.20. For the conceptual hydrologic model, the quartiles of the empirical CDF are shown. In the case of the fuzzy arithmetic approach, the supporting points of the trapezoidal fuzzy number are displayed. With regard to comparability, they refer to the 'A-variant' with crisp input. The 75 % - quartiles (Q3) are approximately the centre of the core of the fuzzy numbers. At the same time, they are similar to the modal values of the histograms in Figure 7.21 or Appendix B, respectively. The maximal values of the empirical distribution are slightly higher than the upper bound of the corresponding fuzzy numbers. The median values of the CDF (Q2) correspond to the lower bound of the fuzzy numbers.

The reference value based on groundwater modelling $Q_{GWM}$ = 68 mio m³/a is similar to the 75 % - quartiles values for α-cut levels $\alpha$ = 0.40 (maximal considered extent) and $\alpha = 0.45$. As mentioned above, these quartiles correspond to the modal values of the respective CDFs.

Table 7.20: Compilation of long-term average estimates $Q_{MFR}$ [mio m³/a] for selected α-cuts $FRA_\alpha$ based on the conceptual hydrologic model and fuzzy arithmetic (A-variant – crisp input)

| α | conceptual hydrologic model (quartiles of empirical CDF) | | | | fuzzy arithmetic variant A (crisp input) | | | |
|---|---|---|---|---|---|---|---|---|
| | Q1 ($\tilde{x}_{0.25}$) | Q2 ($\tilde{x}_{0.50}$) | Q3 ($\tilde{x}_{0.75}$) | max. $\tilde{x}_{1.00}$ | a (μ=0) | b (μ=1) | c (μ=1) | d (μ=0) |
| 0.40 | 46.6 | 59.9 | 70.6 | 83.3 | 60.9 | 63.7 | 75.3 | 78.5 |
| 0.45 | 44.0 | 56.7 | 66.8 | 79.0 | 57.8 | 60.5 | 71.5 | 74.6 |
| 0.50 | 41.8 | 54.0 | 63.7 | 75.5 | 55.1 | 57.8 | 68.4 | 71.4 |
| 0.55 | 31.6 | 42.3 | 50.6 | 61.0 | 42.7 | 45.4 | 54.8 | 57.6 |
| 0.60 | 26.7 | 36.5 | 44.3 | 54.0 | 36.6 | 39.0 | 47.7 | 50.3 |

### 7.4.2 *Time-dependent estimates*

Exemplarily for all considered parameterisations of the conceptual hydrologic model, Figure 7.24 shows the amount of groundwater recharge per month (cumulated over the whole balance area) and subsurface outflow from the mountain aquifer $Q_{MFR}$. It is based on an aquifer model as outlined in section 7.3.5. Obviously, the mountain aquifer can attenuate the high temporal variability of infiltration-recharge processes considerably. Consequently, the aquifer generally yields even in dry periods. It has to be mentioned, that translation, i.e. the consideration of time lags between rainfall event and peak of the groundwater response, is not yet included in this approach. Moreover, according to availability of reference data, a distinction of parameterisations for different response units may be reasonable. To date, the database to consider these issues is limited to selected aflaj hydrographs showing a time lag of 3 to 6 months (see section 7.3.5). Groundwater observations in the alluvial basin aquifer next to the mountain front are not available for the time being.

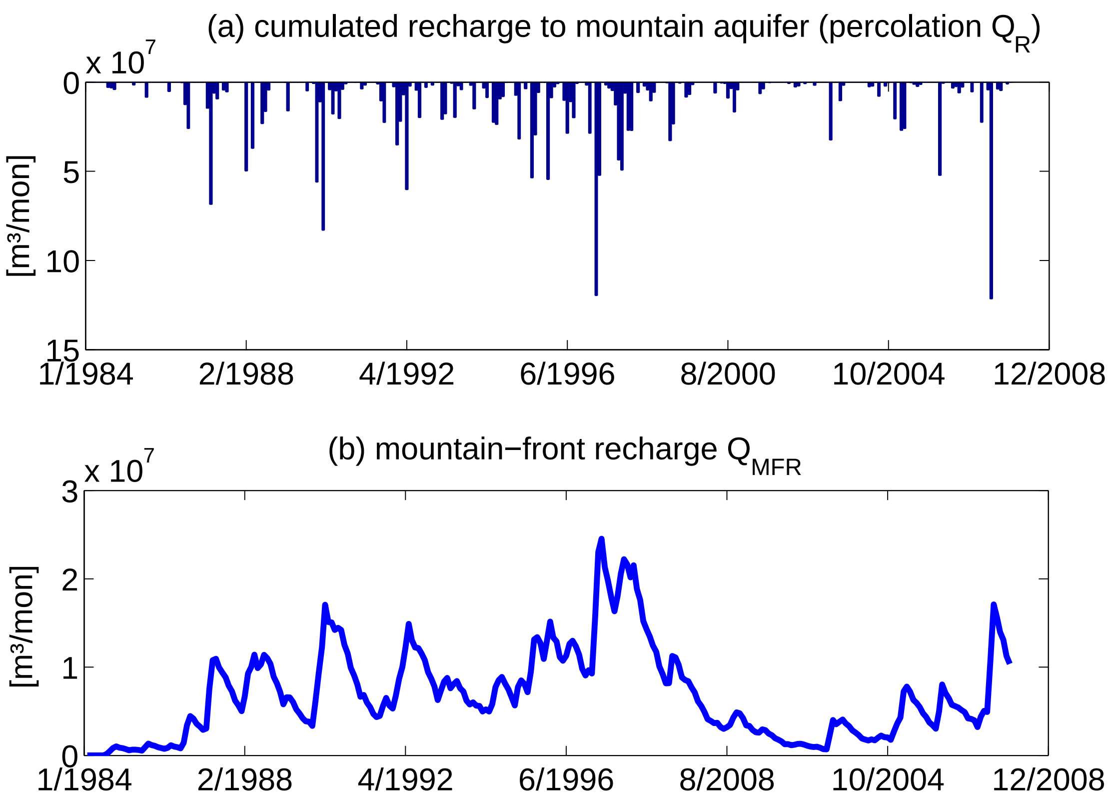


Figure 7.24: Total yield and subsurface outflow under consideration of retention in the mountain aquifer (parameter set 47, $\alpha$-cut $FRA_{0.5}$)

## 7.5 Consideration of uncertainties

Parameter uncertainties, i.e. the uncertainties in recharge rates as percentage of rainfall, were already considered. In the case of the conceptual hydrologic model, this was done based on different parameter sets covering a wide range of values for each parameter and different possible combinations.

In the fuzzy arithmetic approach, parameter uncertainty it is implicitly included due to fuzzy numbers of recharge rates or parameters of the APLIS-approach, respectively. In the following, input uncertainties are considered based on variant B of the fuzzy arithmetic approach which was presented in section 7.3.4. Exemplarily, Figure 7.25 shows the total mountain front recharge $Q_{MFR}$ for both variants A and B. The result of the 'B-variant' (fuzzy numbers for rainfall and crop water use) is obviously fuzzier than the outcome of the A-variant. With decreasing membership degrees, the confidence ranges of the correspondent α-cuts are increasing considerably. This covers the possible combinations of increased or reduced rainfall, cropped area and crop water use per area.

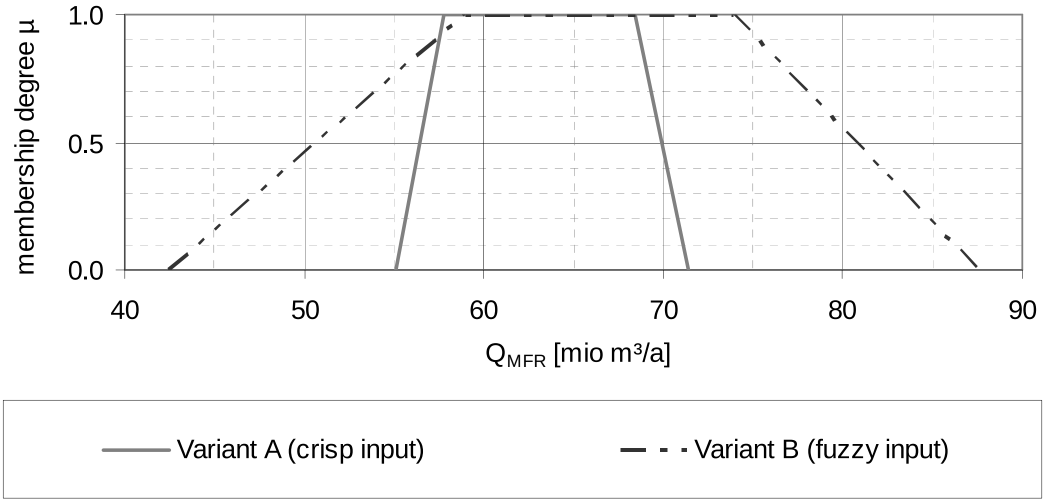


Figure 7.25: Results of both fuzzy arithmetic approaches A and B for α-cut $FRA_{0.5}$

Figure 7.26 shows the results of the B-variant for all 5 considered α-cut levels. Together, they give a picture of the range of possible values for the mean annual mountain-front recharge $Q_{MFR}$. Accordingly, the core values for the different spatial extents range from about 40 to 80 mio m³/a. The highest overall value is 94 mio m³/a (for $\alpha = 0.40$), while the lowest for $\alpha = 0.60$ amounts to 27 mio m³/a.

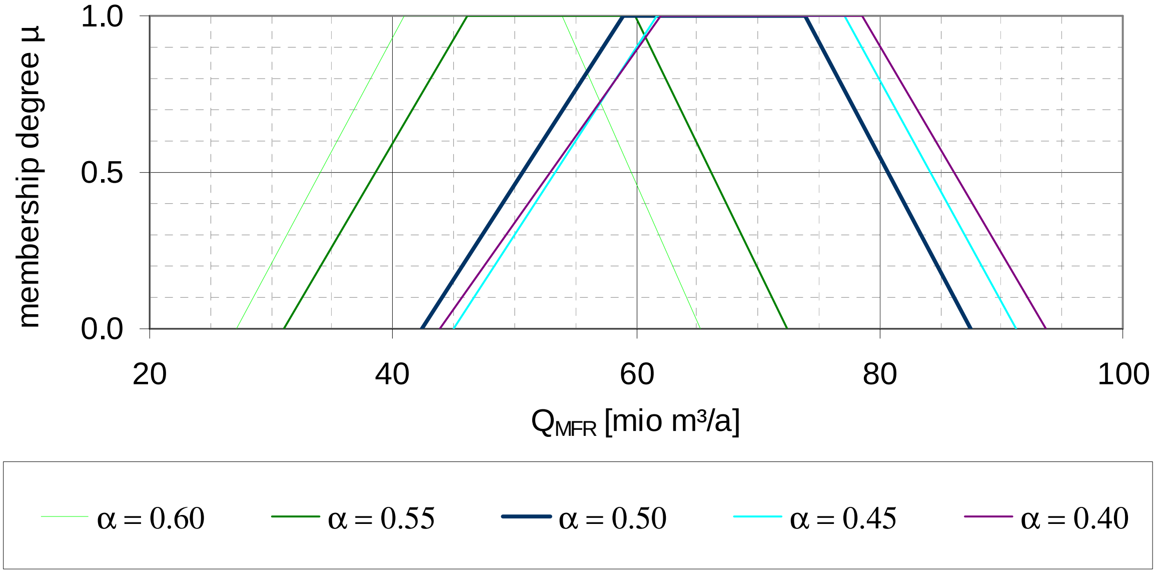


Figure 7.26: Results of the fuzzy arithmetic approach (Variant B) for all considered a-cut levels

The consideration of input uncertainties is limited to long-term average considerations so far. Though, uncertainties in (seasonal) crop water use or (event-specific) rainfall input are subject to temporal variations. Consequently, uncertainty assessment in a higher temporal resolution seems to be indicated to consider above mentioned issues. This, in turn, requires adequate climate data in a relatively high spatial resolution. In addition, crop water use depends strongly on cropping patterns which are mostly not available for the considered study area. Hence, a more sophisticated uncertainty analysis has necessarily to be based on various assumptions. In how far this is useful or necessary depends on the context in which assessment of mountain-front recharge is being done. In the frame of an integrated water resources management, it may be reasonable to compare the uncertainties of different water balance variables and their influencing parameters to decide on the each necessary degree of resolution.

It is therefore concluded, that the proposed fuzzy arithmetic approach is an efficient option to consider uncertainties which is suitable for large scale water balance assessment on the long-term. If a more sophisticated analysis is indicated, then the fuzzy arithmetic tool should be applied on a monthly time step including time-varying input. Alternatively, a probability based uncertainty assessment based on the conceptual hydrologic model is possible. For this purpose, appropriate stochastic input parameter sets are necessary.

## 7.6 Discussion & Conclusions

### *7.6.1 Water resources assessment in the study area*

Consideration of rainfall characteristics:

Compared to former water balance studies in the study area, this study considers the contribution of areas outside of the (surface) drainage divide of Wadi Maawil to the groundwater basin of the Maawil ‘plume’. For the first time, available rainfall stations in the high altitudes above 1800 m a.s.l. were considered in water balance computations. They show significantly higher rainfall amounts, than considered so far in stations of lower altitudes. The detailed analysis of seasonal rainfall characteristics in distinct altitude zones including stations above 1000 m a.s.l. supports the conceptual modelling approach.

Water balance assessment:

The conceptual model is based on monthly values. Time-dependent reference values to calibrate mountain-front recharge are lacking. Consequently, plausibility checks are based on long-term average considerations. A total of 75 parameter sets was considered, covering reasonable ranges of the single parameters. Sets resulting in implausible recharge rates were sorted out. For the remaining 56 runs, the recharge rates reflect the expected differences according to the different response units and seasons. They amplify the seasonal distribution of rainfall. They hence confirm the statement of Lerner et al. (1990), that winter rainfall is a main driver of mountain front recharge (MFR). The orders of magnitude of long-term average recharge rates in distinct response units and seasons are conclusive and also plausibly compared to available literature on karst environments in arid and semi-arid regions (Andreo et al., 2008; Hoetzl, 1995). Hence, the approach is able to provide reliable spatially distributed estimates of groundwater recharge.

The 56 model runs mentioned above result in a left skewed empirical distribution of long-term average subsurface outflow at the mountain front. The upper bound of the interquartile range is in good agreement with a reference value based on steady state groundwater modelling of 68 mio $m^3/a$ (Walther et al., 2012) and the complementary water balance approach using fuzzy arithmetic (variant 1). The latter is mainly based on the regionalisation approach APLIS (Andreo et al., 2008). Only for the response unit ‘quaternary’ (alluvium and slope colluvium), recharge was roughly estimated at values up to 15 %. In comparison, the conceptual modelling approach results in up to 17 % recharge in the summer season and up to around 30 % in winter. In the response unit ‘high altitudes’, the conceptual model shows slightly lower recharge rates than the APLIS-approach. In the response unit ‘slopes’, APLIS and the conceptual model result on average in similar recharge rates.

The fuzzy arithmetic approach was applied with crisp numbers of rainfall and crop water demand (variant A), but also with fuzzy numbers (variant B). Consequently, higher rainfall input due to the consideration of assumed measurement errors was considered. Additionally, higher crop water use due to a potentially extended cropped area, and a higher confidence range of crop water demand per area was considered. In summary, these opposed influences resulted in a higher overall fuzziness (regarding the resulting fuzzy number) or confidence interval (regarding a distinct $\alpha$-cut level). This covers the possible combinations of increased or reduced rainfall, cropped area and crop water use per area. Overall, the fuzzy arithmetic tool is an efficient option to consider uncertainties – provided, that the underlying assumptions are plausible. This aspect is guaranteed by the good agreement with the alternative approaches mentioned above.

The proportion of high altitude recharge compared to the total yield:

The relative contribution of the high altitudes to the total groundwater recharge is not as predominant as assumed based on the conclusions of Weyhenmeyer et al. (2002) or Macumber (2003). It is however possible that mountain oases rely on the recharge of the response units ‘slopes’ and ‘quaternary’, while high altitude recharge is flowing mainly to the alluvial basin aquifer via deep percolation and drainage in the mountain aquifer via fracture systems. Hence, the main portion of rainfall recharged in the high altitudes would recharge the alluvial basin aquifer. An option for further investigation is to analyse the aflaj in terms of water geochemistry and isotopy. This could result in conclusions on distinct source areas of aflaj water yield within the mountain catchment.

Fuzzy Recharge Areas:

The choice of the $\alpha$-cut levels presented above represents a range of potential spatial extents of the groundwater basin which is most reasonable considering the available expert knowledge on the study area. In the first instance, an $\alpha$-cut $FRA_{0.5}$ is assumed to be a realistic assessment.

$\alpha$-cuts $FRA_{\alpha}$ with $0.45 \leq \alpha \leq 0.55$ are assumed to be reasonable confidence ranges for water resources assessment in the study area. It has to be mentioned, that the variation in total yield from $\alpha = 0.50$ to $\alpha = 0.55$ is considerable. Due to maximum values of rainfall amounts and recharge rates in the resulting transition zone, the vague spatial extent results in a confidence interval of about 30 % of the total subsurface outflow at the mountain front.

From the viewpoint of water resources assessment it is recommended to consider an extended study area including the western Farah ‘plume’ as well as the groundwater basins south to the Jebel Akhdar for future work to substantiate this issue in the frame of a large scale assessment. The consideration of adjacent groundwater basins is supported by the concept of the Fuzzy Recharge Areas (see section 3.2). Consequently, the approaches presented above can easily be extended to adjacent groundwater basins.

Time-dependent estimates and (inverse) groundwater modelling:

Groundwater monitoring data in the alluvial basin aquifer is only available about 5 km downstream to the mountain front zone. Hence, at the time being, there is no observed reference data available to check time-dependent assessment of MFR. A reliable transfer between time-dependent subsurface outflow at the mountain front and (transient) upstream inflow to the groundwater model domain is lacking. Consequently, supplementary groundwater stations and additional bore profiles in close distance to the mountain front as well as between mountain front and actually available bores on the Batinah plain are desirable. This would allow a more direct link of the mountain catchment, which mainly recharges the alluvial basin aquifer and the groundwater model domain.

If one takes this thought further, even a best possible assessment of agricultural water use in the coastal zone is a contribution to the assessment of natural water yield in the mountain catchment. Its accuracy influences the reliability of the groundwater model, which is, in turn, an important means to cross-check time-dependent assessment of mountain front recharge. In other words, groundwater management and assessment of sink and source terms are interlinked. An increased reliability of one component supports the assessment of the other ones.

### *7.6.2 Modelling approaches*

Based on the sensitivity analysis in section 6.4.2 and on the results of the case study application it is concluded, that the proposed non-linear seasonal rainfall relationships based on water balance considerations are a reasonable approach for reliable water balance estimates in data scarce arid mountain regions. Compared to the assessment approaches discussed in section 2.3, the conceptual hydrologic model is most comparable to the approach of Hughes et al. (2008). Both approaches are spatially distributed. However, in comparison to Hughes et al., the presented model incorporates more process knowledge for it considers the main recharge mechanisms in deriving the response functions.

The conceptual hydrologic model is based on a monthly time step. This integration over time is one of the main simplifications of this approach. This concerns especially the estimation of the maximum (cumulated) infiltration, which does not only include the number of rainy days per month, but also the temporal distribution of rainfall intensity within an event. According to Al-Rawas and Valeo (2009), this is highly variable. Consequently, the infiltration parameter has definitely to be considered as a calibration parameter. Its physical meaning is limited to reasonable proportions between the response units (promotion of infiltration) or seasons (proportion of hours with significant rainfall). A way to substantiate its estimate would be to consider the temporal distributions of long duration events (> 6 h), which were not considered yet. All in all, only a sub-daily resolution is able to describe this aspect more adequately. A daily time step would be once again a compromise in this regard.

The applied approach for derivation of the non-linear rainfall-recharge relationships shows a high sensitivity to changes in the assumed mean seasonal soil moisture deficit (SMD). The deeper the soil profile, the higher the potential SMD and, thus, the uncertainties related to its estimates. Analogously, vegetation cover is challenging for this simple consideration of soil moisture status. It is concluded, that the approach is reliable for rock outcrops, raw and shallow soils with only scattered vegetation. This is in accordance with the envisaged application, namely the assessment of mountain front recharge in arid environments.

In the case of a considerable vegetation cover, the suitability of the model approach has to be proved. At least, a supplementary assessment of mean seasonal crop water use is useful to estimate the seasonal SMD. This can result in a revision or refinement of the seasons.

The application of the approach in similar settings is highly desirable to corroborate the approach, but also to gather experiences regarding appropriate response functions or parameters for their derivation in different hydrogeologic conditions. This could be a way towards a more widespread application by analogy with the SCS Curve Number methodology (SCS-CN) (SCS, 1956) which is used to estimate effective rainfall. This approach was derived based on empirical observations in various catchments of the USA. Actually, it is applied all over the world including the Arabian peninsula, for example by Wheater et al. (1995).

As outlined in Table 2.1, drainage from the actual location of recharge to the mountain front can follow either the alluvial valleys (predominantly indirect recharge), or the mountain aquifer after deep percolation (predominantly direct recharge from high altitudes). The conceptual hydrologic model is, in principle, adaptable so that distinct response functions for direct, localised and indirect recharge and even for surface runoff could be defined. Accordingly, the layer 'Fuzzy Recharge Areas' could be subdivided into different layers representing the recharge mechanisms mentioned above. In another words, parameterisation and drainage paths could be treated separately. This would allow including the observed surface runoff as an additional objective in model calibration besides subsurface flow components.

Moreover, the fundamental structure would allow to overcome the usual restriction of surface drainage direction and to implement drainage patterns which are, so far, reserved to physically based 3D numerical models or to highly conceptual watershed models. Thus, in a technically easy way, the model structure would allow considering available expert knowledge or, alternatively, assumptions on surface and subsurface drainage patterns, in combination with a robust approach to estimate the magnitudes of the respective fluxes.

# 8 Summary

Reliable estimates of mountain-front recharge are urgently needed in the context of integrated water resources management in arid regions. Time dependent estimates are highly desirable as boundary condition for prognostic transient groundwater management. To date, this is not yet state-of-the-art. The scarce and uncertain database implies the need for new approaches with reduced complexity but exploiting all the qualitative and quantitative information contained in available data. To achieve this goal, a novel strategy for rainfall based estimates of mountain-front recharge was developed.

An innovative conceptual hydrologic modelling approach based on non-linear seasonal rainfall-recharge relationships is considered to be the best possible solution for monthly estimates of mountain-front recharge under data scarcity. The algorithm to derive the response functions is based on a mass balance equation which includes, among other variables, direct recharge at site and indirect recharge during lateral movement of water. Their assessment is a function of parameters representing initial losses, infiltration, long-term mean seasonal soil moisture deficit, and transmission losses. Retention in the mountain aquifer is considered via serial two-reservoir models. The analysis of seasonality in relationships between altitude, rainfall amounts and occurrence is an important contribution to the parameterisation of the model. Moreover, it is a step forward in the analysis of arid zone rainfall characteristics in general.

A complementary approach, which is likewise based on spatially distributed rainfall, provides estimates of long-term mean annual groundwater recharge. It uses fuzzy arithmetic to assess the uncertainties of recharge estimates and crop water use in mountain oases.

Fuzzy regions are used to portray uncertainties with respect to the actually unknown extent of groundwater basins in specific geological settings. Selected subsets ($\alpha$-cuts) are the discrete spatial reference in applying the two assessment approaches mentioned above. Available expert knowledge on groundwater recharge areas and flow paths based on isotopy, geochemistry, or 3D geological modelling can be included. Furthermore, the use of fuzzy regions supports the complementary consideration of adjacent basins. This enhances large scale water resources assessment in multi-basin systems, where regional groundwater flow crosses surface drainage divides.

The proposed strategy was tested in a large-scale arid mountain area. The adequacy of the new approach was confirmed by comparing the outcome of the proposed models with the inversely computed inflow to a steady state groundwater model for the adjacent basin aquifer. The recharge rates, which result from the conceptual hydrologic model for distinct terrain types and seasons, are in accordance with scientific literature. This is an argument in favour of the hypothesis, that an approach which incorporates process knowledge, though with reduced complexity, is able to provide reliable results on the large scale. In contrast to available empirical approaches, it models variability both in time and space. In addition, it is regionally transferable because it incorporates process knowledge. Its application is not limited by the availability of high resolution rainfall data. Thus, it is comparatively easy to provide input time series which are long enough to represent wet and dry periods or periodical cycles in rainfall, as observed in the pilot study area.

The transition zone between the different aquifer systems in the investigated study area is located in the high-altitude region, where high rainfall amounts coincide with relatively high recharge rates. As a consequence, the uncertainty in the actually unknown extent of the groundwater basins is quantitatively important for the considered water resources system. It is therefore concluded that the use of the fuzzy regions to assess this source of uncertainties is an essential contribution to water resources management under uncertainty in similar settings.

As a summary, the proposed strategy provides more reliable estimates of mountain-front recharge in the face of scarce and uncertain data.

# 9 Prospects for future work

Hydrogeologic survey and groundwater monitoring in the alluvial basin aquifer near to the mountain front zone is the most promising option to enhance water resources assessment in the discussed study area. This would allow the extension of the groundwater modelling domain towards the mountains, which mainly recharge the alluvial basin aquifer. On this basis, the calibration of the conceptual hydrologic model could be improved. Moreover, the routing of mountain-front recharge towards the coastal zone could be improved.

Beyond this study, the request for data acquisition in the mountain front zone mentioned above can be understood as a general recommendation for mountain block systems in general and, first and foremost, for selected, well investigated experimental catchments. This would contribute to understand the complex surface-groundwater interactions at the interface between mountain blocks and alluvial basin aquifers.

The application of the new conceptual hydrologic modelling approach in similar settings is desirable. The comparison of the each suitable parameter sets or response functions would be a step towards urgently needed options for inter-site comparisons, or even regionalisation in arid mountain environments.

## List of Figures

## List of Tables

## List of Symbols

| | |
|---|---|
| $\alpha$ | cut level of a fuzzy set [-] |
| A | area [$L^2$] |
| $\overline{\mathbf{A}}$ | complement of A |
| $A_c$ | cropped area |
| crisp | "not fuzzy", distinct |
| $\delta$ | deviation from vienna standard [‰] |
| $\Delta$ | increment |
| ET | evaporation |
| $ET_0$ | reference evapotranspiration [mm] |
| $ET_{actual}$ | actual evapotranspiration |
| $ET_C$ | crop evapotranspiration [L/T] |
| ETP | evapotranspiration |
| $ET_{surface}$ | surface wetting loss |
| *falaj* (pl. *aflaj*) | traditional irrigation system; similar to the iranian *qanat* systems |
| K | reservoir constant [d] |
| $k_c$ | crop coefficient |
| $\mu$ | membership degree [-] |
| max | maximum |
| min | minimum |
| n | sample size |
| $n_{SMR\ alluvium}$ | model parameter (n-th root) |
| $n_{transm\ loss}$ | model parameter (n-th root) |
| P | precipitation |
| $P_{break}$ | model parameter (rainfall value of breakpoint) |
| $P_{eff}$ | effective precipitation |
| $P_{sill}$ | model parameter (rainfall threshold) |
| Q | discharge [$L^3/T$] |
| Q1, Q2, Q3 | quartiles of a distribution function |
| $Q_C$ | crop water use [$L^3/T$] |
| $Q_{MFR}$ | mountain-front recharge or subsurface outflow at mountain front [$L^3/T$] |
| $Q_R$ | groundwater recharge [$L^3/T$] |
| $Q_{R,\ direct}$, $Q_{R,\ indirect}$ | direct / indirect recharge [$L^3/T$] |
| $Q_{wadi}$ | (surface) wadi runoff [$L^3/T$] |
| R | groundwater recharge rate [% of P] |
| $\Re$ | real number |
| R.H. | relative humidity [%] |
| $R_{break}$ | model parameter (recharge value of breakpoint) |
| Rh | recharge to high permeable storage [%] |
| Rl | recharge to low permeable storage [%] |
| Sh | high permeable storage |
| Sl | low permeable storage |
| supp. | support |
| V | storage volume [$L^3$] |

## List of Abbreviations

| | |
|---|---|
| 1D, 2D, 3D | one-dimensional, two-dimensional, three-dimensional |
| ANFIS | adaptive network based FIS |
| ANN | artificial neural network |
| CDF | cumulated distribution function |
| CL | classical (binary, two-valued) logic |
| CMB | chloride mass balance |
| DIFGA | Differenzenganglinienanalyse; approach for runoff component analysis according to Schwarze et al. (1999) |
| EDK | external drift kriging |
| FIS | fuzzy inference system |
| FL | fuzzy logic |
| FR | fuzzy region |
| FRA | fuzzy recharge area |
| GWML | global meteoric water line |
| HBV | Hydrologiska Byråns Vattenbalansavdelning; hydrologic model according to Bergström (1995) |
| HGRU | hydrogeologic response unit |
| HRU | hydrologic response unit |
| Inf | infiltration |
| init loss | initial loss |
| IQR | interquartile range |
| ITCZ | inter-tropical convergence zone |
| IWRM | integrated water resources management |
| LMWL | local meteroric water line |
| LTA | long-term average |
| m a.s.l. | meters above sea level |
| MAF | Ministry of Agriculture and Fisheries |
| MD | membership degree |
| MF | membership function |
| MFR | mountain-front recharge |
| MRMWR | Ministry of Rural Municipalities and Water Resources |
| MWR | Ministry of Water Resources |
| RMSE | root mean square error |
| SLR | single linear reservoir |
| SMD | soil moisture deficit |
| SMR | soil moisture replenishment |
| SO | southern oscillation |
| SVAT | soil-vegetation-atmosphere |
| WMO | World Meteorological Organization |
| WRA | water resources assessment |
| WT | wetting threshold |

# Appendix

A: Sensitivity of the response function to variations of the different model parameters

B: Histograms of subsurface outflow at the mountain front $Q_{MFR}$ based on different parameterisations of the conceptual hydrologic model

# A: Sensitivity of the response function to variations of the different model parameters

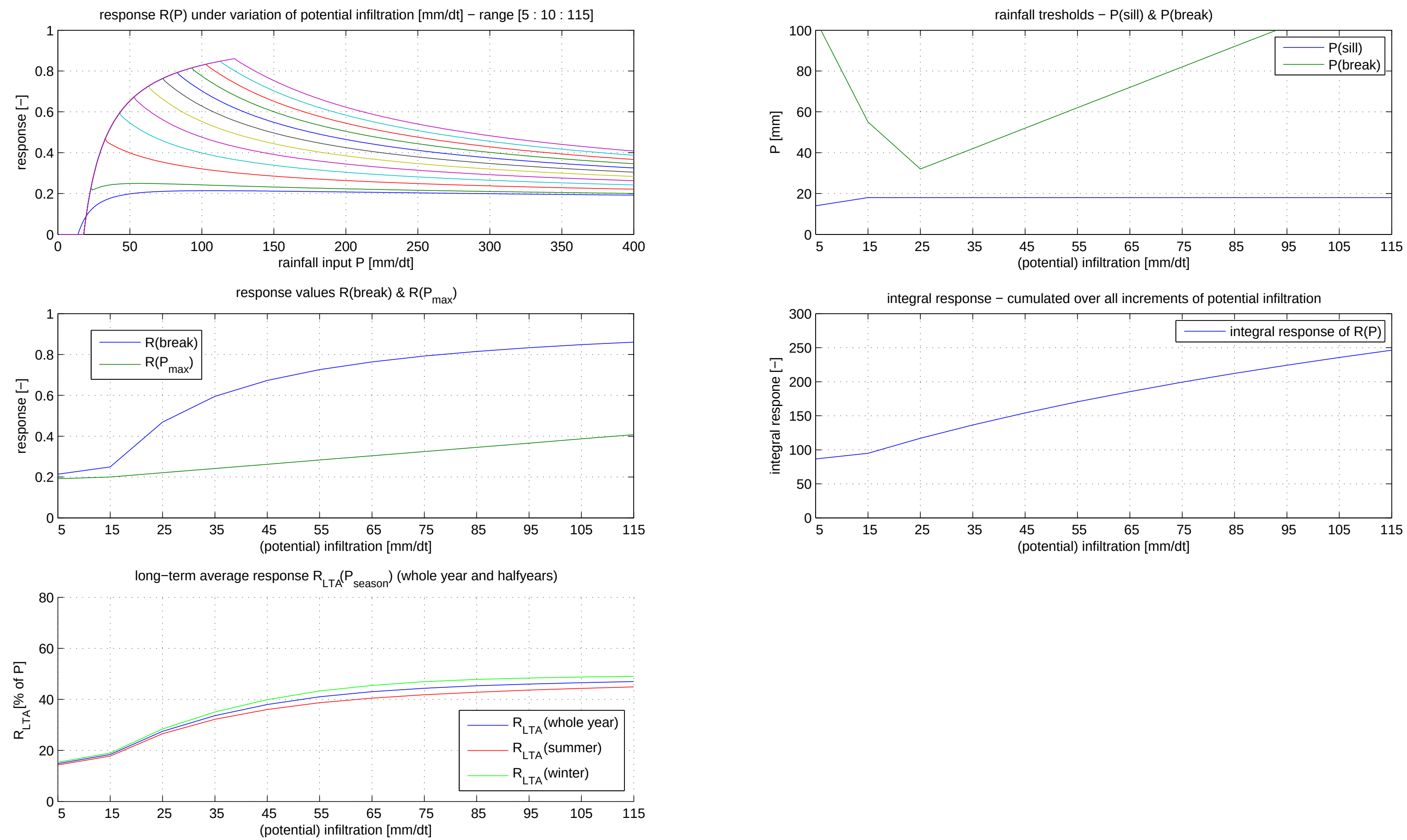


## A.1: Sensitivity of the response function to variations of (potential) infiltration

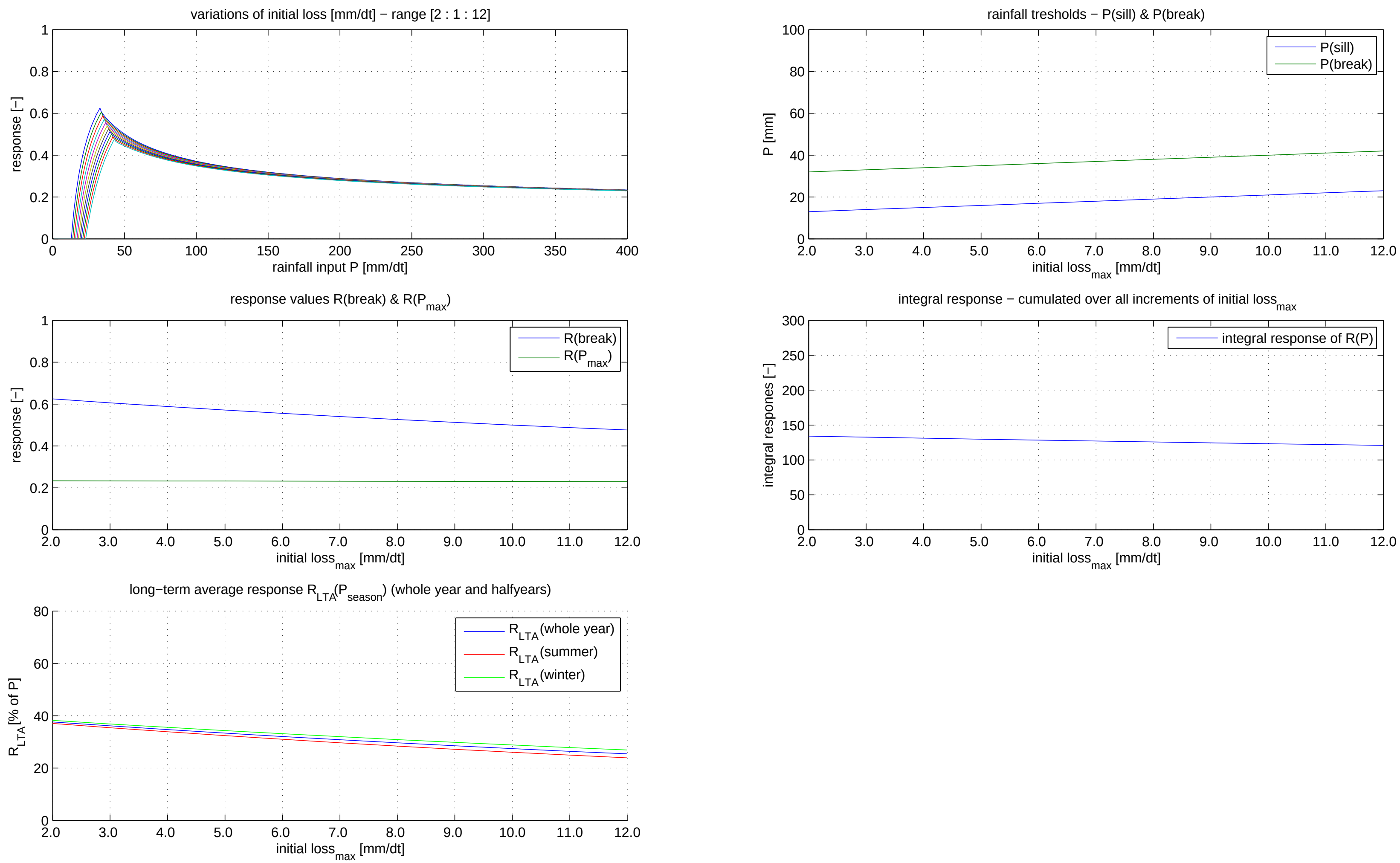


A.2: Sensitivity of the response function to variations of (potential) initial losses

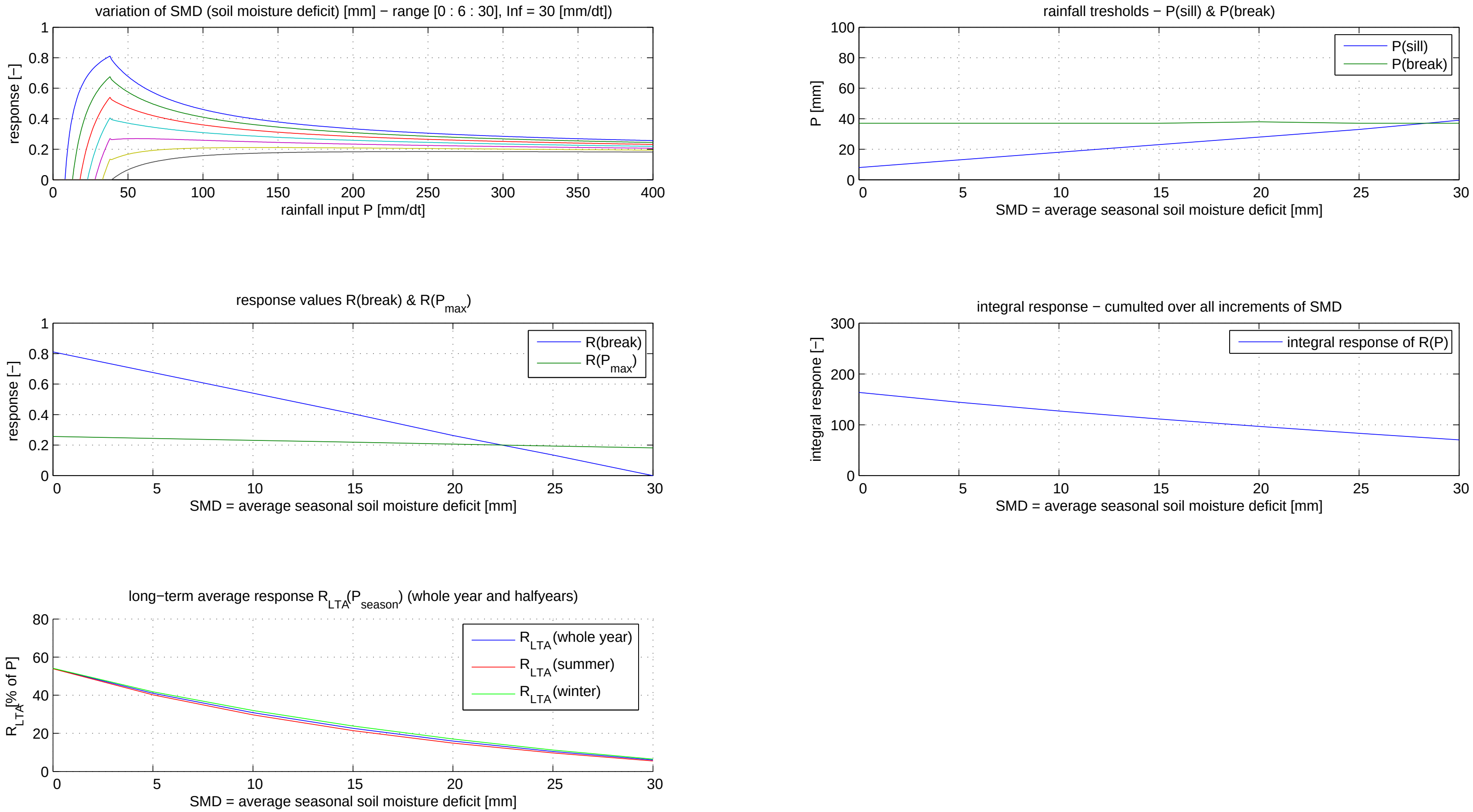


A.3: Sensitivity of the response function to variations of soil moisture deficit SMD (potential infiltration = 30 mm/dt)

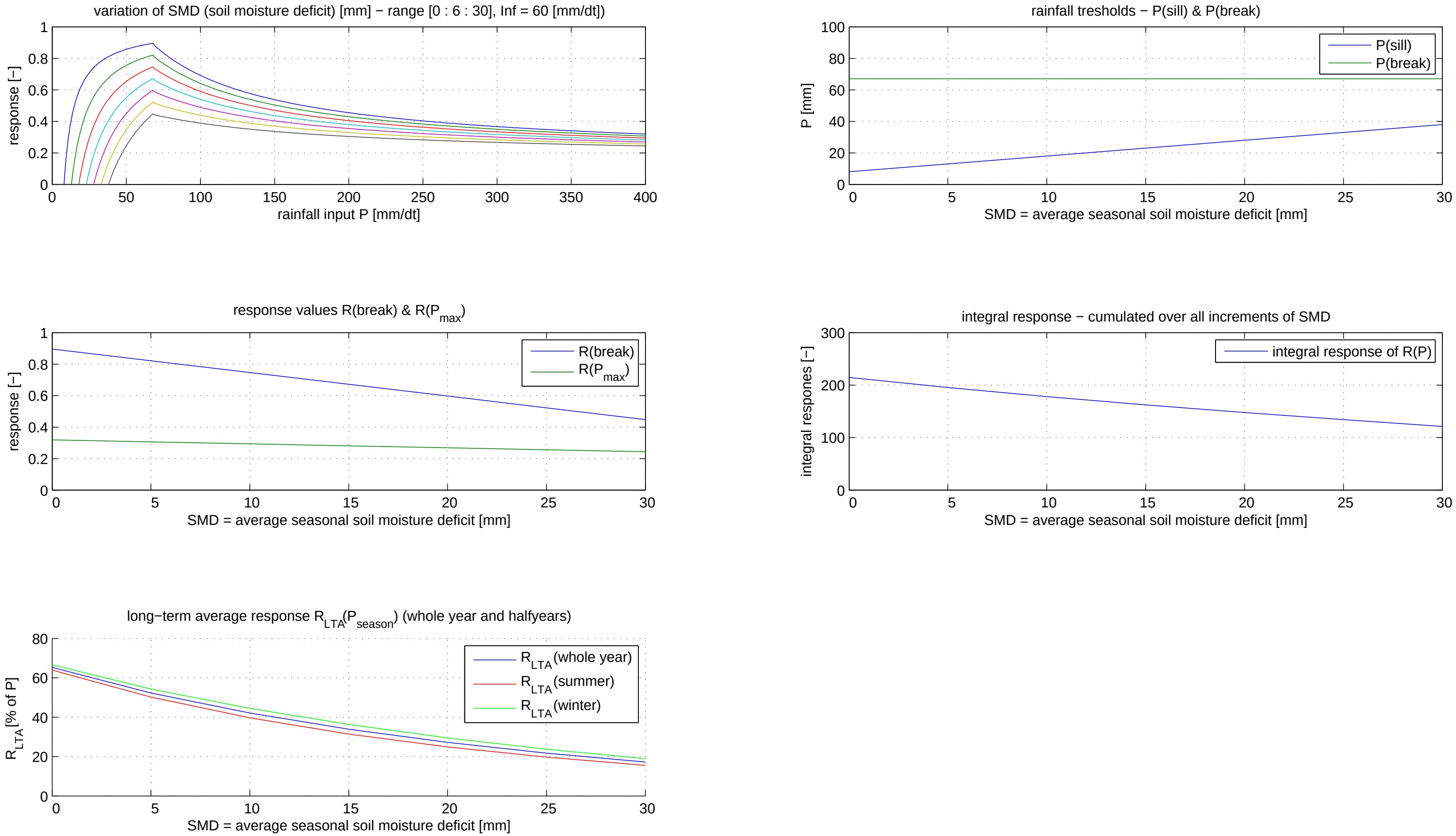


A.4: Sensitivity of the response function to variations of soil moisture deficit SMD (potential infiltration = 60 mm/dt)

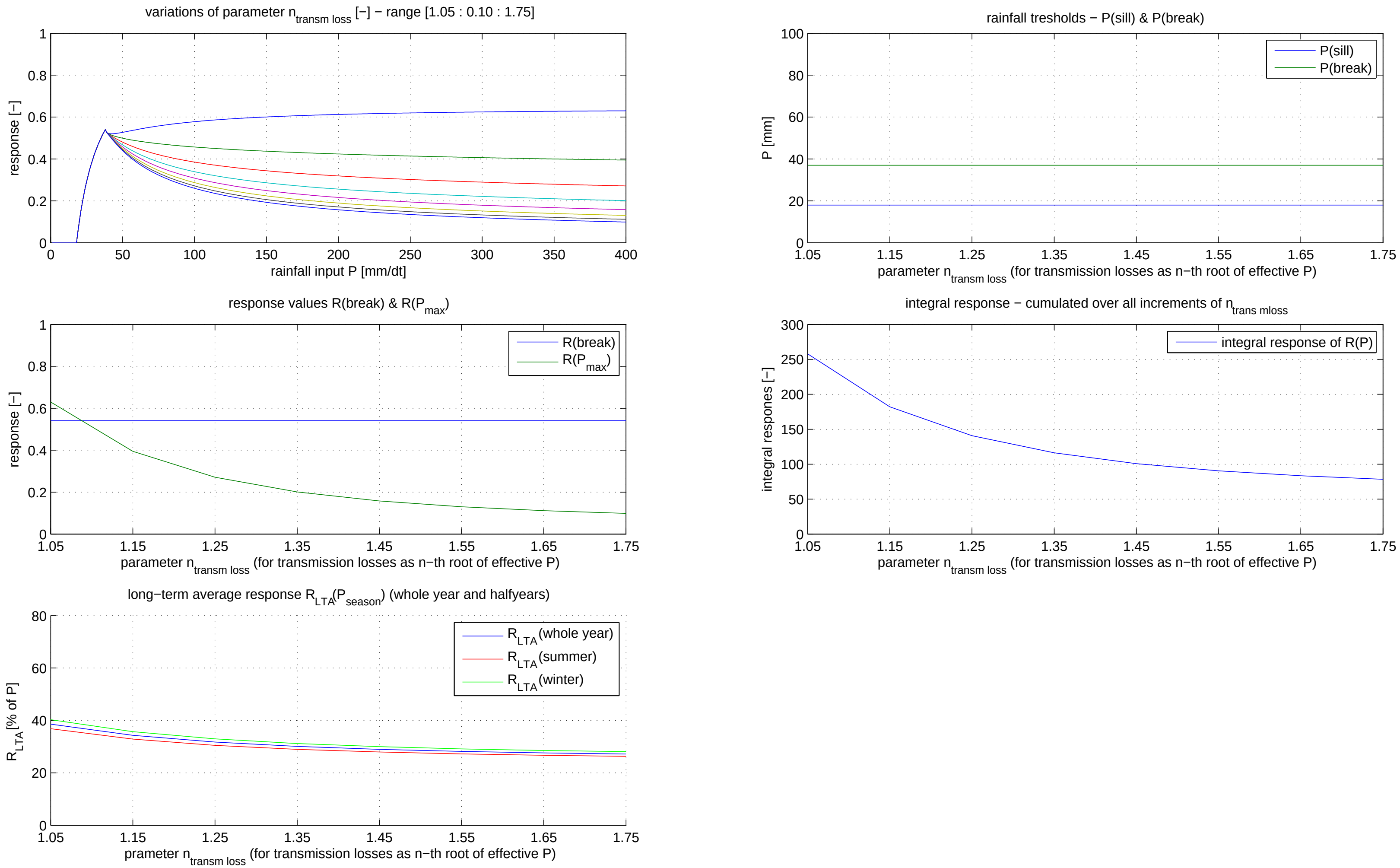


A.5: Sensitivity of the response function to variations of transmission losses

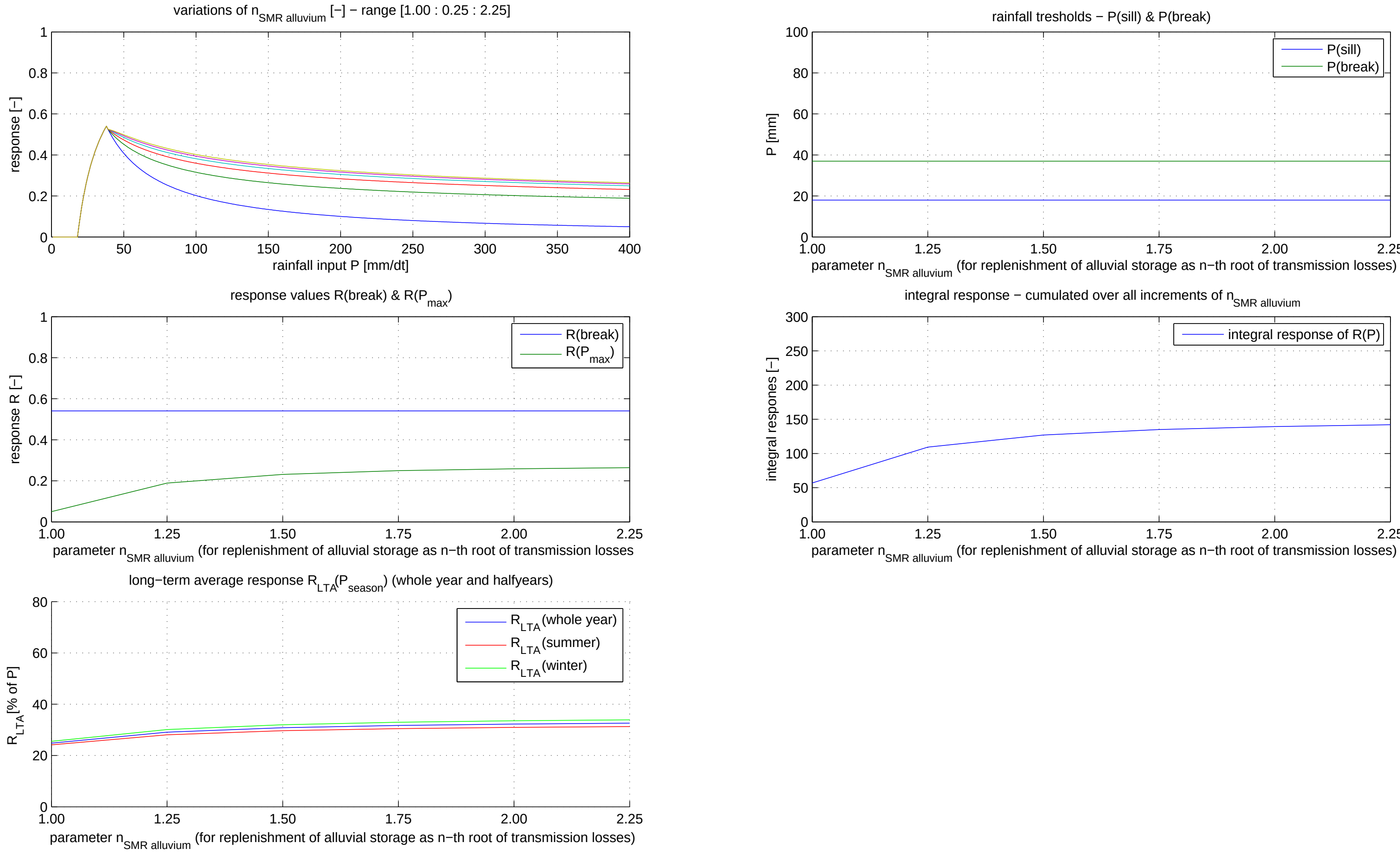


A.6: Sensitivity of the response function to variations of soil moisture replenishment in alluvial channels $SMR_{alluvium}$

## B: Histograms of subsurface outflow at the mountain front $Q_{MFR}$ based on different parameterisations of the conceptual hydrologic model

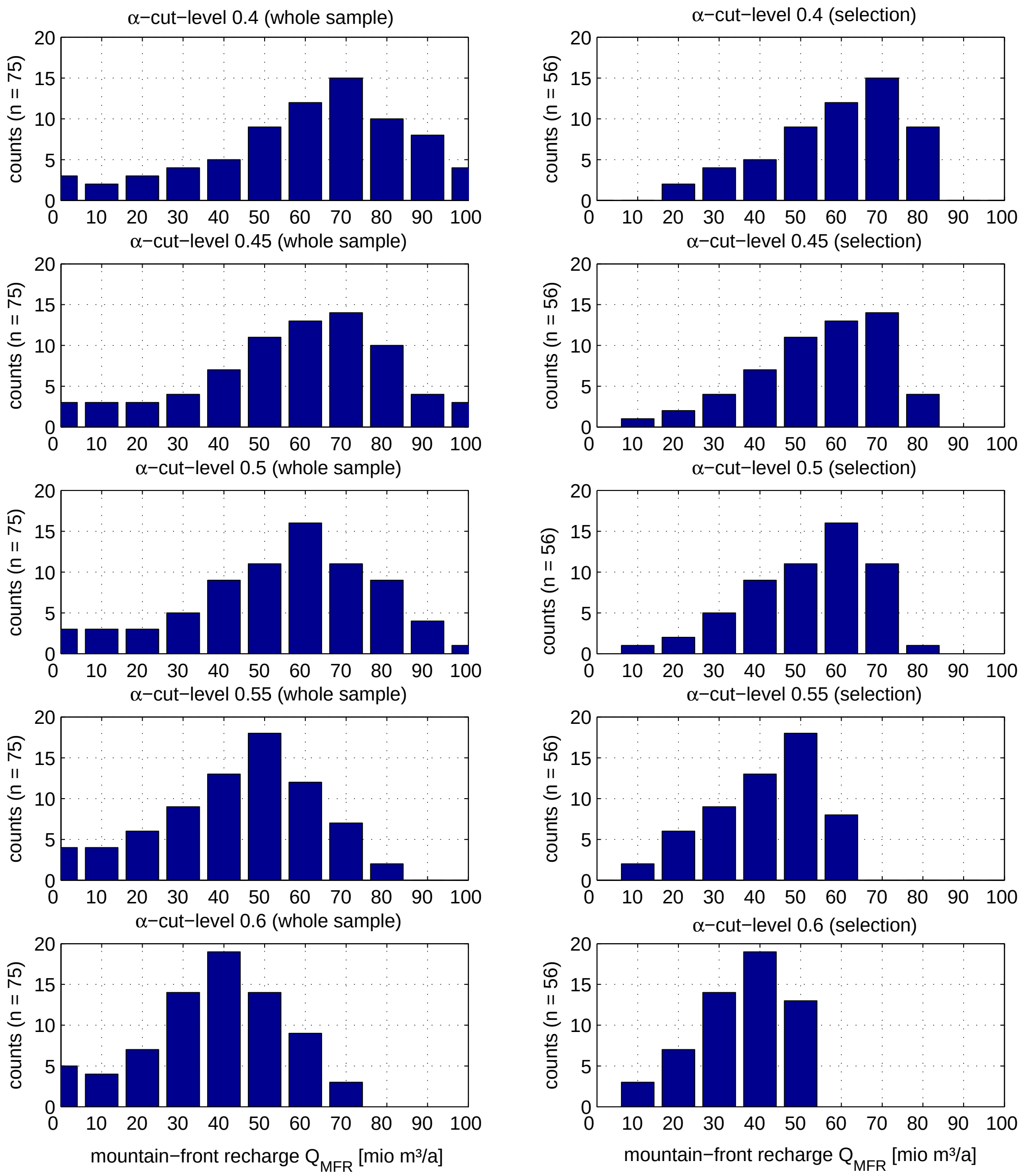


B: Histograms of subsurface outflow at the mountain front QMFR based on different parameterisations of the conceptual hydrologic model

## References


Ahmed, S., Maréchal, J.C., Ledoux, E. and Marsily, G.d., 2008. Groundwater flow modelling in hard-rock terrain in semi-arid areas: experience from India. In: H. Wheater, S. Sorooshian and K.D. Sharma (Editors), Hydrological modelling in arid and semi-arid areas. Cambridge University Press, pp. 157-189.

Al-Hattaly, S. and Al-Kindy, M., 2008. Water Resources Assessment and the Evaluation of Expected Impacts of Climatic Change in Oman., First International Conference Water Resources & Climate Change in the MENA Region, 2-4 Nov. 2008, Muscat, Sultanate of Oman.

Al-Qurashi, A., McIntyre, N., Wheater, H. and Unkrich, C., 2008. Application of the Kineros2 rainfall-runoff model to an arid catchment in Oman. Journal of Hydrology, 355(1-4): 91-105.

Al-Rawas, G.A. and Valeo, C., 2009. Characteristics of rainstorm temporal distributions in arid mountainous and coastal regions. Journal of Hydrology, 376(1-2): 318-326.

Al Shaqsi, S., 2004. The Socio-Economic and Cultural Aspects in the Implementation of Water Demand Management: A Case Study in the Sultanate of Oman, University of Nottingham, 370 pp.

Alkhoury, W., 2011. Hydrological modelling in the meso scale semiarid region of Wadi Kafrein / Jordan -The use of innovative techniques under data scarcity, Universtität Göttingen, 227 pp.

Allen, R.G., Pereira, L.S., Raes, D. and Smith, M., 1998. Crop Evapotranspiration (guidelines for computing crop water requirements), FAO - Food and Agriculture Organization of the United Nations, Rome.

Anderholm, S.K., 2001. Mountain-front recharge along the eastern side of the Middle Rio Grande Basin, Central New Mexico. USGS Water Resources Investigations Report 00–4010.

Andreo, B., Vias, J., Duran, J.J., Jimenez, P., Lopez-Geta, J.A. and Carrasco, F., 2008. Methodology for groundwater recharge assessment in carbonate aquifers: application to pilot sites in southern Spain. Hydrogeology Journal, 16(5): 911-925.

Bárdossy, A., 1997. Introduction to Geostatistics, Stuttgart, pp. 100.

Bergström, S., 1995. The HBV model. In: V.P. Singh (Editor), Computer Models of Watershed Hydrology. Water Resources Publications, Highlands Ranch, CO, pp. 443-476.

Beven, K., 1993. Prophecy, reality and uncertainty in distributed hydrological modelling. Advances in Water Resources, 16(1): 41-51.

Blöschl, G., 2006. Hydrologic synthesis: Across processes, places, and scales. Water Resour. Res., 42(3): W03S02.

Boussinesq, J., 1903. On a simple mode of flow of infiltration water tables with a horizontal stream bed, with a vertical ledge all around, when a part of this ledge is taken away from the surface to the bottom. Comptes Rendus Hebdomadaires Des Seances De L Academie Des Sciences, 137: 5-11.

Bredenkamp, D.B., 1990. Quantitative estimation of groundwater recharge by means of a simple rainfall-recharge-relationship. In: D.N. Lerner and R. Ababou (Editors), Groundwater Recharge: a guide to understanding and estimating natural recharge. International Contributions to Hydrogeology. Heise, Hannover (Germany), pp. 247-256.

Brook, G.A. and Sheen, S.W., 2000. Rainfall in Oman and the United Arab Emirates: Cyclicity, influence of the Southern Oscillation, and what the future may hold. The Arab World Geographer, 3(2): 78-96.

Canton, Y., Villagarcia, L., Jose Moro, M., Serrano-Ortiz, P., Were, A., Javier Alcala, F., Kowalski, A.S., Sole-Benet, A., Lazaro, R. and Domingo, F., 2010. Temporal dynamics of soil water balance components in a karst range in southeastern Spain: estimation of potential recharge. Hydrological Sciences Journal, 55(5): 737-753.

Chwala, C., Gmeiner, A., Qiu, W., Hipp, S., Nienaber, D., Siart, U., Eibert, T., Pohl, M., Seltmann, J., Fritz, J. and Kunstmann, H., 2012. Precipitation observation using microwave backhaul links in the alpine and pre-alpine region of Southern Germany. Hydrology and Earth System Sciences, 16(8): 2647-2661.

de Vries, J.J. and Simmers, I., 2002. Groundwater recharge: an overview of processes and challenges. Hydrogeology Journal, 10(1): 5-17.

Dewandel, B., Lachassagne, P., Boudier, F., Al-Hattali, S., Ladouche, B., Pinault, J.L. and Al-Suleimani, Z., 2005. A conceptual hydrogeological model of ophiolite hard-rock aquifers in Oman based on a multiscale and a multidisciplinary approach. Hydrogeology Journal, 13(5-6): 708-726.

Dooge, J.C.I., 1997. Searching for Simplicity in Hydrology. Surveys in Geophysics, 18(5): 511-534.

Dubois, D. and Prade, H.M., 1992. Fuzzy sets and systems / theory and applications. Academic Press, New York, 393 pp.

Eder, G., Nachtnebel, H.-P. and Sivapalan, M., 2005. Water Balance Modeling with Fuzzy Parameterizations: Application to An Alpine Catchment, pp. 125 - 146.

Fetter, C.W., 2001. Applied Hydrogeology. Prentice Hall, Upper Saddle River, New Jersey.

Fleckenstein, J.H. and Fogg, G.E., 2008. Efficient upscaling of hydraulic conductivity in heterogeneous alluvial aquifers. Hydrogeology Journal, 16(7): 1239-1250.

Flint, A.L., Flint, L.E., Kwicklis, E.M., Fabryka-Martin, J.T. and Bodvarsson, G.S., 2002. Estimating recharge at Yucca Mountain, Nevada, USA: comparison of methods. Hydrogeology Journal, 10(1): 180-204.

Freeze, R.A., Massmann, J., Smith, L., Sperling, T. and James, B., 1990. Hydrogeological Decision Analysis: 1. A Framework. Groundwater, 28(5): 738 - 766.

Gebremichael, A.W., 2010. Analysis and correction of rainfall data as a basis for water balance calculation: Al-Batinah Region, Oman, TU Dresden, Dresden, 40 pp.

Germann, U., Galli, G., Boscacci, M. and Bolliger, M., 2006. Radar precipitation measurement in a mountainous region. Quarterly Journal of the Royal Meteorological Society, 132(618): 1669-1692.

Gerner, A., Schütze, N. and Schmitz, G.H., 2012. Portrayal of fuzzy recharge areas for water balance modelling - a case study in northern Oman. Advances in Geosciences, 31(1): 1-7.

Geyer, T., Birk, S., Liedl, R. and Sauter, M., 2008. Quantification of temporal distribution of recharge in karst systems from spring hydrographs. Journal of Hydrology, 348(3-4): 452-463.

Giese, M., 2011. Abflussschätzung mittels Fuzzy Logic für ausgewählte Einzugsgebiete im Sultanat Oman, TU Dresden, Institute of Hydrology and Meteorology, Dresden, 96 pp.

Gleeson, T. and Manning, A.H., 2008. Regional groundwater flow in mountainous terrain: Three-dimensional simulations of topographic and hydrogeologic controls. Water Resour. Res., 44(10): 1-16.

Glennie, K.W., 1974. Geology of the Oman Mountains. Verhandelingen Koninklijk Nederlasnds Geologisch Mijnboukundig Genootschap, 31.

Grundmann, J., 2010. Analyse und Simulation von Unsicherheiten in der flächendifferenzierten Niederschlag-Abfluss-Modellierung, TU Dresden, Dresden, 137 pp.

Grundmann, J., Schütze, N., Schmitz, G.H. and Al Shaqsi, S., 2012. Towards an integrated arid zone water management using simulation based optimisation. Journal of Environmental Earth Sciences, 65(5): 1381-1394.

Gunkel, A. and Lange, J., 2011. New Insights Into The Natural Variability of Water Resources in The Lower Jordan River Basin. Water Resources Management, 10.1007/s11269-011-9903-1: 1-18.

Healy, R. and Scanlon, B., 2010. Estimating Groundwater Recharge. Cambridge University Press.

Hoetzl, H., 1995. Groundwater recharge in an arid karst area (Saudi Arabia), Application of Tracers in Arid Zone Hydrology (Proceedings of the Vienna Symposium, August 1994). IAHS Publ. no. 232, pp. 195-207.

Hughes, A.G., Mansour, M.M. and Robins, N.S., 2008. Evaluation of distributed recharge in an upland semi-arid karst system: the West Bank Mountain Aquifer, Middle East. Hydrogeology Journal, 16(5): 845-854.

Hundecha, Y., Bardossy, A. and Theisen, H.W., 2001. Development of a fuzzy logic-based rainfall-runoff model. Hydrological Sciences Journal-Journal Des Sciences Hydrologiques, 46(3): 363-376.

Jacobs, E., 2007. Modellierungsmuster für GIS und Unschärfe- Fuzzy-Methoden zur multiattributiven Raumbewertung, Humbolt-Universität Berlin.

Kessler, H., 1967. Water balance investigations in the karstic regions of Hungary. Actes du colloque de Dubrovnik. IAHS-UNESCO, Paris, pp. 91-105.

Khazaei, E., Spink, A.E.F. and Warner, J.W., 2003. A catchment water balance model for estimating groundwater recharge in arid and semiarid regions of south-east Iran. Hydrogeology Journal, 11(3): 333-342.

Király, L., 2002. Karstification and Groundwater Flow. In: F. Gabrovšek (Editor), Conference on Evolution of Karst: From Prekarst to Cessation, Postojna-Ljubljana, pp. 155-190.

Kraemer, S., Verworn, H.-R., Pfister, A. and Treis, A., 2012. Path-integrated rainfall measurements using a dual-frequency microwave link and quantification of radar signal attenuation. Hydrologie und Wasserbewirtschaftung, 56(2): 59-77.

Kwarteng, A.Y., Dorvlo, A.S. and Kumar, G.T.V., 2009. Analysis of a 27-year rainfall data (1977-2003) in the Sultanate of Oman. International Journal of Climatology, 29(4): 605-617.

Lange, J., Greenbaum, N., Husary, S., Ghanem, M., Leibundgut, C. and Schick, A.P., 2003. Runoff generation from successive simulated rainfalls on a rocky, semi-arid, Mediterranean hillslope. Hydrological Processes, 17(2): 279-296.

Lange, J., Leibundgut, C., Greenbaum, N. and Schick, A.P., 1999. A noncalibrated rainfall-runoff model for large, arid catchments. Water Resources Research, 35(7): 2161-2172.

Lerner, D.N., 1997. Groundwater Recharge. In: O.M. Saether and P. De Caritat (Editors), Geochemical Processes, Weathering and Groundwater Recharge in Catchments. A. A. Balkema, pp. 42.

Lerner, D.N., Issar, A. and Simmers, I., 1990. Groundwater recharge; a guide to understanding and estimating natural recharge. International Contributions to Hydrogeology, 8.

Lodwick, W.A., Anile, M. and Spinella, S., 2008. Introduction and Interpolation with Data containing Interval, Fuzzy, and Possibilistic Unvertainty Fuzzy Surfaces in GIS and Geographical Analysis: Theory, Analytical Methods, Algorithms, and Applications. In: W.A. Lodwick (Editor). CRC Press, pp. 1-47.

Love, D., Uhlenbrook, S. and van der Zaag, P., 2011. Regionalising a meso-catchment scale conceptual model for river basin management in the semi-arid environment. Physics and Chemistry of the Earth, 36(14-15): 747-760.

Macumber, P.G., 1998. The Cable Tool Program and Groundwater Flow in the Eastern Batinah Alluvial Aquifer, Ministry of Water Resources, Muscat.

Macumber, P.G., 2003. Lenses, Plumes and Wedges in the Sultanate of Oman: A Challenge for Groundwater Management. In: W.W. Wood and A.S. Alsharhan (Editors), Water Resources Perspectives: Evaluation, Management and Policy. Developments in Water Science. Elsevier, pp. 349-370.

MAF, 1990. Soil Atlas of Oman. Ministry of Agriculture and Fisheries, Muscat, Sultanate of Oman.

Makropoulos, C.K., Butler, D. and Maksimovic, C., 2008. Building Decision Support Systems based on Fuzzy Inference. In: R.J. Abrahart, D.P. Solomatine and L.M. See (Editors), Practical Hydroinformatics. Computational Intelligence and Technical Developments in Water Applications. Water Science and Technology Library. Springer, pp. 215-228.

Manning, A.H. and Solomon, D.K., 2003. Using noble gases to investigate mountain-front recharge. Journal of Hydrology, 275(3-4): 194-207.

MathWorks, 2008. Matlab 2008b. The MathWorks, Inc., Natick, MA.

Matter, J.M., Waber, H.N. and Matter, A., 2005. Recharge areas and geochemical evolution of groundwater in an alluvial aquifer system in the Sultanate of Oman. Hydrogeology Journal, 14(14): 203-224.

Maxey, G.B. and Eakin, T.E., 1950. Groundwater in White River Valley, White Pine, Nye, and Lincoln Counties, Nevada. NV State Eng Water Resour Bull 8: 59.

Menzel, L., 1997. Modellierung der Evapotranspiration im System Boden-Pflanze-Atmosphäre, ETH, Zürich, 122 pp.

Messer, H., Zinevich, A. and Alpert, P., 2012. Environmental Sensor Networks Using Existing Wireless Communication Systems for Rainfall and Wind Velocity Measurements. Ieee Instrumentation & Measurement Magazine, 15(2): 32-38.

Morin, E. and Gabella, M., 2007. Radar-based quantitative precipitation estimation over Mediterranean and dry climate regimes. Journal of Geophysical Research-Atmospheres, 112(D20): 13.

Morris, a. and Kokhan, S.A.A., 2007. Abstracts Geographic Uncertainty in Enviroanmental Security. In: a. Morris and S. Kokhan (Editors). Springer.

MRMWR, 2001. Aflaj Inventory Project Summary Report, Ministry of Regional Municipalities, Environment and Water Resources.

MWR, 1995. Water Resources of the Sultanate of Oman. An introductory guide. Ministry of Water Resources, Muscat, Sultanate of Oman.

MWR, 1996. Jabal Akhdar Hydrogeological Assessment, Ministry of Water Resources, Groundwater Department, Hydrogeology Section.

Pakosch, S., 2011. Development of a fuzzy rule based expert system for flood forecasts within the meso-scale Upper Main basin, Universität der Bundeswehr München, 162 pp.

Peleg, N. and Morin, E., 2012. Convective rain cells: Radar-derived spatiotemporal characteristics and synoptic patterns over the eastern Mediterranean. Journal of Geophysical Research-Atmospheres, 117(D15): 17.

Penman, H.L., 1948. Natural evaporation from open water, bare soil and grass. Proceedings of the Royal Society A, 193: 120–145.

Peters, R., Schwärzel, K. and Feger, K.H., 2011. Fuzzy-Inference-Systeme zur Regionalisierung des Standortswasserhaushaltes von Wäldern. Waldökologie, Landschaftsforschung und Naturschutz(12/2011): 111-117.

Philipp, A. and Grundmann, J., 2013. An Integrated Modeling System for Flash Flood Routing in Ephemeral Rivers under the Influence of Groundwater Recharge Dams. Journal of Hydraulic Engineering, 10.1061/(ASCE)HY.1943-7900.0000766(Apr. 13, 2013).

Rayitsfeld, A., Samuels, R., Zinevich, A., Hadar, U. and Alpert, P., 2011. Comparison of two methodologies for long term rainfall monitoring using a commercial microwave communication system. Atmospheric Research, 104: 119-127.

Scanlon, B.R. and Cook, P.G., 2002. Theme issue on groundwater recharge - Preface. Hydrogeology Journal, 10(1): 3-4.

Scanlon, B.R., Healy, R.W. and Cook, P.G., 2002. Choosing appropriate techniques for quantifying groundwater recharge. Hydrogeology Journal, 10(2): 18-39.

Scanlon, B.R., Keese, K.E., Flint, A.L., Flint, L.E., Gaye, C.B., Edmunds, W.M. and Simmers, I., 2006. Global synthesis of groundwater recharge in semiarid and arid regions. Hydrological Processes, 20(15): 3335-3370.

Schwarze, R., 2004. Regionalspezifische Untersuchungen zum Wasser- und Stofffluss im Festgesteinsbereich. In: A. Becker and W. Lahmer (Editors), Wasser- und Nährstoffhaushalt im Elbegebiet und Möglichkeiten zur Stoffeintragsminderung. - Konzepte für die nachhaltige Entwicklung einer Flusslandschaft. Weißenseeverlag, Berlin, pp. 183 - 225.

Schwarze, R., Dröge, W. and Opherden, K., 1999. Regional analysis and modelling of groundwater runoff components from catchments in hard rock areas Regionalization in Hydrology. IAHS, pp. 221-232.

SCS, 1956. Hydrology. National Engineering Handbook, Supplement A. Soil Conservation Service, USDA, Washington, D.C.

Seibert, J., 2002. HBV light version 2, User's manual. Environmental Assessment, SLU, Uppsala.

Sen, Z., 2010. Fuzzy logic and hydrological modeling. CRC Press, Boca Raton, Fla. , 340 pp.

Sheffer, N.A., Dafny, E., Gvirtzman, H., Navon, S., Frumkin, A. and Morin, E., 2010. Hydrometeorological daily recharge assessment model (DREAM) for the Western Mountain Aquifer, Israel: Model application and effects of temporal patterns. Water Resources Research, 46(W05510): 16.

Siebert, S., Nagieb, M. and Buerkert, A., 2007. Climate and irrigation water use of a mountain oasis in northern Oman. Agricultural Water Management, 89(1-2): 1-14.

Sorooshian, S., Hsu, K.-L., Imam, B. and Hong, Y., 2008. Global precipitation estimation from satellite imagery using artificial neural networks. In: H. Wheater, S. Sorooshian and K.D. Sharma (Editors), Hydrological modelling in arid and semi-arid areas. Cambridge University Press, pp. 21-28.

Stanger, G., 1985. Coastal Salinization - a case-history from Oman. Agricultural Water Management, 9(4): 269-286.

Stanger, G., 1986. The Hydrogeology of the Oman Mountains. PhD Thesis, Open University, Milton Keynes, 355 pp.

Tavares Wahren, F., Tarasiuk, M., Mykhnovych, A., Kit, M., Feger, K.-H. and Schwaerzel, K., 2012. Estimation of spatially distributed soil information: dealing with data shortages in the Western Bug Basin, Ukraine. Environmental Earth Sciences, 65(5): 1501-1510.

Viviroli, D., Dürr, H.H., Messerli, B., Meybeck, M. and Weingartner, R., 2007. Mountains of the world, water towers for humanity: Typology, mapping, and global significance. Water Resour. Res., 43(W07447): 13.

Walther, M., Delfs, J.O., Grundmann, J., Kolditz, O. and Liedl, R., 2012. Saltwater intrusion modeling: Verification and application to an agricultural coastal arid region in Oman. Journal of Computational and Applied Mathematics, 236(18): 4798-4809.

Warner, T.T., 2004. Desert Meteorology. Cambridge University Press, 595 pp.

Weyhenmeyer, C.E., Burns, S.J., Waber, H.N., Aeschbach-Hertig, W., Kipfer, R., Loosli, H.H. and Matter, A., 2000. Cool glacial temperatures and changes in moisture source recorded in Oman groundwaters. Science, 287(5454): 842-845.

Weyhenmeyer, C.E., Burns, S.J., Waber, H.N., Macumber, P.G. and Matter, A., 2002. Isotope study of moisture sources, recharge areas, and groundwater flow paths within the eastern Batinah coastal plain, Sultanate of Oman. Water Resour. Res., 38(10): 1-22.

Wheater, H. and Al-Weshah, R.A., 2002. Hydrology of wadi systems. 55, IHP regional network on wadi hydrology in the Arab region In co-operation with the Arab League Educational, Cultural and Scientific Organization (ALECSO) and the Arab Centre for Studies of Arid Zones and Dry Lands (ACSAD).

Wheater, H., Jolley, T.J. and Peach, D., 1995. A water resources simulation model for groundwater recharge studies: an application to Wadi Ghulaji, Sultanate of Oman, Proc. Int. Conf. on Water Resources Management in Arid Countries, Muscat, pp. 502-510.

Wheater, H.S., Onof, C., Butler, A.P. and Hamilton, G.S., 1991. A Multivariate spatial-temporal model of rainfall in southwest Saudi-Arabia. 2. Regional Analysis and long-term performance. Journal of Hydrology, 125(3-4): 201-220.

Wheater, H.S., Woods Ballard, B. and Jolley, T.J., 1997. An integrated model of arid zone water resources: Evaluation of rainfall-runoff simulation performance In: D. Rosbjerg, N.-E. Boutayeb, A. Gustard, Z.W. Kundzewicz and P.F. Rasmussen (Editors), Sustainabilily of Water Resources under Increasing Uncertainty. IAHS Publication. IAHS, pp. 395-405.

Wilson, J.L. and Guan, H., 2004. Mountain-Block Hydrology and Mountain-Front Recharge Groundwater recharge in a desert environment: the southwestern United States Water Science and Application 9. In: J.F. Hogan, F.M. Phillips and B.R. Scanlon (Editors). American Geophysical Union, pp. 1-23.

Wu, Y., Wang, W., Toll, M., Alkhoury, W., Sauter, M. and Kolditz, O., 2011. Development of a 3D groundwater model based on scarce data: the Wadi Kafrein catchment/Jordan. Environmental Earth Sciences, 64(3): 771-785.

Zadeh, L.A., 1965. Fuzzy sets. Information and control, 8(3): 338-353.

Zhan, F.B. and Lin, H., 2003. Overlay of Two Simple Polygons with Indeterminate Boundaries. Transactions in GIS, 7(1): 67-81.